The role of the Glucocorticoid Receptor in intestinal inflammation and tumorigenesis in a murine model of colitis and colitis-associated colorectal cancer

Dissertation

for the award of the degree
"Doctor rerum naturalium"
of the Georg-August-Universität Göttingen

within the doctoral program
GGNB (Göttingen Graduate School for Neurosciences, Biophysics, and Molecular Biosciences), Molecular Medicine
of the Georg-August University School of Science (GAUSS)

submitted by
Chiara Muzzi

From Grosseto, Italy

Göttingen, May 2022

Thesis Committee

Dr. Sybille Reichardt
Institute for Cellular and Molecular Immunology
University Medical Center, Göttingen

Prof. Dr. Lutz Walter (1st Referee)
Department of Primate Genetics
German Primate Center, Göttingen

Prof. Dr. Matthias Dobbelstein (2nd Referee)
Institute of Molecular Oncology
University Medical Center, Göttingen

Additional Members of the Examination Board

Prof. Dr. Heidi Hahn
Department of Human Genetics, Section of Developmental Genetics
University Medical Center, Göttingen

Prof. Dr. Ralf Dressel
Institute for Cellular and Molecular Immunology
University Medical Center, Göttingen

Dr. Shiv K. Singh
Department of Gastroenterology and Gastrointestinal Oncology
University Medical Center, Göttingen

Date of submission: 23/05/2022
Date of oral examination: 25/07/2022

Part of this work have been published or submitted in the following articles:

Muzzi, C., Watanabe, N., Twomey, E., Meers, G. K., Reichardt, H. M., Bohnenberger, H., & Reichardt, S. D. (2021). The Glucocorticoid Receptor in Intestinal Epithelial Cells Alleviates Colitis and Associated Colorectal Cancer in Mice. *Cellular and molecular gastroenterology and hepatology*, *11*(5), 1505–1518. https://doi.org/10.1016/j.jcmgh.2020.12.006

Table of Contents

Table of Contents

Table of Contents

Table of Contents

Abstract

Ulcerative colitis (UC) is a life-threatening disease with constantly increasing incidence. Glucocorticoids (GCs) are one of the first choices for the treatment of this disease thanks to their anti-inflammatory action and their low costs. However, they are associated with adverse effects. GCs exert their function by binding to the GC receptor (GR), which is ubiquitously expressed and can impact gene transcription by different mechanisms.

To obtain new insights into the mechanism of GCs in the context of UC, we chemically induced colitis in a mouse strain with impaired GR DNA-binding (GR^{dim}). Here we found that disease symptoms were reduced compared to littermate controls, and that expression of pro-inflammatory genes was downregulated. We also observed a differential expression of genes associated with colon permeability in untreated GR^{dim} mice, which presumably confers a protective effect during colitis. When we induced colitis-associated colon cancer by additionally injecting a cancerogenic agent, we observed a lower number of tumors in GR^{dim} mice. Impaired GR DNA-binding activity thus seems to be beneficial in colitis and cancer progression, indicating that more selective GR agonists could improve UC treatment.

Intestinal epithelial cells (IECs) are essential in maintaining gut homeostasis and play a crucial role in the pathogenesis of UC, but the function of the GR in this cell type has not been investigated yet. To study this issue, we used mice carrying an inducible deletion of the GR in IECs (GR^{villin}) and subjected them to the same chemically induced UC model. Epithelial permeability in the colon and the expression of pro-inflammatory genes in IECs were increased in GR^{villin} mice. Recruitment of immune cells into the lamina propria was compromised in mutant mice, presumably leading to an impaired clearance of pathogens. In contrast, the infiltrating cells were hyperactivated in GR^{villin} mice leading to a perpetuation of inflammation. Taken together, a lack of the GR in IECs aggravates colitis. These data underscore the importance of GC action in IECs in controlling colonic inflammation and raise the question if a drug administered to directly target them might be an option for improved treatment of UC.

List of Figures

List of Tables

Abbreviations

5-ASA	5-aminosalicylic acid
6-MP	Mercaptopurine
ACTH	Adrenocorticotropic hormone
AF	Activation function
AJ	Adherent junction
AMP	Antimicrobial peptide
AOM	Azoxymethane
AP-1	Activator protein 1
APC	Antigen-presenting cell
AZA	Azathioprine
CACRC	Colitis-associated colorectal cancer
CCL	C-C chemokine ligand
CCR	C-C chemokine receptor
CD	Crohn's disease/ Cluster of Differentiation
cDNA	Complementary DNA
COX	Cyclooxygenase
CRH	Corticotropin releasing hormone
CXCL	C-X-C chemokine ligand
CXCR	C-X-C chemokine receptor
DAI	Disease activity index
DBD	DNA-binding domain

Abbreviations

DC	Dendritic cells
ddH2O	double-distilled water
DEPC	diethylpyrocarbonate
Dex	Dexamethasone
DNA	Deoxyribonucleic acid
dNTP	Deoxynucleoside triphosphate
DSS	Dextran sulfate sodium
EB	Evans blue
EDTA	Ethylenediaminetetraacetic Acid
EGF	Endothelial Growth Factor
ELISA	Enzyme-linked Immunosorbent Assay
ERK	Extracellular signal-regulated kinases
FACS	Fluorescence Activated Cell Sorting
FAP	Familial adenomatous polyposis
FCS	Fetal calf serum
FDA	Food and Drug administration
FITC	Fluorescein isothiocyanate
FKBP	Immunophilin FK binding protein
FoxP3	Forkhead box P3
GCs	Glucocorticoids
GI	Gastrointestinal
GILZ	Glucocorticoid-induced leucine zipper

Abbreviations

GR	Glucocorticoid receptor
GrB	Granzyme B
GRE	Glucocorticoid Response Elements
H&E	Hematoxylin and eosin
HGF	Hepatocyte growth factor
Hif	Hypoxia-Inducible Factor
HLA	Human leukocyte antigen
HNPCC	Hereditary non-polyposis colorectal cancer
HPA	Hypothalamic-pituitary-adrenal
HPRT	hypoxanthine phosphoribosyl transferase
Hsp	Heat shock protein
IBD	Inflammatory bowel disease
IEC	Intestinal epithelial cells
IFC	Integrated Fluidic Circuit
IFN	Interferon
Ig	Immunoglobulin
IGIP	Immunoglobulin A-inducing protein
IL	Interleukin
IRAK-M	Interleukin-1 receptor-associated kinase 3
JAK	Janus Kinase
K-RAS	Kirsten Rat Sarcoma
LBD	ligand-binding domain

Abbreviations

LOH	Loss of heterozygosity
LP	Lamina propria
LPC	Lamina propria cell
Lypd8	Ly6/PLAUR domain containing 8
MAdCAM-1	Mucosal address cell adhesion molecule-1
MAM	Methylazoxymethanol
MEP1A	Meprin 1A
MHCII	Class II major histocompatibility complex
MMP	Matrix metalloproteinase
MR	Mineralocorticoid receptor
mRNA	Messenger RNA
mTOR	Mammalian target of rapamycin
MYOD1	Myogenic Differentiation 1
NFAT	Nuclear factor of activated T cells
NF-κB	Nuclear factor-κB
NK	Natural Killer
NL	Nuclear localization signals
NOD	Nucleotide-binding oligomerization domain-like
NOS	Nitric oxide synthase
NP	Nanoparticles
NR3C1	Nuclear receptor subfamily group C member 1
NTD	N-terminal domain

Abbreviations

PBS	Phosphate Buffered Saline
PCR	Polymerase chain reaction
PGE2	Prostaglandin E2
PPAR-γ	Proliferator activated receptor gamma
PRR	Pattern Recognition Receptor
PVN	Paraventricular nucleus
RA	Retinoic acid
RegIII	Regenerating islet-derived 3
RNA	Ribonucleic acid
ROS	Reactive oxygen species
RT	Room temperature
RT-qPCR	Quantitative reverse transcription PCR
SCFA	Short-chain fatty acid
SCID	Severe combined immunodeficient
SEGRAM	Selective GC antagonist and modulator
SEM	Standard error of the mean
SIgA	Secretory IgA
SNPs	Single nucleotide polymorphisms
sPLA2	Secretory phospholipase A2
STA	Specific Target Amplification
STAT	Signal Transducers and Activators of Transcription
TCR	T-cell receptor

Abbreviations

TGF	Transforming growth factor
Th	T helper
TJ	Tight junction
TLR	Toll like receptor
TNBS	Trinitrobenzene sulfonic acid
TNF	Tumor necrosis factor
Treg	T regulatory
TSLP	Thymic Stromal Lymphopoietin
UC	Ulcerative colitis
UV	Ultraviolet
VEGF	Vascular Endothelial Growth Factor

1. Introduction

1.1 Colon Homeostasis

The colon is the widest part of the large intestine, which includes the cecum, the appendix, the entire colon, the rectum, and the anal canal. The colon itself is divided in four parts, the ascending, transverse, descending and sigmoid part. It begins at the end of the ileum and ends with the rectum and the anus. The colon has the typical histological structure of the digestive tract and is composed of the mucosa (*lamina epithelialis*), connective tissue (*lamina propriae mucosae*), the submucosa and the inner circular musculature (*tunica muscularis*) (Kahai et al., 2022). Due to its role in water absorption from indigestible contents, electrolyte balance and as a reservoir of stools, the colon is constantly exposed to the external environment and antigens. Hence, protection against harmful microorganism requires a complex interaction between intestinal epithelial cells (IECs), lamina propria cells (LPCs) and the intestinal microbiota (S.D. Reichardt et al., 2021). A dysregulation of the colon homeostasis such as immune dysregulation or dysbiosis can lead to severe intestinal inflammation and clinical manifestations like ulcerative colitis (UC) and Crohn´s disease (CD), which are commonly comprised as Inflammatory Bowel Disease (IBD) (Okumura & Takeda, 2016). To understand the pathology of the disease it is important to analyze the specific roles that the microbiota as well as the LPCs and IECs play in the gut homeostasis and how an impaired balance between them can lead to an abnormal immune response against components of the digestive system.

1.1.1 Microbiota

The gut microbiota is composed of trillions of bacteria which colonize the intestinal lumen. This ecosystem consists of commensal bacteria living in symbiosis with the host and is necessary for several aspects of human health like gut homeostasis and the development and function of the immune system (El-Aidy et al., 2013; Lin & Zhang, 2017). Microbiota's antigens are continually sensed and processed by Pattern Recognition Receptors (PRRs) such as Toll like receptors (TLRs) and Nucleotide-

binding oligomerization domain-like (NOD) receptors present on IECs, macrophages and dendritic cells (DCs) without eliciting a pro-inflammatory immune response. The mechanisms behind this hyporesponsiveness towards the microbiota are complicated, although it was demonstrated that some components of commensal bacteria play a role in inhibiting inflammatory pathways. It was demonstrated that bacteria as *L. reuteri*, *B. infantis* and *L. salivarius* can suppress Tumor necrosis factor (TNF) production in IECs in a NF-κB-dependent manner and *L. casei* can suppresses invasive *S. flexneri*-induced transcription of pro-inflammatory and adhesion molecules in IECs thanks to the regulation of the ubiquitin/proteasome pathway moreover it can also inhibit the nuclear translocation of NF-κB. In addition, *B. thetaiotaomicron* induces the export of the RelA subunit of NF-κB associated with PPARγ from the nucleus thereby regulating the NF-κB pathway (Vanderpool et al. 2008, Yan & Polk, 2010). The microbiota has a role in the induction and balance between Treg and Th17 cells as well. *Clostridium* species and short-chain fatty acids (SCFAs) like butyrate and propionate for instance, promote the development of $Foxp3^+$ Treg cells, a subpopulation of T cells that modulate the immune system, maintain tolerance, and prevent autoimmunity, in the large intestine by inducing Transforming growth factor β (TGF-β) production from IECs (Artis, 2008; Okumura & Takeda, 2016; Omenetti & Pizarro, 2015). Moreover, the absence of the microbiota in germ-free mice was associated to several immune problems and a compromised function of Treg cells (Atarashi et al., 2013; Macpherson & Harris, 2004).

1.1.2 Intestinal Epithelial Cells

IECs reside between the intestinal lumen and the lamina propria (LP) and act as a physical and biochemical barrier between both compartments. Namely, the mucosa is lined by a single-layered columnar epithelium with a thin brush border and includes several different cells with various roles such as absorptive enterocytes that represent the majority of the intestinal cells, goblet cells, enteroendocrine cells, and Paneth cells (Kaur et al., 2020, Henderson et al., 2011). The intestinal epithelium is folded leading to the formation of intestinal crypts known as ‘crypts of Lieberkühn’. They are the

site of IEC generation since it is here where the intestinal stem cells reside (van der Flier & Clevers, 2009). IECs mainly fulfill two roles, one of which is "segregation", which means that they separate the immune cells in the LP from the gut microbiota, thereby preventing conflicts between them. This is mainly possible thanks to the presence of intracellular junction, such as tight junctions (TJs), adherent junctions (AJs) and desmosomes which contribute to the barrier efficiency and integrity (Hossain & Hirata, 2008). Another crucial factor is the presence of a layer of mucus on the surface of IECs. The mucus, which is mainly composed of mucin that confers the gel-like properties, is secreted by goblet cells and prevents antigen infiltration into the tissue (Herath et al., 2020; Pelaseyed et al., 2014). Moreover, IECs produce a variety of antimicrobial peptides (AMPs), which are secreted into the mucus layer and help maintaining the IECs' integrity. Enterocytes produce a variety of antimicrobial peptides such as regenerating islet-derived 3 (RegIII) γ and Ly6/PLAUR domain containing 8 (Lypd8). In addition, they mediate the transfer of IgA produced within the LP to the intestinal lumen. Paneth cells which reside in the basal region of the crypts secrete lysozyme, α-defensins, secretory phospholipase A2 (sPLA2), and RegIIIγ, and produce molecules with anti-inflammatory activity such as trefoil factor 3 (Goto, 2019). The second role of IECs is being a "mediator". The intestinal epithelium delivers signals that communicate between bacteria and immune cells, IECs sense microbiota's molecules and in response produce immune mediators such as cytokines which regulate the immune responses thereby promoting tolerance or, in the case of infection, a protective response (Okumura & Takeda, 2017). The presence of PRRs such as TLRs and NODs and class II major histocompatibility complex (MHCII) molecules is necessary for IECs to fulfill the mediator role. Thanks to these receptors IECs can act as antigen-presenting cells (APCs), induce T cells polarization, interact with LP immune cells, and secrete pro- or anti-inflammatory molecules. TLR signaling under steady state condition seems to have a protective effect on the intestinal epithelium by inducing anti-apoptotic and proliferative factors and promoting IECs restitution and fortifying TJs (Maloy & Powrie, 2011). IECs communicate directly with DCs, too, thanks to the release, under steady state

condition, of Thymic Stromal Lymphopoietin (TSLP), TGF-β, retinoic acid (RA) and IL-25. This leads to the generation of a Treg-polarizing $CD103^+$ tolerogenic DC phenotype and supports IgA class switch (Heuberger et al., 2021; Rutella & Locatelli, 2011). $CD103^+$ tolerogenic DCs are essential for tolerance against commensal bacteria and food antigens, they migrate from the LP to the mesenteric lymph nodes and induce the differentiation of gut homing $FoxP3^+$ regulatory T cells (Villemin et al., 2020, Scott et al., 2011).

1.1.3 Immune cells of the gut

The LP is located underneath the intestinal epithelium and is composed of connective tissue elements such as elastin and collagen, myofibroblast, vascular elements, lymphatic vessels, nerve endings and several immune cells which are key regulators in gut homeostasis. DCs, macrophages, $CD4^+$ and $CD8^+$ T cells, B cells, IgA plasma cells, Natural Killer (NK) cells, mast cells and innate lymphoid cells reside in this tissue (Bruellman & Llorente, 2021). DCs in the LP are essential in shaping the immune response. Different subtypes of DCs are found in this tissue and they are implicated in both immune tolerance and protective immune responses as a result of their ability to sense and integrate signals from the local environment (Sun et al., 2020). To interact with the intestinal environment DCs have the ability to extend their dendrites across the intestinal epithelium to sample luminal antigens (Kelsall and Rescigno, 2004). These extensions occur without compromising the integrity of the epithelial barrier, probably due to the presence of TJs structure between the dendrites and IECs (Chieppa et al., 2006). Under steady-state conditions, DCs migrate to secondary lymphoid organs where they present self and innocuous antigens to maintain tolerance. Moreover, under tolerogenic conditions, intestinal DCs can induce anergy in antigen-specific T cells or induce the generation of $FoxP3^+$ Treg cells (Rutella & Locatelli, 2011). $CD8^+$ T cells in the colon are, under homeostatic condition, anergic thanks to the continuous antigen stimulation and interaction with tolerogenic DCs, $FoxP3^+$ Treg cells and cytokines like IL-10 (Casalegno Garduño & Däbritz, 2021). The presence of $FoxP3^+$ Treg cells is essential for immune tolerance

and barrier integrity, preventing an immune response, but, on the other hand, the presence of Th17 cells, which are proinflammatory cells, is also essential for the gut immune response and protection against several antigens such as bacteria and fungi. The equilibrium between these two types of T lymphocytes is needed for both tolerance and protective immune responses and is mainly controlled by DCs, macrophages, integrated signal from IECs, and the gut microbiota (Omenetti & Pizarro, 2015; van Wijk & Cheroutre, 2010). FoxP3$^+$ Treg cells in the colon produce IL-10, which decreases the secretion of pro-inflammatory Th1 cytokines such as IFN-γ and IL-12. Hence, mice lacking IL-10 develop spontaneous colitis and enhanced effector T cells activity (Okumura & Takeda, 2016). Intestinal macrophages reside mainly under the layer of IECs and are mainly polarized to the M2 anti-inflammatory phenotype under homeostatic conditions although M1 macrophages are also present in low numbers. The M2 phenotype in the colon is mainly driven by a combination of signals from TLRs, IL-10 signaling, and the interactions with both IECs and the gut microflora (Isidro & Appleyard, 2016). They are highly phagocytic and responsible for cleaning apoptotic cells and for capturing and eliminating bacteria that cross the epithelial barrier. Their role in the LP is similar to the one of DCs, since it was demonstrated that they can sample luminal bacteria to regulate the immune response and can balance FoxP3$^+$ Treg cells and Th17 cells through the secretion of IL-10, TGF-β and IL-1β. Moreover, thanks to the secretion of prostaglandin E2 (PGE2), hepatocyte growth factor (HGF) and Wnt ligands they promote barrier integrity and IEC renewal (Bain & Schridde, 2018; Bording-Jorgensen et al., 2021; Panea et al., 2015). DCs and macrophages play a key role for B cells and Plasma cells within LP as well. Plasma cells in the gut secrete IgA, which is the most abundant antibody isotype in the colonic mucosa. IgA antibodies are secreted in the LP and then transported through the IECs directly into the intestinal lumen (Gutzeit et al., 2014). DCs and macrophages induce the differentiation of B cells in the LP into Plasma cells and support class switch and homing thanks to the secretion of RA, immunoglobulin A-inducing protein (IGIP), APRIL and TGF- β (Spencer & Sollid, 2016). Once reaching the intestinal lumen, IgA resides mainly in the mucus layer and

is called secretory IgA (SIgA). They block both harmful and non-harmful bacteria preventing their adhesion to IECs and their infiltration into the LP. In addition, they mediate the removal of antigens in the LP, transporting and releasing them in the intestinal lumen (Figure 1) (Strugnell & Wijburg, 2010).

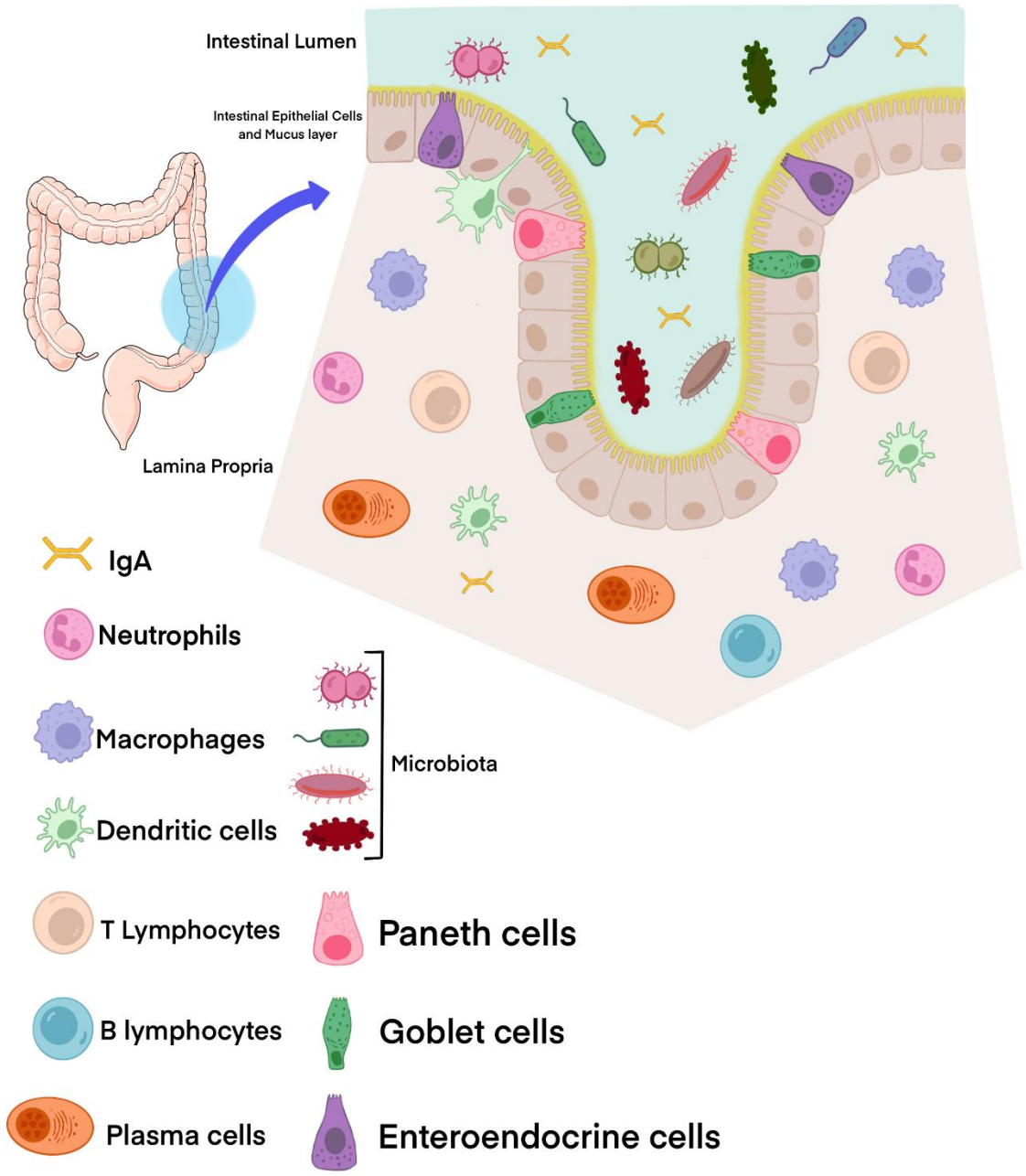

Figure 1: Gut homeostasis. The different types of IECs segregate the immune cells within the LP from the gut microbiota in the intestinal lumen. Figure created with Procreate.

1.2 Ulcerative Colitis

1.2.1 Epidemiology of UC

UC, a subform of IBD, is a chronic multifactorial inflammatory disease, which affects the colonic mucosa. In contrast to CD, which affects the entire gastrointestinal (GI) tract from the mouth to the anus and where the lesions have a patchy pattern, UC usually starts in the rectum and affects the whole colon in a continuous inflammatory pattern and the formation of ulcers. The prevalence of UC is constantly rising worldwide, particularly in newly industrialized countries such as South America, Asia, Africa, and the Middle East, although the prevalence remains low in these areas compared to western countries. The incidence ranges from 8.8 to 23.1 per 100,000 person-years in North America, 0.6 to 24.3 per 100,000 person-years in Europe, and 7.3 to 17.4 in Oceania, and the estimated annual direct and indirect costs related to UC range from 12.5 to 29.1 billion € in Europe and 8.1 to 14.9 billion $ in the US (Gajendran et al., 2019; Ungaro et al., 2017, Du & Ha, 2020). Despite the increasing number of UC diagnoses, the mortality has been decreasing over time thanks to therapeutic advantages and the optimization of surgical techniques (da Silva et al., 2014). UC affects women and men equally and occurs at any age. The peak of the disease's onset is between 30 and 40 years of age and in elderly individuals. Symptoms are numerous, including incontinence, urgency, fatigue, mucus discharge, increased bowel movements, and abdominal cramps. In severe forms of UC, fever and weight loss can also be present. Furthermore, UC can be associated with extraintestinal manifestations, which usually involve skin, joints, liver, and eyes. The disease is also associated with a high risk of developing colitis-associated colorectal cancer (CACRC) (Lu et al., 2018, Feuerstein & Cheifetz, 2014). Risk factors associated with UC are related to alterations in the gut microbiota and damage of the intestinal mucosa that can lead to an abnormal immune response and include GI infections, lifestyle, drugs, and antibiotics (Du & Ha, 2020). The use of oral contraceptives, hormone replacement therapy, tetracyclines and non-steroidal anti-inflammatory drugs have been associated with an increased risk of UC, while

adenectomy at young age seems to have a protective effect. Regarding lifestyle, cigarette smoking has a protective effect whereas an urban lifestyle is a risk factor. The impact of the diet has been evaluated in several studies and a diet rich in fat and sugar was found to be associated with UC while a diet rich in fiber reduces the risk of the disease. Enteric infections leading to a mucosal barrier disruption and interferences with the gut microbiome increase the risk of UC in individuals who develop IBD due to GI inflammation. In fact, *Salmonella* and *Campylobacter* are the most usually stated triggers (Arnone et al., 2021; Feuerstein & Cheifetz, 2014; Ungaro et al., 2017) Around 8-14% of patients with UC have a family history of IBD, and those with afflicted first-degree relatives are four times more likely to develop the disease. Although the genetic risk factors are not completely understood up to now, around two hundred risk loci have been identified. Variants of the HLA gene such as HLA-DqA1 seem to be most strongly associated with UC, as well as genes associated with epithelial barrier function, such as CHD1 and LAMB1, and genes encoding cytokines and inflammatory markers (Du & Ha, 2020; Feuerstein et al., 2019; Ungaro et al., 2017).

1.2.2 Diagnosis and classification of UC

The diagnosis of UC is based on an overall interpretation of clinical manifestations, laboratory tests, endoscopic evidence of inflammation, as well as histologic and radiologic findings (Kucharzik et al., 2020). Biopsy specimens are usually used as confirmation of chronic active colitis. Histologically, inflammation is restricted to the mucosal layers, with lymphocytes, plasma cells, and granulocytes infiltrating in variable degrees. Other histologic findings include crypt architectural distortion with crypt shortening and disarray, as well as crypt atrophy, abscesses, and branching. Furthermore, Paneth cell metaplasia is symptomatic of a long-term inflammatory condition. Even though inflammation is continuous, in some instances of proctitis, proctosigmoiditis, or left-sided colitis, a cecal patch, which is an isolated region of inflammation in the cecum, can be present (typically near the appendiceal orifice) (Feuerstein et al., 2019).

UC is usually classified according to the Montreal classification, which comprises several parameters: age of diagnosis, location, the extent of the colonic involvement, and behavior and severity of the colitis (Figure 2) (Satsangi et al., 2006).

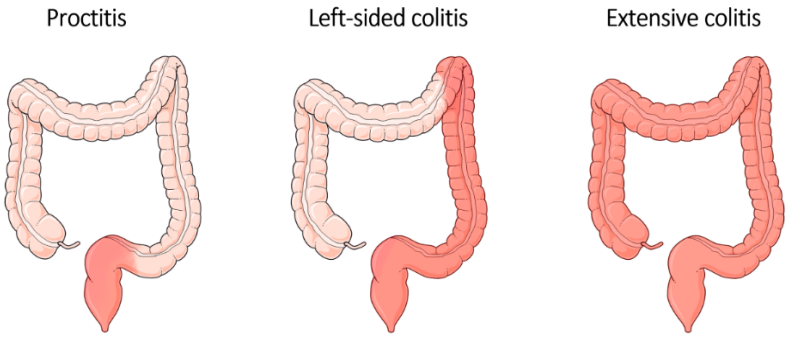

Extent		Anatomy
E1	Ulcerative proctitis	Involvement limited to the rectum
E2	Left sided UC	Involvement limited to a proportion of the colorectum distal to the splenic flexure
E3	Extensive UC (pancolitis)	Involvement extends proximal to the splenic flexure

Figure 2: Illustration of the different types of UC according to the extension of the colonic inflammation and the Montreal classification (Satsangi et al., 2006)

1.2.3 Pathogenesis of UC

The pathology of UC is complicated since there is not a clear triggering factor and the underlying events in the initiation of inflammation can be manifold. One factor which is associated with UC is dysbiosis, a change in the microbiota composition. There are three different classifications of dysbiosis: loss of beneficial microbial organisms, expansion of pathobionts, and loss of overall microbial diversity. These three types of dysbiosis are not mutually exclusive and may occur in parallel. The causes are related mainly to the western lifestyle and to the excessive use of antibiotics, due to their inability to distinguish between commensal and pathogenic bacteria (Petersen & Round, 2014). Dysbiosis can cause inflammatory responses and results in increased number of harmful bacteria and the accumulation of other pathogens such as viruses in the intestine. The release of enterotoxin, which increases

intestinal mucosal permeability, and the production of immunological mediators can lead to immune dysfunction and IEC damage which triggers a vicious cycle of inflammation and aggravates the intestinal immune response (Shen et al., 2018). A reduction in Firmicutes and Bacteroides species associated with an overgrowth of proteobacteria is commonly observed in patients with UC (Frank et al., 2007). A defect in the colonization with *F. prausnitzii* was also linked to UC, while the recovery of this bacteria in the lumen after a disease relapse is associated with clinical remission (Varela et al., 2013). Due to the role of the microbiota in immune regulation and barrier integrity, dysbiosis could also impair these aspects. A decreased production of SCFAs, which is common in IBD patients, affects the differentiation and expansion of FoxP3$^+$ Treg cells, while the high number of *Desulfovibrio* results in an overproduction of hydrogen-sulfate and leads to damage of intestinal epithelium (Nishida et al., 2018).

Defects in intestinal epithelial barrier function are one of the characteristic features of UC. These defects affect different levels of IECs protective mechanisms causing an impaired defense against pathogens (Antoni, 2014). The causes of IECs disruption are multifold such as dysbiosis, genetic factors or an abnormal immune response. Intestinal barrier damage favors the contact of immune cells with microbes thus increasing the inflammatory response. During inflammation, the production of pro-inflammatory cytokines such as TNF-α, IFN-γ and IL-13 induces IEC damage due to a dysregulation of TJ-associated-proteins like Claudin 2, Claudin 1 and Occludin (Landy et al., 2016). Single nucleotide polymorphisms (SNPs) in loci associated with IECs integrity were also observed in patients with UC. SNPs in *meprin 1A* (*MEP1A),* a protein that cleaves TJ protein, for instance, are associated with the disease in patients with active UC, moreover the downregulation of Hepatocyte nuclear factor 4α (HNF4α), which regulates the expression of protein involved in intestinal permeability was observed in patients with UC. Genetic alterations were also observed E-cadherin gene (Coskun, 2014). During the disease the mucus layer appears thinner and less continuous, and it might cause less effective retention of

AMPs and an increased IECs damage. These changes make the segregation less effective and lead to the initiation of inflammation. Furthermore, a deficiency of *Muc2* in mice leads to a thinner mucus layer and develop of spontaneous colitis (Van der Sluis et al., 2006, Coskun, 2014). In the mucus of UC patients, an impaired mucin glycosylation was also detected, while glycans are shorter and have a less complex structure and reduced sulfation (Antoni, 2014). Due to the barrier disruption and increased contact with pathogen associated molecular patterns (PAMPs), PRRs expressed on IECs are hyperactivated. A sustained PRRs activation drives a dysregulation in the immune response and leads to chronic intestinal inflammation (Maloy & Powrie, 2011). Dysregulation of TLR expression in IECs was also observed during IBD. A significant upregulation of TLR2 and TLR4 could compromise the capability to distinguish between commensals and pathogens and induce an abnormal immune response (Roda, 2010; Szebeni et al., 2007).

Immune cells in the LP are hyperactivated during UC due to barrier disruption and an increased uptake of luminal antigens. An abnormal DC and macrophage response and the subsequent expression of pro-inflammatory cytokines due to TLR signaling, lead to a pro-inflammatory T cells response with a high reactivity against intestinal bacteria. The production of TNF-α and IL-12 and the subsequent Janus Kinase (JAK) signaling potentiate lymphocytes activation and proliferation (Du & Ha, 2020). Moreover, an imbalance between Th17 and Treg cells, favoring Th17 cells thanks to the secretion of IL-17 and IL-23 was observed in UC (Rescigno & di Sabatino, 2009). During UC $CD8^+$ T cells are activated and present in increased numbers in the inflamed area (Müller et al., 1998), in fact, patients have an increased number of these cells in peripheral blood and high levels of IFN-γ (Funderburg et al., 2013). These activated $CD8^+$ T lymphocytes produce IFN-γ, TNF-α, granzyme B (GrB), and perforin that enhances the inflammation in the gut and disrupt TJs. IFN-γ and TNF-α are involved in the damage of TJs and they can change the lipid composition and fatty acyl substitutions of phospholipids in the membrane of the TJs microdomain (Li et al., 2008). Chronic exposure to IFN-γ seems to increase IEC apoptosis due to the

blockade of the Wnt pathway (Nava et al., 2010). Moreover, macrophage polarization changes during UC as well. It was demonstrated that an imbalance between pro-inflammatory M1 and anti-inflammatory M2 cells occurs. Namely, M1 macrophages increased and M2 macrophages decreased in number during colitis, accompanied by an induction of IL-23 and TNF-α and a suppression of IL-10 (Zhu et al., 2014). Th2 cells also play a role in the development of UC. They produce IL-13 which impairs epithelial barrier function due to its effects on IECs apoptosis, TJs and healing (Heller et al., 2005). Lastly, alterations in genes that encode for inflammatory pathways were also detected in UC patients. HLA mutations are the most common ones. 7.4%–11% of UC patients with extensive disease or pancolitis carry the rare *HLA DRB1*0103* variant in the MHC class II region (Toyoda et al., 1993). Mutations in the *IL23R* gene and components of its pathway such as *L12B, JAK2*, and *STAT3* were observed. *IL23* mutations activate pro-inflammatory pathways and Th17 cells. In fact, the blockade of this pathway suppresses gut inflammation in several murine models (M. F. Neurath, 2019). SNPs in the *IL10* gene were found as well, thus dysregulating its anti-inflammatory effects on the immune system (Thompson & Lees, 2011).

Collectively it is clear that the function of the whole colon is tightly regulated by the environment, IECs, microbiota and immune cells. A balance of all these factors is essential for gut homeostasis and a dysregulation of one or more of these factors in combination with the patient's genetic predisposition is associated with disease development (Figure 3) (Rescigno & di Sabatino, 2009).

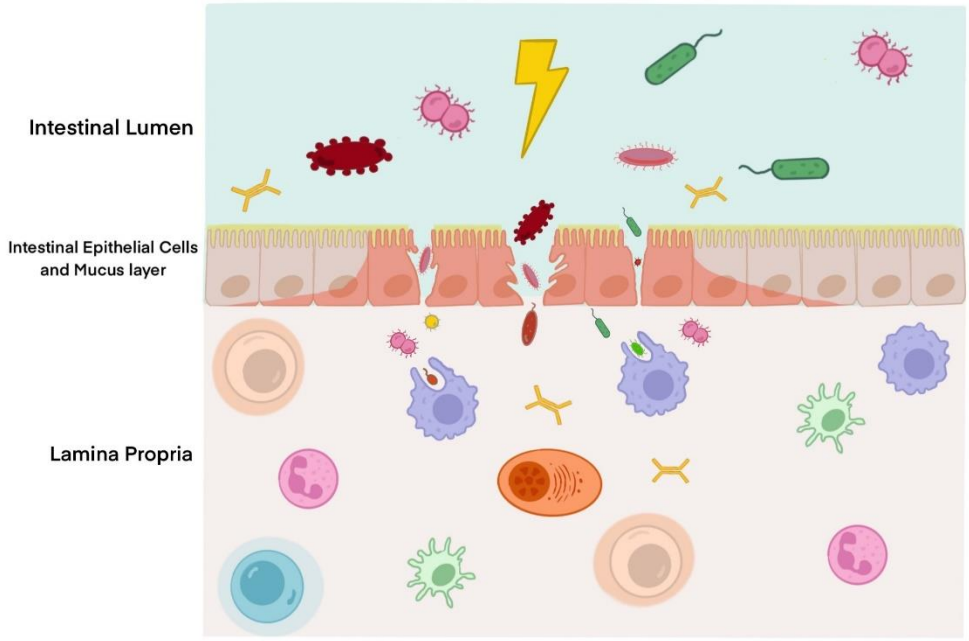

Figure 3: Pathogenesis of UC. During the disease, the intestinal epithelial barrier and the mucus layer are compromised. The bacteria invade the LP causing an activation of the immune cells and an increased uptake of luminal antigens. For legend see Figure 1. Figure created with Procreate.

1.2.4 UC Treatments

The choice for the best UC treatment is based on several factors and is not the easiest choice considering that several aspects must be kept in mind. Given that there are multiple distribution patterns, disease activities and disease courses, several scenarios could be present during UC and must be analyzed for the choice of the best treatment. Moreover, other factors such as age, concomitant diseases, infection, extraintestinal manifestation, and previous surgery and treatment must be considered (Meier & Sturm, 2011). The aim of the treatment is not only the clinical resolution of the symptoms, but also the healing of the mucosa since it is associated with long-term clinical remission and avoidance of colectomy (Kayal & Shah, 2020). In mild to moderate colitis, the first-line treatment for induction of remission is 5-aminosalicylic acid (5-ASA) (Xu et al., 2004). 5-ASA was synthesized in 1940 for the treatment of

rheumatoid arthritis and later it was found to be effective against UC as well (Chibbar & Moss, 2020). The mechanism of action is not well understood. While it interferes with several inflammatory pathways such as cyclooxygenase/lipoxygenase signaling and blocks IL-1β and TNF-α, it also seems to induce apoptosis of lymphocytes and inhibit macrophage and neutrophil functions (Chibbar & Moss, 2020; Mezzina et al., 2018). There are several formulations of 5-ASA, such as enema, foam, pill and suppository and the choice depend mainly on the extent of the disease and its localization since some formulations cannot reach the inflamed area in the inner part of the colon. The dosage usually ranges from 1.0 - 4.8 g/ day in one or more daily doses. The oral formulations are usually taken in a dosage between 2.0 - 4.8 g in two, three or four doses a day, the suppository formulation is usually 1 g one or twice daily and the enema solution usually contains 4 g of the drug and is given once or twice daily (Kayal & Shah, 2020). Symptoms should ameliorate after 2-3 weeks of 5-ASA treatment, if improvements are not observed a therapy with glucocorticoids (GCs) alone or in combination with 5-ASA can be considered (Probert, 2013). Second-generation GCs such as budesonide, budesonide multimatrix and beclomethasone dipropionate, are mainly used for the treatment of mild to moderate disease when a local anti-inflammatory action is required. Topical and oral beclomethasone dipropionate and Budesonide multimatrix (9 mg/ day for 2 months), are usually prescribed for patients who show no response to 5-ASA. These GCs are associated with fewer adverse effects (Hussenbux & de Silva, 2021). Some first-generation GCs such as methylprednisolone (12–48 mg/day) and prednisone, if used in combination with other drugs, such as sulfasalazine also can cause symptom improvement. Prednisone is usually prescribed in moderate-severe UC, the dosage is 1 mg/ kg up to 40–60 mg/ day (Bruscoli et al., 2021).

In moderate to severe UC thiopurines and biologics are also used. Thiopurines are immunosuppressive drugs that act on T cells by deactivating T cell processes and reducing the inflammatory response since they target the enzyme Rac1, a GTPase, which is essential for T cells activation (Neurath, 2010). Thiopurines are mainly used

as maintenance therapy for patients which cannot be treated with 5-ASA, are steroid-dependent or have relapses (Mezzina et al., 2018). The recommended dosage for this compound varies between the guidelines and also depends on the type of thiopurine used. The European Crohn's and Colitis Organization recommend daily doses of 1.5-2.5 mg/ kg AZA and 0.75-1.5 mg/kg 6-MP. However, the dosage may also differ between different ethnicities (Frei et al., 2013).

If other treatments are not effective various biologics can be used for the treatment of UC. The first biologic to be approved by the FDA was Infliximab. It consists of a chimeric IgG1 monoclonal antibody that binds to soluble and cellular membrane TNF-α and induces cytotoxicity and T cells apoptosis. Later on, Adalimumab and Golimumab were approved and are now used to treat UC. Other biologics which target different molecules have also been approved: the integrin receptor antagonist, Vedolizumab and Etrolizumab and the JAK inhibitor Tofacitinib (Park & Jeen, 2015). Vedolizumab is a fully humanized monoclonal IgG1 antibody that inhibits the interaction between the α4ß7 integrin and mucosal address cell adhesion molecule-1 (MAdCAM-1). Etrolizumab is a next-generation anti-integrin antibody with dual action which inhibits both α4ß7 and αEß7 integrins. Their function is mainly the blockade of immune cells trafficking into the gut thus reducing local inflammation (Sandborn et al., 2020; Scribano, 2018). Tofacitinib is the first JAK inhibitor approved for UC. It acts by inhibiting the JAK-STAT pathway leading to the blockade of several cytokines at the same time, thus reducing inflammation (D'Amico et al., 2019). The use of biologic drugs is associated with high costs and sometimes also severe side effects, which may include opportunistic infections and malignancies. In addition, complications such as injection reactions, autoimmunity, heart failure and acute infectious diseases may occur (Stallmach et al., 2010).

For the treatment of acute severe UC, currently approved therapies are intravenously applied GCs, Infliximab, Cyclosporine A, and colectomy. Intravenously administered GCs are the first therapy of choice. Methylprednisolone is given at a dose of 60 mg/ day or 100 mg hydrocortisone every 6 hrs. Treatment duration is usually limited to 7

to 10 days. For patients not responding to intravenous GCs, calcineurin inhibitors like intravenous Cyclosporin A are used with a dosage of 2 mg/ kg per day (Kedia, 2014). It is a peptide that inhibits the immune response by forming a complex that inhibits calcineurin, an enzyme involved in T cells activation leading to the blockade of production of IL-2 by Th cells. Furthermore, it interferes with B cell function since it blocks the production of IFNγ and B cell activating factors (Mezzina et al., 2018). Another calcineurin inhibitor is Tacrolimus. Its effect is the same as the one of Cyclosporin A. It blocks calcineurin through the binding of the immunophilin FK binding protein (FKBP) and prevents the dephosphorylation of the nuclear factor of activated T cells (NFAT) and the transcription of the IL-2 gene. Even though the action of tacrolimus is like Cyclosporin A, the immunosuppressive properties have been reported to be 100 times greater both *in vivo* and *in vitro* (Matsuoka et al., 2015). Infliximab also has shown good therapeutic results for the treatment of acute severe UC (Halpin et al., 2013) and helps to avoid colectomy (Aratari A et al., 2008). Nevertheless, treatment with GCs is used at all stages of UC. This is due to their efficacy in suppressing the abnormal immune response which characterizes the disease. The treatment with GCs remains one of the first choices for IBD in the clinic thanks to their lower price compared to biologics and their effectiveness during the inflammatory response and flare-up. Regarding the price, it was demonstrated that for the usage of biologics for the treatment of asthma the price for all biologics exceeds measures of cost-effectiveness (Anderson & Szefler, 2019). Anyway, due to their various side effects, the mechanism and application of GCs are still studied to maximize their benefits and reduce adverse reactions.

1.3 Colitis-associated Colorectal Cancer

Patients affected by UC have an elevated risk of developing colorectal cancer. IBD is the third most common cause of intestinal cancer, after familial adenomatous polyposis (FAP) and hereditary non-polyposis colorectal cancer (HNPCC), and the risk rises with increased duration and severity of the disease. Patients with extensive colitis have a 19-fold higher risk of developing cancer, and the risk is higher when

colitis starts at a youthful age. Moreover, there also seems to be a correlation with the localization of colitis. In fact, the risk of cancer increases from 1.7-fold in proctitis and 2.8-fold in left-sided colitis to 14.8-fold in pancolitis, and the use of anti-inflammatory drugs reduce the risk of cancer (Ekbom et al., 1990; Kulaylat & Dayton, 2010, Lakatos & Lakatos, 2008). Genetic and environmental factors contribute to the development of CACRC. However, dysregulation of gut homeostasis is probably the most important mechanism in tumorigenesis (Lakatos & Lakatos, 2008). CACRC develops in a multi-step process that starts from an initial chronic inflammation to a hyper-plastic colon, early dysplasia and ends with invasive carcinoma (Kulaylat & Dayton, 2010). This sequence implies sequential alteration at the molecular level that causes changes in tissue structure and genetics (Seril et al., 2003; Vogelstein et al., 1988). Expression of pro-inflammatory cytokines such as IL-1β and TNF-α during the inflammatory process in the gut, together with the accumulation of DCs, neutrophils, macrophages and activated mesenchymal myofibroblasts at the inflamed site and the expression of reactive oxygen species (ROS), nitric oxide synthase (NOS), growth factors and morphogens have an important impact on the genetic of IECs and colonic stem cells. The overproduction of ROS and NOS by immune cells increases the oxidative damage of the DNA and together with the epithelial injury, causes a continuous cycle of regeneration which increases the risk of mutations. Moreover, the high proliferation rate could also lead to chromosomal instability and the accumulation of chromosomal aberrations (Humphries et al., 2012; Sobczak et al., 2014). The continuous stem cells proliferation in the crypts could also compromise Wnt signaling, which has a role in IECs homeostasis and regeneration. The overactivated Wnt pathway results in abnormal proliferation and leads to the accumulation of several mutations in key genes such as TP53 and *K-RAS* (Humphries et al., 2012). Loss of heterozygosity (LOH) of p53 is commonly observed in UC-associated carcinoma and dysplasia. LOH was observed in 70% of cancer tissue and 45% of dysplastic lesions and it was observed in the inflamed epithelium (Fogt et al., 1997; Seril et al., 2003).

DNA methylation of several genes was also observed in patients. ER, MYOD1, CSPG2 and p16 genes appear to be highly methylated in the dysplastic tissue (Issa et al., 2001), and methylation of the Wnt gene is also frequently observed in UC and CACRC. Methylation seems to occur early during the disease and is associated with the progression from inflammation to cancer (Dhir et al., 2008). Several cytokines and their associated pathway were observed to be implicated in tumor progression, an example of which is the NF-κB pathway. It was observed to be active also in cancer, and its target genes, such as BCL-2, BCL-X_L, TNF-α, COX-2, IL-6, VEGF and MMPs, have anti-apoptotic activity and promote cell invasion, angiogenesis, and inflammation (Oshima et al., 2012). TNF- α and IL-6 were found to be overexpressed in cancer tissue and they are associated with tumor progression and metastasis. Moreover, IL-6 was also associated with angiogenesis and Th17 cell regulation (Grivennikov et al., 2009; Sobczak et al., 2014). T lymphocytes play a role in tumor progression as well: $CD4^+$ effector T cells promote inflammation and sustain cancer progression, and cytotoxic $CD8^+$ T cells can aggravate chronic inflammation and thereby support tumor development. Thanks to their immunosuppressive action, Treg cells can dampen chronic inflammation and protect against cancer development (Waldner & Neurath, 2009).

1.4 Glucocorticoids

GCs are a group of steroid hormones, which regulate several pathological and physiological processes, namely metabolism, the immune response, growth, reproduction, and development. Moreover, thanks to their anti-inflammatory activity, synthetic GCs are used for the treatment of inflammation, allergy, autoimmune diseases such as rheumatoid arthritis, asthma, and IBD (Timmermans et al., 2019). Despite their broad use for the treatment of several diseases, the long-term application of synthetic GCs is associated with several adverse effects such as osteoporosis, weight gain, osteonecrosis, infections, hyperglycemia, diabetes, and hypertension (Gensler, 2013).

The long process that has led to the discovery of GCs started in 1855 when Thomas Addison observed a disease, today known as Addison's disease, characterized by atrophy of the adrenal glands; later Edouard Brown-Séquard demonstrated that the removal of the adrenals of small animals was associated with muscle weakness, respiratory, cardiac irregularities, and death. In 1927 Julius Rogoff and George Stewart demonstrated that they were able to keep alive animals without adrenals thanks to the injection of extracts from the adrenal cortex (Patrick, 2013). The turning point was then during the 1930s when Tadeus Reichstein and his colleagues extracted corticosterone. Sometimes later, Edward C. Kendall, thanks to the results of Rogoffs and Stewarts, decided to isolate the active compound from the adrenal complex. This process required several years and international efforts and led to the isolation of several molecules. Kendall named these steroid molecules with letters: Compound A was 11-dehydrocorticosterone, Compound B was corticosterone, Compound E was cortisone (17-hydroxy-11-dehydrocorticosterone), and Compound F was cortisol (hydrocortisone or 17-hydroxycorticosterone) (Simoni et al., 2002). In 1950, Kendall, Reichstein, and Hench received the Nobel Prize in Physiology and Medicine for their work in studying and describing GCs (Ahmed et al., 2019).

1.4.1 Mechanism of Glucocorticoids

The biosynthesis of steroid hormones occurs in the *zona fasciculata* of the adrenal cortex. It starts from cholesterol, which is the precursor of all the steroid hormones, and pregnenolone is finally converted into cortisol in the mitochondria. This process is mainly accomplished by cytochrome P450 family enzymes. Daily, between 5 and 30 mg of active cortisol are produced (Strehl et al., 2019). The process is controlled by the hypothalamic-pituitary-adrenal (HPA) axis in a negative feedback loop. In response to stress, neurons in the paraventricular nucleus (PVN) of the hypothalamus release corticotropin releasing hormone (CRH) into the blood. CRH then stimulates the pituitary gland to produce and secrete adrenocorticotropic hormone (ACTH). Next, ACTH induces GCs synthesis and their release from the adrenal glands (Sheng et al., 2021). GCs are secreted in a circadian manner or in response to external stress, such as inflammation or pain.

GCs are lipophilic steroid hormones with low molecular weight and can pass the cellular membrane and bind to the GC receptor (GR) in the cytosol (Strehl et al., 2019). The GR is part of the nuclear receptor superfamily, it is expressed in almost every cell of the body, and its cellular response is variable (Oakley & Cidlowski, 2013). The GR is encoded by the nuclear receptor subfamily group C member 1 (NR3C1) gene, which is located on chromosome 5 (5q31) in humans. The gene is related to NR3C2, which encodes the mineralocorticoid receptor (MR), to gene NR3C3, which encodes the progesterone receptor (PR), and to NR3C4, which encodes the androgen receptor (AR) (Weikum et al., 2017). The GR is composed of three functional domains: the N-terminal domain (NTD), the DNA-binding domain (DBD), and the ligand-binding domain (LBD). The DBD is a conserved region and contains two zinc fingers that are essential for DNA binding and recognition. The NTD contains the active ligand-independent activation function (AF-1), which is essential for the transcriptional activation of the receptor, and it is the site for interaction with co-regulators and the basal transcription machinery. The LBD comprises the ligand-dependent activation function 2 (AF-2), which has a role in the

interaction with co-chaperone proteins, co-regulators, and other transcription factors (Petta et al., 2016). The nuclear translocation of the receptors is controlled by a flexible hinge region located between the DBD and LBD, where the two nuclear localization signals NL1 and NL2 are located (H.M. Reichardt et al. 1998). The *NR3C1* pre-mRNA consists of 9 exons, the last 2 exons are named 9α and 9β and their alternative splicing can generate two isoforms of the receptor, one incorporates exon 9α to form GRα and the other incorporates 9β and form GRβ (Oakley et al., 1996). GRα has a fully active LDB domain and upon ligand binding, it regulates the gene expression. On the other hand, GRβ has an LBD that is unable to bind GCs and acts as a negative regulator, failing in the activation of transcription. High levels of GRβ are associated with GC-resistant asthma and rheumatoid arthritis (Jain et al., 2014). In the absence of the ligand, the GR is found in the cytosol bound to heat shock proteins (Hsp) 90, 70, the co-chaperone p23, and immunophilins which keep the receptor inactive but, at the same time, favor binding of the ligand (Kirschke et al., 2014; Noddings et al., 2022; Tatro et al., 2009). Upon the interaction with its ligand, the GR mainly acts through two different mechanisms which are either DNA-binding-dependent or -independent (Ahmed et al., 2019). Once GCs bind to the receptor, the GR changes its conformation and dissociates from the protein complex, which favors its translocation into the nucleus where it can regulate gene expression through different mechanisms: either by direct interaction with specific regions of the DNA, direct interaction with other transcription factors or interaction with composite elements (Meijsing, 2015). The GR generally binds DNA as a homodimer in specific regions called GC-responsive elements (GREs) thus promoting gene expression. DNA binding induces the recruitment of coregulators and a chromatin-remodeling complex and influences the activity of RNA polymerase II. Negative GREs (nGREs) are also present in some genes. In this case the GR represses gene expression thanks to the recruitment of corepressors and histone deacetylase (Ramamoorthy & Cidlowski, 2016). The regulation of the gene expression in the nucleus can also be exerted without the binding of GREs. The GR can interact as a monomer directly with other transcription factors employing a so-called “tethering” mechanism, which

stimulates or inhibits the transcription of target genes (Xavier et al., 2016). The tethering process was observed to be essential in the regulation of the inflammatory response, since the GR binds several transcription factors that are key players in inflammatory processes like AP-1 and NF-κB, thus inhibiting inflammation (Reichardt H. M. et al., 2001; Weikum, de Vera, et al., 2017). For some genes the GR acts in a composite manner, it binds to a GRE and to a transcription factor bound to the next DNA site at the same time (Figure 4) (Ramamoorthy & Cidlowski, 2016). Non-genomics effects of GCs involve interaction with the cell membrane, interaction with the cytosolic GR or with a membrane-bound GR. These effects affect several aspects of the cell like the level of intracellular calcium, the function of the skeletal and smooth muscle as well as ROS and NOS generation. These effects are variable and depend on the cell type (Panettieri et al., 2019).

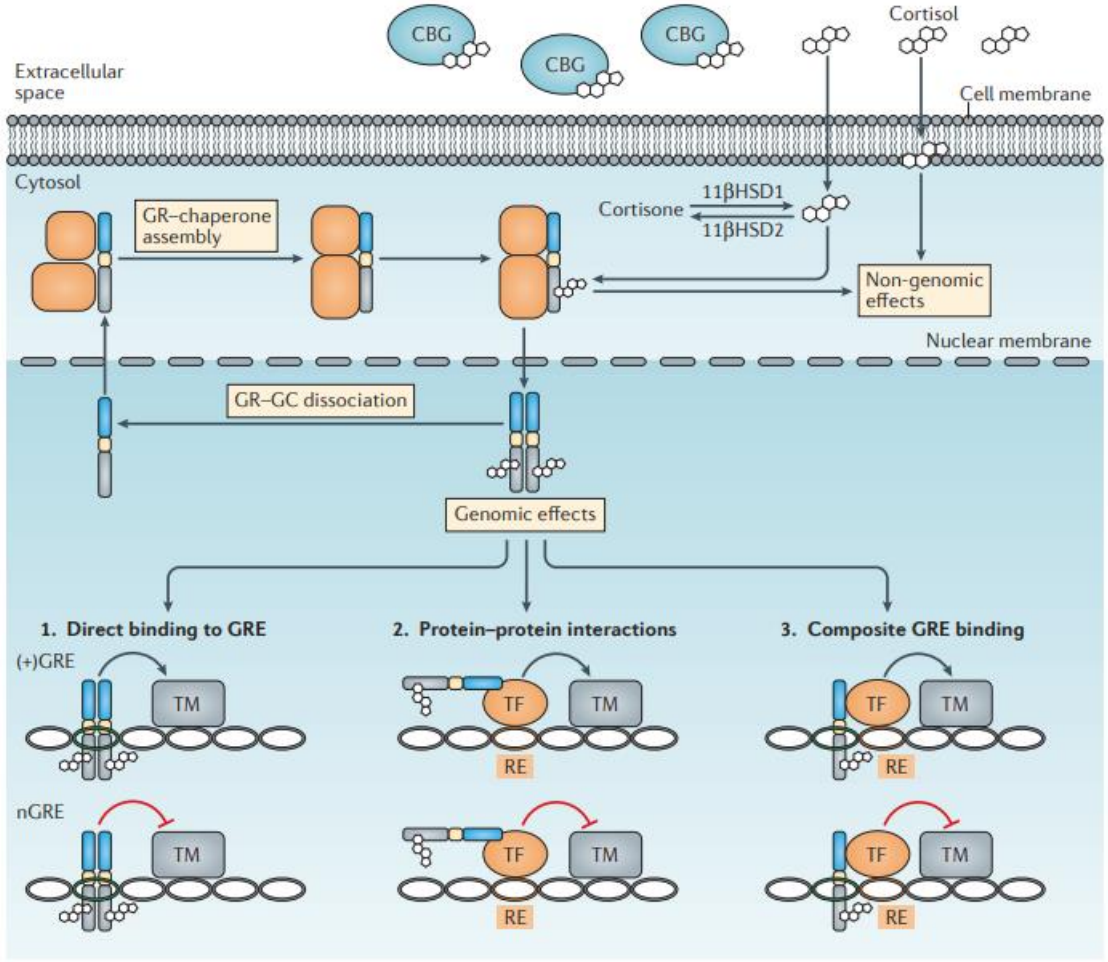

Figure 4: Mechanism of GCs. GCs pass the cell membrane and bind to the GR in the cytoplasm. The GR translocate in the nucleus and exerts its mechanism of gene regulation by binding the DNA in GRE or nGRE regions, by binding directly other proteins or by composite action. The GR can also exert its function in a non-genomic way. Figure from Cain and Cidlowski, 2017.

1.4.2 Glucocorticoids and immunity

GCs are regulators of the immune system; their effects modulate all the phases of the inflammatory response. The immunosuppressive action of GCs targets pathways of both innate and adaptive immunity. This is possible thanks to the interaction with several components of the PRR system thus reducing the inflammatory response. It is well known that GCs interact with the NF-κB, and AP-1 signaling on many levels. GCs induce expression of IκBα which keeps the NF-κB molecules inactive (Auphan et al., 1995) and it was observed that GCs can also upregulate IRAK-M and interact with p65 leading to the downregulation of pro-inflammatory responses (Miyata et al., 2015; Scheinman et al., 1995). Furthermore, the GR binds to NF-κB when it interacts with the promoter region, blocking the expression of pro-inflammatory genes (Nissen & Yamamoto, 2000). Regarding AP-1, GCs seem to inhibit the JNK phosphorylation thus blocking its activity, and additionally, the GR acts through the tethering mechanism (Herrlich, 2001; Victoria González et al., 2000). GCs can also upregulate DUSP-1 expression, leading to the suppression of the MAPK pathway including p38, JNK, and ERK, and thereby reduce the expression of pro-inflammatory cytokines (Shimba et al., 2021). Glucocorticoid-induced leucine zipper (GILZ) is a GC-inducible gene that fulfills a role in the regulation of these transcription factors. GILZ prevents the up-regulation of the Fas/FasL system induced by NF-κB and inhibits COX-2 and prostaglandins expression thanks to the inhibition of NF-κB. GILZ can also dimerize with AP-1 pathway components, thereby blocking its activity (Ronchetti et al., 2015). The presence of nGREs in several promoter regions of pro-inflammatory genes such as *IL1B*, *IL6* and *TSLP* also explains the reduction of the inflammatory response exerted by GCs (Cain & Cidlowski, 2017). GCs regulate the migration of leukocytes, too. They downregulate the expression of the adhesion molecules ELAM-1, ICAM-1 and VCAM-1 thus reducing leucocytes migration (Atsuta et al., 1999; Cronstein et al., 1992). Several immune cells are also influenced by the immunosuppressive action of GCs. DCs treated with GCs showed higher endocytic activity, in impaired antigen-presenting function, a diminished ability to

secrete cytokines and a reduced expression of MHCII thus a reduced ability to activate T cells (Piemonti et al., 1999; Valerio Di Carlo Sironi et al., 1999). GCs also impair the differentiation of DC and promote the polarization of DCs into tolerogenic DCs which are incapable of inducing a potent immune response. In these cells, expression of IL-2, p70 and TNFα was reduced while the expression of TLR 2, 3 and 4 seems to increase upon GC treatment. Moreover, the treatment with GCs decreases the number of circulating DCs and abrogates plasmacytoid DCs (Bros et al., 2007; Rozkova et al., 2006). During an inflammatory response GCs also act on macrophages and induce their switch from a pro-inflammatory M1 to an anti-inflammatory M2 type (Zhang et al., 2009). These M2 macrophages are characterized by the expression of CD163, MERTK and CD206, and the production of anti-inflammatory cytokines such as IL-10 and TGF-β (Ehrchen et al., 2019). GCs seem to further impact macrophage migration, phagocytic activity, and survival. While migration seems to be reduced, survival and phagocytic activity are upregulated, probably to sustain the healing of inflammation (Desgeorges et al., 2019).

Myeloid and lymphoid cells closely cooperate during immune responses. Hence, GC effects on DCs and macrophages shape T cells responses as well. Namely, the pro-inflammatory cytokine production and the increased secretion of anti-inflammatory molecules upon GC treatment favor the polarization of T cells into Th2 and Treg cells (Cain & Cidlowski, 2017). GCs inhibit the Th1 response by reducing IFN-γ secretion and IFN regulatory factor-1 expression in T cells and inhibit the phosphorylation of Stat4, both driven by IL-12 (Franchimont et al., 2000). They also interact directly with T-bet, which is essential for Th1 polarization and IFN-γ production, by blocking the transcriptional activity of T-bet through direct protein-protein interaction (Liberman et al., 2007). The inhibitory effects on the AP-1 and NF-κB pathways and the expression of GILZ also interfere with TCR signaling, dampen T cell activation, and inhibit T cell proliferation (Cain & Cidlowski, 2017). Moreover, the GR seems to interact directly with the TCR. This reduces LCK and FYN activity which leads to the suppression of TCR signaling (Löwenberg et al., 2007). Finally, GCs induce Treg cell polarization and $FOXP3^+$ expression thanks to the expression of GILZ (Furukawa

et al., 2016). However, GCs interact directly with Treg cells, too. It was observed that GCs applied in the absence of Treg cells failed to control inflammation and that GR deficiency in Treg cells abolished the anti-inflammatory effects of GCs in mice (D. Kim et al., 2020; Rocamora-Reverte et al., 2019).

1.4.3 Novel GC therapies for UC

GCs are potent anti-inflammatory drugs, which makes them the first choice for the treatment of UC. However severe adverse effects associated with GCs can reduce the treatment's benefits (S. D. Reichardt et al., 2021). Several GC derivatives have been developed to directly target the disease or to activate only some GC genes and reduce harmful effects. Some of the first GC-derived molecules created belong to the family of selective GC antagonists and modulators (SEGRAMs). These compounds can induce the GR's transrepression activity, meaning that the GR still binds to other proteins blocking their activity while transactivation, i.e., the direct binding to DNA is mainly blocked. This mechanism of action was developed due to the hypothesis that most of the GC side-effects derive mainly from the direct binding of the GR to DNA. Unfortunately, it was demonstrated that the mechanism is more complicated. While it could be shown that many of the adverse effects such as hyperglycemia and muscle wasting are mediated by transactivation, some others such as the suppression of the HPA-axis are mostly mediated by transrepression or both pathways (Sundahl et al., 2015). The anti-inflammatory effects of GCs were analyzed via *in vivo* studies, Hua and colleagues have shown that the anti-inflammatory effects of CpdX and CpdX-D3 are comparable to those of Dex for the treatment of several inflammatory diseases such as Dextran sulfate sodium salt (DSS) induced colitis and probably associated with less adverse effects (Hua et al., 2019). Their effects were also analyzed in a mouse model of acute Trinitrobenzene Sulfonic Acid (TNBS) induced colitis by Reuter and colleagues. Mice suffering from TNBS-induced colitis were treated with CpdA and ZK216348, and both compounds reduced the severity of the disease, tissue damage, and inflammation. Moreover, diabetogenic effects, HPA-axis suppression, or development of GC resistance were not observed (Reuter et al., 2012).

VBP15, with the commercial name of Vamorolone, was also tested for the treatment of TNBS-induced colitis in mice. It significantly reduced the *in vitro* production of CCL5, IL-6, IL-8 and reduced colitis symptoms while decreasing or avoiding side effects (Damsker et al., 2016).

A targeted GC delivery system using nanoparticles (NPs) for the treatment of UC is also a promising therapeutic approach for the reduction of adverse effects and for targeting the inflamed area. Several delivery systems for drugs have been evaluated including liposomes, NPs, and inorganic scaffolds and their efficacy was investigated both i*n vitro* and *in vivo* experiments. (Lühder & Reichardt, 2017). Cholesteryl butyrate-solid lipid nanoparticles (DxCb-SLN) containing Dex were studied by Dianzani and colleagues *in vitro* and DSS-induced colitis in mice. The treatment caused reduced cytokine expression and reduced cell adhesion (Dianzani et al., 2017). Oral Chitosan-modified lipid NPs were also developed. These NPs have the capability to target the colon and release the drug directly in the inflamed area thanks to the esterase-responsive properties of the NPs. This treatment showed benefits in both cell and mouse experiments with a decreased cytokine expression and an improvement of colitis symptoms (Chen et al., 2020). Another colon-targeted drug delivery system is Eudragit® S100-aminoclay double-coated liposomes that contain budesonide. These orally administrated NPs are a pH-sensitive drug carrier that releases the GCs at the high pH that is present in the intestinal fluid and caused a decreased pro-inflammatory cytokine expression (H. Y. Kim et al., 2020). Despite the presence of new delivery systems and their good efficiency *in vivo* and *in vitro*, their effectiveness in the clinic remains unknown.

1.5 Mouse Models of UC and CACRC

1.5.1 DSS-induced Colitis

IBD is a complex disease, and several aspects must be elucidated to better understand the etiology and find the best therapeutic approach. To this end, several murine models of the disease were developed through the years. One of the most used murine models of colitis involves the use of DSS, which is a water soluble sulfated polysaccharide with a highly variable molecular weight ranging from 5 to 1400 kDa, and is negatively charged (Chassaing et al., 2014). The use of DSS for colitis induction was first described by Okayasu and colleagues in 1990 when they observed that the administration of this molecule via drinking water was associated with acute colitis and clinical manifestations such as diarrhea, rectal bleeding, and weight loss. Moreover, the post-mortem examination revealed crypt changes and disruption, colon erosion and prominent regeneration of the colonic mucosa (Okayasu et al., 1990). The molecular mechanisms by which DSS exerts its function and enters into IECs are not completely clear. One proposed mechanism for the penetration of DSS through the intestinal epithelium seems to be the formation of nano-lipocomplexes with Medium-Chain length fatty acids in the colon. This lipocomplex seems to help the DSS to penetrate the cells and exert its function (Laroui et al., 2012). DSS action affects mainly the intestinal epithelium, causing a disruption of the epithelial barrier thus leading to the entry of luminal antigen into the LP thereby initiating an inflammatory response (Eichele & Kharbanda, 2017). This disruption of the IEC layer seems to be caused by several DSS actions also on TJs, one is the loss of the protein ZO-1 which is associated with TJs. The loss of this protein was observed starting on day 1 of DSS treatment and increased the colon permeability (Poritz et al., 2007). In addition, DSS seems to act also on the microbiota causing changes in its composition and leading to enhanced mucosal inflammation and mucin dysregulation. A probiotic therapy consequently ameliorates the disease (Eichele & Kharbanda, 2017). DSS colitis seems to be triggered only with the help of the innate immunity, since the cytokines produced by innate cells are enough to initiate the

inflammatory events. Experiments have shown that DSS colitis can occur also in immunodeficient mice like SCID and Rag1-/- (Dieleman et al., 1994; Krieglstein et al., 2002).

For an experimental setting, several factors must be evaluated: the concentration of DSS, which is usually between 1% and 5%, the duration of DSS treatment to establish an acute or chronic inflammation model, the molecular weight of the manufactured DSS, the sex and the microbial environment of the animals (Egger et al., 2000; Eichele & Kharbanda, 2017; Mähler et al., 1998). Furthermore, DSS can be used in combination with Azoxymethane (AOM) to induce initial colitis and subsequent CACRC formation.

1.5.2 AOM/DSS-induced CACRC

The AOM/DSS-induced model of CACRC was first described in 2003 by Tanaka and colleagues who described this new method for inducing colitis-associated cancer in murine models (Tanaka et al., 2003). AOM is usually injected intraperitoneally on day 1 of DSS treatment and mice then develop cancer several weeks later. This method is a model that utilizes chemical induction of DNA damage following acute colitis. AOM is a pro-carcinogen that must be metabolized before it becomes effective. The isoform CYP2E1 of the cytochrome p450 converts AOM into methylazoxymethanol (MAM) which is a highly reactive alkylating species. This molecule induces O^6 methylguanine adducts in DNA resulting in G to A transitions. It is excreted into the bile and then taken up by IECs, where it exerts its carcinogenic effect (Parang et al., 2016). Several protocols were developed for cancer formation in mouse models. In general, DSS must be administrated for at least 7 days. The AOM/DSS treatment depends also on the mouse strain used for the experiment and AOM alone seems not to be enough for cancer development (Suzuki et al., 2005). Studies addressing the cellular effects of the AOM/DSS model have demonstrated its reliability in terms of mimicking the human CACRC microenvironment and the molecular events associated with it. Dysregulation of the Wnt pathways associated with pro-inflammatory responses results in high levels of c-myc, an activator of cell

cycle progression and a known oncogene. Moreover, the inflammation caused by DSS treatment enhances the possibility of mutations as described in human CACRC. In essence, due to its similarity with the human CACRC progression, in terms of histological, pathological, and molecular features, the AOM/DSS model represents one of the best models for investigating the development and progression of this disease (Snider et al., 2016, Proetzel & Wiles, 2010).

1.5.3 Mouse models to address GC effects

DSS colitis is now one of the most used murine models of colon inflammation. It allowed a better understanding of colitis and the pathways that play a key role in its development such as the GR and immune cells.

Meers and colleagues demonstrated that the GR in myeloid cells is essential in the resolution of DSS colitis. Mice lacking the receptor failed to recover from DSS-induced colitis and the expression of pro-inflammatory cytokines in mutant mice was higher (Meers et al., 2018).

Zhang and colleagues investigated the role of GC administration in DSS colitis. They observed that Dex treatment of mice exacerbated colitis severity and potentiated the immune response. Mammalian target of rapamycin (mTOR) was upregulated in IECs during the inflammation, and its deletion was associated with an amelioration of the disease caused by Dex, suggesting that mTOR in IECs plays a role in the exacerbation of DSS-induced colitis by Dex and modulates the immune response in the first stages of the disease (Zhang et al., 2020).

Similarly, Ocón and colleagues demonstrated that the treatment with budesonide in DSS-treated mice has both protective and deleterious effects on colitis. GCs caused anti-inflammatory effects during DSS colitis but an aggravation of the disease such as an increased weight loss, rectal bleeding, an increased deterioration of animal status, bacterial translocation, and endotoxemia was observed simultaneously during the treatment (Ocón et al., 2016).

Introduction

Due to the pleiotropic role of GCs and the GR in the development of colitis and the regulation of the immune response, a lot of aspects remain to be elucidated. The role that GCs play in the clinic for the treatment of IBD is noteworthy, however, a better understanding of the underlying mechanisms and target cells through which GCs exert their function will help to reduce side effects and empower the beneficial effects. To this end, several murine models with cell type-specific deletions of the GR (S. D. Reichardt et al., 2012) or function modifications of the GR were employed to better understand its mechanism of action in immunity and disease (H. M. Reichardt et al., 1998).

The mouse strain $GR^{villinCreERT2}$ is characterized by an inducible knock-out of the GR in IECs and allows the study of the role of the GR in this specific cell type which is essential for maintaining gut homeostasis. Induction of colitis in $GR^{VillinCreERT2}$ mice permits a better understating of the role of endogenous GCs in both UC and cancer development. Another mouse strain which allows a better understanding of the GR's role in inflammatory disease is GR^{dim} mice, which are characterized by a point mutation that impairs dimerization of the GR. In this case, the mouse strain allows an insight into the role of GR gene regulation and a better understanding of how GR dimers affect gene expression.

1.6 Objectives

UC is a multifactorial chronic disease that severely affects the quality of life of afflicted persons. Moreover, patients have an increased risk to develop CACRC and its development is associated with the duration and extent of the inflammatory state. Several drugs are used for its treatment, but GCs remain the gold-standard thanks to their easy use for patients and their low costs. Unfortunately, GCs are associated with severe side effects which affect the whole body. Although different GC formulations and applications were developed to reduce them, many steps forwards must still be done for a better understating of GC action and mechanism eventually leading to a reduction of the side effects.

A better understanding of the role of endogenous GCs in inflammation and cancer development is therefore essential for the development of effective GC formulations with fewer adverse effects. *In vivo* experiments which mimic colitis and subsequent tumor progression in different mouse models outlined in this thesis allow us to study the mechanism of endogenous GCs and the role of the GR in this disease and help to bring new perspectives for GC treatment.

It is also important to keep in mind that due to their pleiotropic effects, GCs can both attenuate or aggravate the inflammatory response, so we investigated the role of GR dimerization in both UC and cancer progression. IECs are key players in the control of intestinal inflammation but the role of the GR in these cells has not been elucidated yet. In this thesis we investigated how GR affects DSS-induced colitis and cancer development with the goal to answer the following questions:

- Does impaired GR dimerization in GR^{dim} mice influence the disease severity of DSS-induced colitis?
- Does impaired GR dimerization in GR^{dim} mice impact the development of CACRC?
- Does GR deficiency in IECs in $GR^{villinCreERT2}$ mice alter UC development in the model of DSS-induced colitis?

2. Materials and Methods

2.1 Materials

2.1.1 Instruments

If not specifically declared, the supplier is located in Germany.

Table 1: Instruments

Equipment	Supplier
Akku-jet® pro-pipette controller	Brand GmbH, Wertheim
Axio Scope A1	Zeiss, Jena
Axio Scope Aplus	Zeiss, Jena
BD FACS Canto II	BD Biosciences, Heidelberg
BioTek® Power Wave 340 Plate Reader	BioTek Instruments, Wetzlar
Centrifuge 2-5	Sigma Laborzentrifugen, Osterode
Centrifuge 5417R	Eppendorf, Hamburg
Centrifuge 5804-R	Eppendorf, Hamburg
Coloscope	Karl Storz, Tuttlingen, Germany
EasyPet 3	Eppendorf, Hamburg
Electrophoresis power supply 301	Amersham Biosciences, Freiburg
Fluidigm BioMark™	Life Technologies Corporation, South San Francisco, California, USA
Freezer Hera freeze -80 ºC	Heraeus, Hanau
Freezer Liebherr Comfort -20 ºC	Liebherr-International Deutschland GmbH, Biberach an der Riss
Freezer VIP plus -150 ºC	SANYO Electric Co., Ltd, Moriguchi, Osaka, Japan
IFC Controller MX	Life Technologies Corporation, South San Francisco, California, USA
Incubator, HERACell 240	Heraeus, Hanau

Laminar airflow cabinet, HERASafe	Heraeus, Hanau
Microscope Primo Star	Zeiss, Jena
Microscope Telaval 31	Zeiss, Jena
Microtom SM2000R	Leica Biosystems, Wetzlar
Microwave R-212	Sharp, Osaka, Japan
Multichannel pipette S-12, 20-200 µl	Brandt, Wertheim
Nanodrop 2000	Peqlab Biotechnology, Erlangen
Neubauer improved haemocytometer	Henneberg-Sander GmbH, Giessen-Lützellinden
Nunc™ Immuno Wash 12	Thermo Fisher Scientific, Wilmington, DE, USA
Pipettes Eppendorf Research plus 2.5 µl, 20 µl, 200 µl, 1000 µl	Eppendorf, Hamburg
Real-Time PCR System 7500	Applied Biosystems, Foster City, CA, USA
Rotilabo® mini-centrifuge	Carl Roth GmbH & Co.KG, Karlsruhe
Scale Acculab ALC-3100.2	Sartorius, Göttingen
Scale TE313S	Sartorius, Göttingen
Shaker GFL 3006/3005	Gesellschaft für Labortechnik, Burgwedel
Thermocycler Mastercycler EP Gradient	Eppendorf, Hamburg
Thermomixer Comfort	Eppendorf, Hamburg
Tissue Homogenizer Ultra Turrax T18 Basic	IKA, Staufen
Tissue Processor Excelsior ES	Thermo Fisher Scientific, Wilmingon, DE, USA
Tissue Tek Prisma Slide Stainer	Sakura Finetek. Staufen
UV System with camera, Gel Imager (Chemostar)	INTAS, Science Imaging Instruments GmbH, Göttingen
Vortex Genie-2	Scientific Industries, Bohemia, New York, USA
Water bath W12	Labortechnik Medingen, Dresden
Water Purification System Arium Pro	Sartorius, Göttingen

2.1.2 Consumables

Table 2: Consumables

Consumable	Supplier
BD Falcon 5 ml Polystyrene tubes with Cell-strainer Cap	BD Biosciences, Heidelberg
BD Micro-Fine + Demi U-100 Insulin Syringes (0.3 ml, 30G)	BD Biosciences, Heidelberg
BD Microlance™ 3 (20G 1.5)	BD Biosciences, Heidelberg
BD Microtainer® SST™ tubes	BD Biosciences, Heidelberg
Black 96-Well Immuno Plates	
Cellstar Culture Plates (6-well, 24-well)	Greiner bio-one GmbH, Frickenhausen
CELLSTAR PS Cell Culture dishes 10 cm	Greiner bio-one GmbH, Frickenhausen
CELLSTAR Culture Flasks 175 cm^2	Greiner bio-one GmbH, Frickenhausen
CELLSTAR serological pipettes (5 ml, 10 ml, 25 ml)	Greiner bio-one GmbH, Frickenhausen
CryoTube™ Vials	Nunc, Rosklide, Denmark
EASYstrainer™ (40 µm, 100 µm)	Greiner bio-one GmbH, Frickenhausen
Falcon 5 ml Polystyrene tubes, round-bottom, non-sterile	Th. Geyer GmbH & Co. KG, Renningen
Falcon tubes (15 ml, 50 ml)	Greiner bio-one GmbH, Frickenhausen
Fluidigm 48.48 Dynamic Array™ IFC	Life Technologies Corporation, South San Francisco, California, USA
Fluidigm Control line fluid	Life Technologies Corporation, South San Francisco, California, USA
Hypodermic needle Sterican® 26G × 0.5, 24G × 1	B Braun, Melsungen
MacrOflow Tissue cassettes	Th, Geyer GmbH & Co. KG, Renningen
Microscope Cover Slips, 24 × 60 mm	Menzel-Gläser, Braunschweig
Microscope Slides SuperFrost Plus	Menzel-Gläser, Braunschweig

Multiply® Pro 8-Strip PCR Microtubes	Sarstedt, Nümbrecht
Nitril® Next Gen® single-use gloves	Meditrade, Kiefersfelden
Nunc-Immuno™ Microwell™ 96 well plates	eBioScience, San Diego, USA
Optical Adhesive Covers	Applied Biosystems, Foster city, USA
Parafilm	Bemis, Neeth, WI, USA
Pasteur pipette	The Gayer GmbH & Co. KG, Renningen
Pipette tips (10 µl, 200 µl, 1000 µl)	Greiner bio-one GmbH, Frickenhausen
PP tubes sterile 14 ml	Greiner bio-one GmbH, Frickenhausen
Reaction tubes, PP natural (1.5 ml, 2 ml)	Greiner bio-one GmbH, Frickenhausen
Saphire Microplate, 96 well for qPCR	Greiner bio-one GmbH, Frickenhausen
Syringe BD Discardit™ II (2 ml, 5 ml)	BD Biosciences, Heidelberg
V-Bottom Plate 96 Well	Thermo Fisher Scientific, Waltham, USA

2.1.3 Reagents and Chemicals

Table 3: Reagents and chemicals

Reagent and Chemical	Supplier
Assay Loading Reagent 2 ×	Life Technologies Corporation, South San Francisco, California, USA
Azoxymethane (AOM)	Sigma-Aldrich, Taufkirchen, Germany
BD FACS Clean solution	BD Biosciences, Heidelberg
BD FACS Flow Sheath fluid	BD Biosciences, Heidelberg
BD FACS Shutdown solution	BD Biosciences, Heidelberg
Bovine serum albumin	Carl Roth GmbH & Co.KG, Karlsruhe
Chloroform	Sigma-Aldrich Chemie GmbH, Taufkirchen
Citric acid	Carl Roth GmbH & Co.KG, Karlsruhe
Dimethylsulfoxid 99.8%	Carl Roth GmbH & Co.KG, Karlsruhe
Dithiothreitol	Sigma-Aldrich Chemie GmbH, Taufkirchen
DNA Binding Dye 20 ×	Life Technologies Corporation, South San Francisco, California, USA
DSS (Dextran sulfate sodium salt 50 kDa)	Sigma-Aldrich Chemie GmbH, Taufkirchen
dNTP Mix PCR	Genaxxon Biosciences, Ulm, Germany
Eosin G	Merck, Darmstadt
Ethanol 99.8%	Carl Roth GmbH & Co.KG, Karlsruhe, Chemsolute® Th. Geyer GmbH & Co. KG, Renningen
Ethidiumbromide solution	Carl Roth GmbH & Co.KG, Karlsruhe
Evans Blue	Sigma-Aldrich Chemie GmbH, Taufkirchen
Exonuclease I Reaction Buffer 10 ×	NEW ENGLAND, BioLabs®, UK
F-518 Phusion® HF buffer with 7.5 mM magnesiumchlorid	Thermo Fischer Scientific, Waltham, USA

Fetal calf serum	Abbvie, Ludwigshafen
FITC-Dextran 4kDa	Sigma-Aldrich Chemie GmbH, Taufkirchen
Formamid ≥99.5%	Carl Roth GmbH & Co.KG, Karlsruhe
Gene Ruler 1kb DNA ladder	Thermo Fischer Scientific, Waltham, USA
Gibco® 2-Mercaptoethanol	Thermo Fischer Scientific, Waltham, USA
Gibco® RPMI1640 + GlutaMAX™	Thermo Fischer Scientific, Waltham, USA
Glycerol	Carl Roth GmbH & Co.KG, Karlsruhe
Guaiac resin	Carl Roth GmbH & Co.KG, Karlsruhe
Hydrogen Peroxide 30%	Carl Roth GmbH & Co.KG, Karlsruhe
Neomycin trisulfate salt hydrate	Sigma-Aldrich Chemie GmbH, Taufkirchen
Nucleoside triphosphate	Genaxxon bioscience, Ulm
OptiLyse® B Lysing solution	Beckman Coulter, Inc., France
Orange G sodium salt	Sigma-Aldrich Chemie GmbH, Taufkirchen
Paraffin wax	Sigma-Aldrich Chemie GmbH, Taufkirchen
Paraformaldehyde, 4%	Carl Roth GmbH & Co.KG, Karlsruhe
PegGOLD Universal Agarose	Peqlab Biotechnology GmbH, Erlangen
Penicillin/Streptomycin (10.000 U/ml)	Invitrogen, Carlsbad, CA, USA
Potassium chloride	Merck KGaA, Darmstadt
Potassium dihydrogen phosphate	Merck KgaA, Darmstadt
Power SYBR® Green Master mix	Applied Biosystems, Foster City, USA
QIAzol™ Lysis buffer	Qiagen, Hilden
Roti®-Histofix 4%	Carl Roth GmbH & Co.KG, Karlsruhe

Sodium carbonate	Merck KgaA, Darmstadt
Sodium chloride, 99.5%	Carl Roth GmbH & Co.KG, Karlsruhe
Sodium hydrogen carbonate	Merck KgaA, Darmstadt
SsoFast EvaGreen Supermix with low ROX 2 ×	Bio-Rad Laboratories GmbH, Munich
Sulfuric acid, 95-98%	Merck KgaA, Darmstadt
Tamoxifen Free Base	Sigma-Aldrich, Taufkirchen, Germany
TaqMan® PerAmp Master mix 2 ×	Applied Biosystems, Foster City, USA
Tween® 20%	Carl Roth GmbH & Co.KG, Karlsruhe
Sevofluran	AbbVie Deutschland GmbH, Ludwigshafen, Germany

2.1.4 Buffers and Solutions

Table 4: Buffers and Solutions

Buffer	Component
Agarose-gel	1% Agarose in TAE-buffer
DNA Suspension buffer	10 mM Tris 0.1 mM EDTA in ddH2O, pH 8.0
DSS solution 1.2%	12g DSS in 1 liter of H_2O
DSS solution 3.5%	35g DSS in 1 liter of H_2O
ELISA Assay diluent	10 % FCS in PBS
ELISA Coating buffer	1000 ml ddH2O 8.4 g NaHCO3 3.56 g Na2CO3, pH 9.5
ELISA Developing solution	ELISA Substrate buffer 1 % TMB in DMSO 0.2 % H2O2
ELISA Stop solution	1 M H2SO4 in ddH2O
ELISA Substrate buffer	0.1 M Citric acid

	0.2 M Na2HPO4 in ddH2O
ELISA Washing buffer	0.05 % Tween® 20 % in PBS
FACS buffer	1.7 % BSA 0.01 % Sodium azide in PBS, pH 7.2
Orange G Loading dye	100 ml ddH2O 100 mg Orange G sodium salt 30 % Glycerol
Phosphate saline buffer (PBS)	137 mM NaCl 2.7 mM KCl 10 µM Na2HPO4 2 mM KH2PO4 in ddH2O
TAC buffer	20 mM Tris 155 mM NH4Cl in ddH2O
TAE buffer	40 mM Tris 20 mM Acetic acid 1 mM EDTA in ddH2O

2.1.5 Commercial Kit

Table 5: Commercial Kit

Commercial kit	Manufacture
Biolegnd LEGENDplex™ multiplex assay	BioLegend, San Diego, USA
Dynabeads mRNA DIRECT Kit	Thermo Fischer Scientific, Waltham, USA
ELISA MAX™ Standard set mouse IL-6	BioLegend, San Diego, USA
iScript™ cDNA Synthesis kit	Bio-Rad Laboratories GmbH, Munich
Qiagen Rneasy Plus Universal Mini kit	Qiagen, Hilden
Quick-RNA™ MiniPrep	Zymo Research Epigenetics, Irvine, USA

2.1.6 Enzymes

Table 6: Enzymes

Enzyme	Supplier
Collagenase type 1-A (25 mg/ml)	Sigma-Aldrich Chemie GmbH, Taufkirchen
Collagenase type II (25 mg/ml)	Sigma-Aldrich Chemie GmbH, Taufkirchen
DNase I recombinant, RNase-free (10.000 U/ml)	Merck KGaA, Darmstadt
PfuS DNA Polymerase	Own Production

2.1.7 Media and supplement

Table 7: Media

Media	Supplier
Gibco® RPMI1640 + GlutaMAXTM 1 x	ThermoFischer Scientific, Waltham, USA
Gibco® Advanced DMEM/F-12	ThermoFischer Scientific, Waltham, USA
Matrigel Matrix	Corning, Glendale, AZ, USA
Noggin Conditioned Medium	Own production
Rspo1 Conditioned Medium	Own production
Wnt-3A Conditioned Medium	Own production

Table 8: Supplemented media

Supplemented medium	Component
RPMI++	RPMI1640, 10 % FCS, 1 % Penicillin/ Streptomycin
Advanced DMEM/F-12+++	Advanced DMEM/F-12 5 ml Glutamax 5ml Hepes 5ml Penicillin/ Streptomycin
Organoids medium	See table 9

Table 9: Organoids medium composition

Media and supplements (Volume for 50 ml)	**Supplier**
Advanced DMEM/F-12+++ (7.7 mL)	ThermoFischer Scientific, Waltham, USA
Noggin Conditioned Medium (10 ml)	Own production
Rspo1 Conditioned Medium (5 ml)	Own production
Wnt-3A Conditioned Medium (25 ml)	Own production
N2 100x (500 µl)	Thermo Fisher Scientific, Wilmington, DE, USA
B27 50x (1ml)	Thermo Fisher Scientific, Wilmington, DE, USA
N-Acetylcysteine (50 µl)	Sigma-Aldrich Chemie GmbH, Taufkirchen
ROCK inhibitor 3.4mg/ml (50 µl)	Sigma-Aldrich Chemie GmbH, Taufkirchen
CHIR 33021 5mM (50 µl)	Axon Medchem Groningen Netherlands
A83-01 10mM (2.5 µl)	Sigma-Aldrich Chemie GmbH, Taufkirchen
Nicotinamide 1M (500 µl)	Sigma-Aldrich Chemie GmbH, Taufkirchen
rmEGF 500ug/ml (20 µl)	ImmunoTools GmbH, Friesoythe

2.1.8 Antibodies

Table 10: Antibodies

Antibody	Clone name	Supplier
APC/cy7 anti-mouse Ly-6C	HK1.4	BioLegend
APC anti-mouse Ly-6G	1A8	BioLegend
APC Rat IgG2a κ Isotype Ctrl	RTK2758	BioLegend
APC anti-mouse CD326 (Ep-cam)	G8.8	BioLegend
PE-Cy7 anti-mouse CD11b	M1/70	BD Biosciences,
Trustain FcX (anti-mouse CD16/32)	93	BioLegend

2.1.9 Oligonucleotides

Table 11: Oligonucleotides

Gene	Sequences (5'—3') Forward / Reverse	Accession number
16s rRNA	AGAGTTTGATCCTGGCTCAG AAGGAGGTGATCCAACC	
Arg1	AGCCCGAGCACATGCAGCAG ACCCCTCCTCGAGGCTGTCCT	NM_007482.3
Arg2	AGGTGGCATCCCAACCTGGAGAG AGCCACTTTGGCAGTCTTCA	NM_009705.3
Ccl2	GACCTTAGGGCAGATGCAGT AGCTGTAGTTTTTGTCACCAAGC	NM_011333.3
Ccl3	TCAGGAAAATGACACCTGGCTG ATATGGAGCTGACACCCCGA	NM_011337.2
Ccl5	CGACTGCAAGATTGGAGCAC CTCACCATATGGCTCGGACA	NM_013653.3
Ccl7	CTCGACCCACTTCTGATGGG CCCTGGGAAGCTGTTATCTTCAA	NM_013654.3
Claudin 2	TGTCTCTGGCAAGCTGACTT ACGGCTCCGTTTTCTAGATGC	NM_001193659.1
Cx3cr1	TCGCCCAAATAACAGGCC TGTCCACCTCCTTCCCTGAA	NM_009987.4

Cxcl1	CTCCGTTACTTGGGGACACC ACCGAAGTCATAGCCACACTC	NM_008176.3
Cxcl2	CAGGTACGATCCAGGCTTCC TGAACAAAGGCAAGGCTAACTG	NM_009140.2
Cxcl5	AGCTTTCTTTTTGTCACTGCCC TGCCCTACGGTGGAAGTCAT	NM_009141.3
Cxcl10	TCACTCCAGTTAAGGAGCCC CCACGTGTTGAGATCATTCC	NM_021274.2
Cxcr2	CTTAATCCTGCAGTAGTAGTTCTACGA CTTCCAGTTCAACCAGCCCT	NM_009909.3
Cxcr3	AGCAGTAGGCCATGACCAGAAG AATGCCACCCATTGCCAGTAC	NM_009910.3
Egf	AGCATACTCAGCGTCACAGC GCAGGACCGGCACAAGTC	NM_010113.4
Ep-4	GCTTGACAAGTTCCGCACTG GCTCAGGCCTCAGATGTTCA	NM_001136079.2
Hif-1α	GAATATGGCCCGTGCAGTGA CACAGAAATGGCCCAGTGAGA	NM_001313919.1
Hprt	GGGACGCAGCAACTGACATT GTCCTGTGGCCATCTGCCTA	NM_013556.2
Il1b	AAGCAGCCCTTCATCTTTTG CTCATCTGGGATCCTCTCCA	NM_008361.4
Il6	CAGAATTGCCATTGCACAAC AGTTGCCTTCTTGGGACTGA	NM_031168.2
Il10	CGGGAGAAATCGATGACAGCGCC AGGCAGAGAAGCATGGCCCAG	NM_010548.2
Mlck	CTCCTTGTTCTCCTCCGGGC TTCCAGAATTCCAAGGTGGCTG	NM_139300.3
Mmp9	AATGGCCTTTAGTGTCTGGCT GGTCTTCCCCAAAGACCTGAAA	NM_013599.5
Mmp13	TGGTCCAGGCGATGAAGA TGCAGGCGCCAGAAGAAT	NM_008607.2
Occludin	AAGATAAGCGAACCTGGCCG GTCCTCCTGGCTCAGTTGAA	NM_008756.2
Oct	TGCTGCAAAATTCGGGATGC TGCTGCAAAATTCGGGATGC	NM_008769.4
Ptgs2	GATACACCTCTCCACCAATGACC CAGACAACATAAACTGCGCCTT	NM_011198.4
Tlr2	CATCCTCTGAGATTTGACGCTTT CTGGAGCATCCGAATTGCA	NM_011905.3
Tlr4	TAGGAACTACCTCTATGCAGGG TGGTTGCAGAAAATGCCAGG	NM_021297.3
Tnf-α	CTTGGTGGTTTGCTACGACG ATGGCCTCCCTCTCATCAGT	NM_013693.3

Tnfr2	TGGGTTTTCAAGGCGGCAGTA ACCACTGACCAGGTGGAGAT	NM_011610.3
Vegf	AAAGGCTTCAGTGTGGTCTG GGTTGGAACCGGCATCTTTA	NM_001287056.1
Ym1	AATGATTCCTGCTCCTGTGG ACTTTGATGGCCTCAACCTG	NM_009892.3

2.1.10 Software

Table 12: Software

Software	Company
7500 System SDS software version 1.4.0.25	Applied Biosystems, Foster City, CA, USA
BD FACS Diva™ software version 6.1.2	BD Biosciences, Heidelberg
BioMark™ Data collection software	Life Technologies Corporation, South San Francisco, CA, USA
BioMark™ Real-Time PCR analysis software	Life Technologies Corporation, South San Francisco, CA, USA
BioTek® Gen 5 version 1.09.8	BioTek Instruments, Bad Friedrichshall
FlowJo version 10 and 7.6.5	Tree Star, Inc., Ashland, USA
GraphPad Prism 5	GraphPad Software, La Jolla, CA, USA
ImageJ 1.52n	Wayne Rasband Nat. Inst. Of Health, USA
The LEGENDplex™ Data Analysis Software Suite	Biolegend, San Diego, CA, USA
Nanodrop 2000	Thermo Scientific, Wilmington, WA, USA
Office Suite For Windows	Microsoft Corporation, Redmond, WA, USA

2.1.11 Cell lines

Table 13: Cell lines

Cell line	Supplier
HEK293T Rspondin1-Fc	kindly provided by Schulz-Heddergott Group
HEK293T Noggin-Fc	kindly provided by Schulz-Heddergott Group
HEK293T Wnt3a	kindly provided by Schulz-Heddergott Group

2.2 Methods

2.2.1 Animal experimentation

All experiments were performed according to the German animal welfare act and approved by the responsible authority of Lower Saxony (*Niedersächsisches Landesamt für Verbraucherschutz und Lebensmittelsicherheit*). Mice were housed in individually ventilated cages under specific-pathogen-free conditions (SPF) in a 12-hrs. light/dark cycle at the animal facility of the University Medical Center of Göttingen (ZTE). Food and water were supplied *ad libitum*.

2.2.1.1 Mouse strains

Two different mouse strains were used for the DSS-induced colitis model and the AOM/DSS model of colitis-associated cancer: the GR^{dim} mice which provide a model for a modified GR and the $GR^{villinCreERT2}$ which lack of GR within IECs. GR^{dim} mice ($Nr3C1^{tm3GSc}$) with a BALB/c background are characterized by a single point mutation in the DBD region of the GR gene. The mutation was inserted by homologous recombination of murine embryonic stem cells (Reichardt et al., 1998). Due to the replace of alanine with threonine (A458T) in the D-loop of the second Zinc-finger the dimerization of the GR is impaired, the mutation is present in both somatic and germ cells of the mice. $GR^{villinCreERT2}$ (Tg (Vil1-cre/ERT2)23Syr) mice and GR^{flox} ($Nr3C1^{tm2GSc}$) on a C57BBl/6 background were intercrossed to receive GR^{villin} mice (Nr3c1tm2GSc;Tg(Vil1-cre/ERT2)23Syr) and GR^{flox}. The mouse model

is an inducible knock out mouse strain that allows the specific deletion of the GR in the IECs through a Tamoxfien-inducible Cre/loxP recombination (Tronche et al., 1999). The Cre recombinase under the Villin promoter allow a specific deletion of the GR only in the IECs since villin is mainly expressed in these cells. Only female mice were used at the age of 10 to 12 weeks.

2.2.1.2 Induction of recombination by tamoxifen treatment

Before the start of the experiment, $GR^{villinCreERT2}$ mice and GR^{flox}, were treated with tamoxifen. Tamoxifen powder was dissolved in ethanol 70 % and warmed to 37 °C in a 1:30 ratio in sunflower seed oil. A dosage of 150 µl tamoxifen-oil solution at a concentration of 20 mg/ml was administered to each mouse by oral gavage at day eleven, nine and seven before the start of the experiment.

2.2.1.3 Induction of DSS-induced colitis

GR^{villin} and GR^{flox} mice were treated with (DSS) at a concentration of 1.2 % via drinking water for 8 days. The DSS solution was changed every other day. During a subsequent recovery time, mice received tap water until day 10. Control mice received only tap water. All mice were evaluated with a clinical score daily, starting on the third day of treatment.

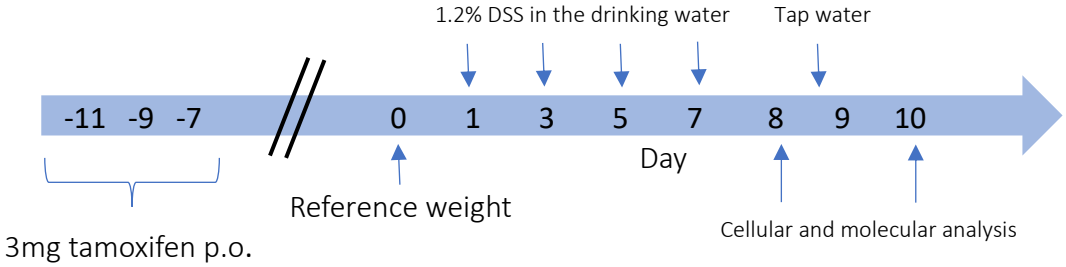

2.2.1.4 Induction of AOM/DSS tumorigenesis

GR^{dim} and GR^{wt} mice were treated with 10-mg/kg AOM intraperitoneally, treated with DSS via the drinking water at a concentration of 3.5% for 8 days and then tap water was administrated. Clinical symptoms of the colitis were evaluated until day 12, and tumor development was monitored by colonoscopy. All mice were evaluated with a clinical score daily, starting on the third day of treatment. Control mice received AOM injection and tap water. Mice were sacrificed at day 8, 12 or after 9 weeks circa, when the tumors were developed (Muzzi et al. 2021).

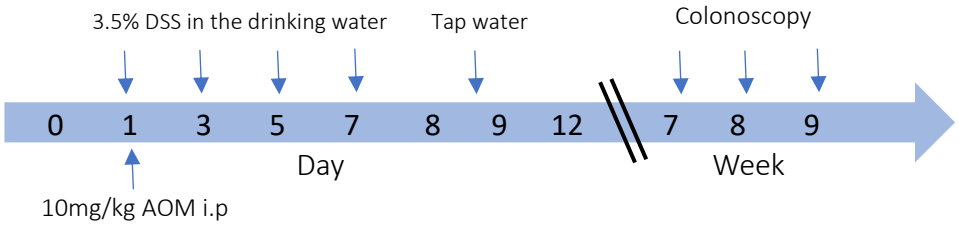

2.2.1.5 Disease assessment

In order to evaluate severity of the colitis and check the health of the animal, mice were scored every day from day 3 of the DSS treatment. Mice were weighed and evaluated for clinical symptoms as rectal bleeding and stool consistency. The disease activity index (DAI) was calculated as sum of the weight loss and clinical symptoms on a scale from 0 to 10.

Weight loss was scored:

- 0 = 0–1%
- 1 = 1–5%
- 2 = 5–10%
- 3 = 10–15%
- 4 = >15%

The stools were evaluated for consistency:

- 0 = normal
- 1 = soft
- 2 = diarrhea

Intestinal bleeding was evaluated:

- 0 = negative hemoccult
- 1 = green hemoccult
- 2 = blue hemoccult
- 3 = blood visible
- 4 = rectal bleeding

Animals that died or had to be sacrificed for ethical reasons were assigned a score of 12 (Meers et al., 2018).

2.2.1.6 Anesthesia

To perform the colonoscopy, all mice were anesthetized with volatile Sevoflurane. A special sealed box was used, and the Sevoflurane was administrated in addition to the oxygen flow with the help of a vaporizer. After a pre-anesthesia performed at a dosage of 5% Vol, the mouse was transferred into the colonoscopy station and the Sevoflurane was administered through a snout mask at 2.5% Vol during colonoscopy.

2.2.1.7 Colonoscopy

Colonoscopy was performed in order to monitor the tumor growth between week 6 and 9 after AOM injection and DSS treatment to check the health of the mouse and to find the time point at which the mice had sufficiently grown tumors. The mouse was fastened on its back and its snout remained in the anesthesia mask. The colonoscope measures are 10 cm in length, 1.9 mm in diameter. The colonoscope was moisturized with H_2O. A continuous air flow allowed the complete view of the colon mucosa. The colonoscopy allows the complete check of the whole descending colon up to the left flexure. The tumors were scored by their size (S1-S5) as shown below (Becker et al., 2006).

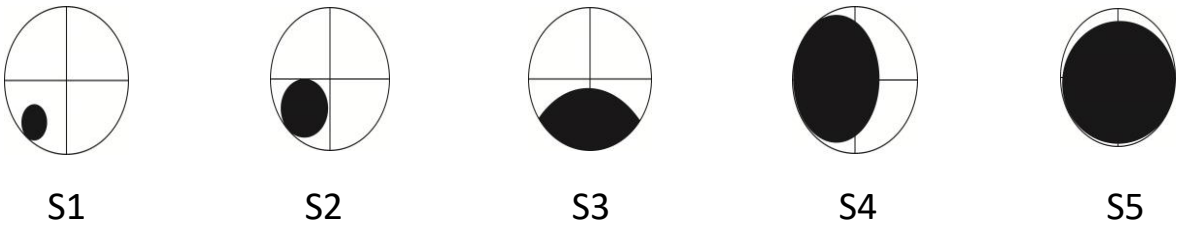

- S1 = less than one quadrant of the colon´s circumference was affected
- S2 = tumors fill a whole quadrant
- S3 = tumors occupy two quadrants
- S4 = tumors fill three or more quadrants
- S5 = tumors occlude the most of the colon

Mice were sacrificed when tumor growth occludes the colon (S3-S4).

2.2.1.8 Isolation of IECs and LPCs

Mice were sacrificed by CO_2 inhalation. The colon was removed, measured in length, and washed with ice-cold PBS to remove contents, then it was opened longitudinally and placed in a 6-well containing PBS + 60 mM EDTA + 3 mM DTT for 1 hr. on ice. After 1 hr. the tissue was transferred into a 50 ml tube filled with 30 ml PBS and shaken vigorously for 1 min twice, a third shaking step was performed with 10 ml, and between each shaking the PBS was filtered through a 40 µm cell strainer into a new 50ml tube. The tube containing the filtered PBS was centrifuged at 300 x g for 7 min and the supernatant was discarded. The IECs pellet was resuspended in 300 µl of PBS, cells were counted and the purity of the IECs was checked by FACS analysis. Cells were stored at -20°C for further analysis.

After IECs isolation, the colon was transferred into a 50 ml falcon containing 5 ml RPMI++ media to eliminate EDTA. Then the colon tissues were cut into small pieces, and then digested with recombinant 500 U DNase I, 4 mg collagenase type II and 4 mg collagenase type 1-A at 37°C for 30 min and samples were vortexed every 10 min. Digested samples were passed through a 40 µm cell strainer, mincing the tissue with the help of a syringe plunge. Then tube was filled with RPMI++ to a total volume of 30 ml and centrifuged at 300 x g for 7 min. The supernatant was removed and the isolated LPCs were used for FACS analysis and stored at -20 for further experiments.

2.2.1.9 Isolation of the colon

Mice were sacrificed by CO2 inhalation and the colon was then removed, measured in length, and washed with cold PBS to remove remaining feces. The colon was prepared for further analysis as gene expression analysis, cytokine quantification via Biolegend LEGENDplex™ Multiplex Assay or histological evaluation.

2.2.1.10 Isolation of the mesenteric lymph nodes

Mice were sacrificed by CO_2 inhalation; the mesenteric lymph nodes were removed from the tissue between the layers of the intestine. The tissue was then frozen at -80°C and used for RT-qPCR.

2.2.1.11 Colon supernatant preparation

For the measurement of the cytokines expression in the colon tissue, after the colon isolation, small pieces of the colon were weighted and then placed into 24-well plates containing 500 µl of RPMI++ media and incubated at 37°C for 24 hrs. After incubation, the tissue was removed from the well. The media was then frozen at -20°C and used for further analysis.

2.2.1.12 Murine colonic organoids preparation

Murine organoids were isolated from the colon. The colon was isolated and washed as described above, then opened lengthwise and the mucus was removed using a tissue. Normal mucosa and tumors were harvested and cut into small pieces. Mucosa and tumors pieces were transferred in two 50 ml falcons each containing 15 ml PBS. A Pasteur pipette was used to pipette the pieces up and down (approx. 10 times) in order to clean the colon, when the colon pieces were settled down, the PBS was removed and the step was repeated at least 3 times, or until the supernatant was clear. 5 ml of 4 mM EDTA in PBS were added to the mucosa tissues and incubated 30 min at 4°C on a roller while tumor tissues were incubated at 37°C with 2mg/ml of collagenase in washing medium. After the incubation time the EDTA was removed from the mucosa tissues and 10 ml PBS were added. The samples were pipetted vigorously several time to isolate the crypts. If the crypts concentration was good the PBS with the crypts was then transferred into a new tube using a 100 µm cell strainer. The step was repeated until the lower number of crypts was isolated. The batch with a good number of crypts and less debris was used for organoids. Tumor tissues, after the incubation, were pipetted up and down to isolate the crypts and the suspension was transferred into a new 50 ml falcon using a 100 um cells strainer. Up to 50 ml

PBS was added to both mucosa and tumor suspensions and centrifuged at 800 x g for 5 min at 4°C with no brake. The supernatant was removed, and 10 ml of washing medium were added, the pellets were resuspended and then centrifuged again. The supernatants were aspirated completely, and the tubes were placed on ice. The crypts were then resuspended in Matrigel. 200 µl of Matrigel was pipetted in 10 drops per well in a 6 well plate and incubated at 37°c for at least 15 min. Once the Matrigel was solid, 2 ml of organoids medium was added to each well. The method was adapted for Balb/c mice from the paper of Klemkle et al. (Klemke et al., 2021).

2.2.1.13 Serum preparation

Blood samples were used to collect serum. Blood was collected by cardiac puncture and left in BD Microtainer SST tubes for coagulation for 30 min. Tubes were centrifuged at 14,000 × g for 2 min. The serum was collected and stored at -20 ºC.

2.2.2 Molecular Biology analysis

2.2.2.1 RNA isolation from cells

Isolation of RNA from cells was performed using the Quick-RNA™ MiniPrep following the manufacturer's protocol. RNA lysis Buffer was added directly to the cells and mixed. The mixture was centrifuged at 10,000 x g for 1 min and the supernatant was transferred into a Spin-Away™ filter in a collection tube. The tube was centrifuged again at 10,000 x g for 1 min. The flow-through was mixed with ethanol and transferred into a Zymo-Spin™ IICG Column in a collection tube and centrifuged for 30 sec. 400 µl of RNA Prep Buffer were added to the column and centrifuged, the flow trough was discarded, and the column was washed with 700 µl RNA wash Buffer and centrifuged. 400 µl of RNA wash Buffer were added to the column and then centrifuged for 2 min at 10,000 x g to ensure the complete removal of the wash buffer. The column was then transferred into a new RNase-free tube and 50 µl of RNase free water were added directly to the column and centrifuged for 30 sec a 10,000 x g. The concentration of the eluted RNA was measured using a Nanodrop, and the integrity was checked with an electrophoresis in a 1% agarose gel

containing ethidium bromide, the gel was then placed under the UV light and if the two bands were visible (28S and 18S rRNA) with a 1:2 ratio the RNA was considered undamaged. The RNA was then stored at -20°C.

2.2.2.2 RNA isolation from tissue

RNA extraction from tissues was performed using the Qiagen RNeasy® Plus Universal Kit. Frozen tissue samples were transferred in a 14 ml sterile tube, 900 µl of QIAzol™ were added and then the tissue was homogenized with the Tissue Homogenizer Ultra Turrax T18 and transferred in a new tube. Samples were mixed with 100 µl of gDNA eliminator and vortexed for 15 sec, then 180 µl of chloroform were also added to the samples, vortexed for 15 sec and then samples were left at RT for 3 min. Samples were centrifuged at maximum speed (14,000 rpm) for 15 min at 4°C. After the centrifugation the upper phase (around 600 µl) was transferred into a new tube and mixed with 600 µl of 70 % ethanol. The mixture was transferred into the RNeasy-Mini columns. Samples were centrifuged at 14,000 rpm for 20 sec at RT and the flow-through was discarded. 700 µl RWT buffer were added to the columns, centrifuged at 10,000 rpm for 20 sec and the flow-through was discarded. Then 500 µl of RPE buffer were added, and the samples were centrifuged at 10,000 rpm for 2 min. The collection tubes were changed with a new one and the columns were centrifuged at 10,000 rpm for 1 min. Columns were placed in a new tube and 35 µl RNase-free water were added to the columns to elute the RNA and centrifugated at 10,000 rpm for 1 min, the last step was repeated twice.

The concentration of the RNA was measured using a Nanodrop, and the integrity was checked with an electrophoresis in a 1% agarose gel containing ethidium bromide, the gel was then placed under the UV light and if the two bands were visible (28S and 18S rRNA) with a 1:2 ratio the RNA was considered undamaged. The RNA was then stored at -20°C.

2.2.2.3 PolyA-mRNA purification

The DSS treatment is known to inhibit real-time polymerase chain reaction (PCR) amplification, so before the cDNA synthesis the PolyA-mRNA must be purified from total RNA (Kerr et al., 2012). The Dynabeads mRNA DIRECT Kit was used. 100 µl of dynabeads were transferred in a microcentrifuge tube and then placed on the magnet until all dynabeads migrated to the tube wall, the supernatant was removed without removing the beads, and 50 µl binding buffer were added to calibrate the beads. The tube was again placed on the magnet and the supernatant was discarded, then the tube was removed from the magnet, and 50 µl of binding buffer were added again. Meanwhile, the RNA volume was adjusted to 50 µl with DPEC-water and then was heated to 65°C for 2 min to disrupt secondary structure and then placed on ice. Once the beads were calibrated, the 50 µl RNA were mixed to the beads. The mixture was then placed on a roller for 5 min a RT to allow the annealing of the mRNA to the beads. Afterwards, the tubes were placed on the magnet and the supernatant was discarded. The RNA-beads mix was washed once with Buffer A and twice with Buffer B and between each step, the tube was placed on the magnet to remove the supernatant. After the washing steps, the mRNA was eluted with 15 µl of mM Tris-HCl, pH 7.5, heated at 80°C for 2 min and placed on the magnet. The eluted mRNA was then transferred to a new tube, the concentration was measured using a Nanodrop and then used for cDNA synthesis.

2.2.2.4 Complementary DNA reverse transcription

1 µg of total mRNA or 5 µl of Poly-A mRNA were used for the transcription into double-stranded complementary DNA (cDNA). The iScript™ cDNA Synthesis Kit was used according to the manufacturer's protocol. The master mix composed of 4 µl of 5 × iScript Reaction Mix and 0.25 µl of iScript Reverse Transcriptase were added to the Poly-A mRNA or total RNA and the final volume was adjusted to 20 µl with Nuclease-free water. A Thermocycler was used to perform the reaction with the following protocol: Priming (5 min at 25 ºC), Reverse Transcription (30 min at 42 ºC), Inactivation (5 min at 85 ºC).

2.2.2.5 Conventional PCR

To assets the cDNA integrity a conventional PCR was performed. The Housekeeping gene hypoxanthine guanine phosphoribosyl transferase (*Hprt*) was amplified.
1 µl of cDNA, 1µl of dNTPs, 1µl Primer mix [10 pmol/µl], 0,3 µl DNA polymerase, and 12,7µl ddH_2O to a final volume of 20 µl were mixed. The PCR was performed as indicated in table 14 with a Thermocycler Mastercycler EP Gradient.

Table 14: Conventional PCR reaction

Process	Temperature (°C)	Time	Cycles
Initial denaturation	98,5	2 min	1
Denaturation	98,5	20 sec	
Annealing	64	15 sec	30
Elongation	72	20 sec	
Final elongation	72	2 min	1

At the end of the reaction the cDNA integrity was analyzed, 5 µl of Orange G loading buffer were mixed with the cDNA and then the samples were loaded on a 1 % agarose gel.

2.2.2.6 Real-time quantitative PCR

To analyze the relative expression of genes of interest, real-time quantitative PCR (RT-qPCR) was performed. The reaction mix was composed of 12.5 µl of SYBR green, 11 µl of ddH2O, 0.5 of µl primer mix [10 pmol/µl] and 1 µl of cDNA and it was pipetted into a 96-well Saphire Microplates, then the plate was sealed with Optical Adhesive Covers. To avoid the presence of bubbles, the plate was shortly centrifuged. After the centrifugation, the plate was loaded into the Applied Biosystem 7500 Real-Time PCR System. Settings are shown in Table 15. The results were analyzed with the ΔΔCt method and normalized to the house-keeping gene (*Hprt*).

Table 15: RT-qPCR reaction

Process	Temperature (°C)	Time	Cycles
Initial denaturation	95	10 min	1
Denaturation	95	15 sec	50
Annealing	60	1 min	
Denaturation	95	15 sec	1

2.2.2.7 Fluidigm® Chip Analysis

- **Preamplification of cDNA**

The DNA was synthesized as previous described. 1 µl of each primer pair (100 µM) was mixed with DNA Suspension Buffer for the preparation of the STA (Specific Target Amplification) mix. The final volume of the STA was 200 µl. Then the preamplification reaction solution was prepared as shown in Table 16.

Table 16: Preamplification reaction solution

	Component	**Volume/ Reaction (µl)**	**Volume for 48 Reactions w/Overage (µl)**
PreAmp-mix	TaqMan PreAmp master Mix	2.5	132
	Pooled STA Master Mix	0.5	26.4
	DNA Suspension Buffer	0.75	36.9
	cDNA (µl)		1.25
	Total volume (µl)		5

1.25 µl of cDNA was mixed with 3.75 µl of the preamplification reaction solution in 8-well strip Micro PCR tubes, the final volume was 5 µl. Samples were vortexed and briefly centrifugated and then placed in a Thermocycler and amplified using the PCR program showed in Table 17.

Table 17: Preamplification PCR Program

Step	Temperature (ºC)	Time	Cycles
Hold	95	10 min	1
Denaturation	95	15 sec	14
Annealing/elongation	60	4 min	
Hold	4	∞	

After the preamplification, a clean-up reaction with the Exonuclease I was performed. 2 µl of the dilute Exonuclease I Master Mix showed in the Table 18 were added to the samples.

Table 18: Exonuclease I Master Mix

Component	Per 5 µl Sample (µl)	48 Samples w/Overage (µl)
DNase-free water	1.4	84
Exonuclease I Reaction Buffer	0.2	12
Exonuclease I (20 U/ µl)	0.4	24
Total volume (µl)	2	120

Tubes were vortexed and centrifuged, then the samples were placed in the Thermocycler and the Exonuclease I PCR program showed in table 19 was performed.

Table 19: Exonuclease I PCR program

Step	Temperature (ºC)	Time
Digestion	37	30 min
Inactivation	80	15 min
Hold	4	∞

The final products were diluted with 18 µl of DNA Suspension Buffer (5-fold dilution) to reach the final volume of 25 µl. The samples were stored at -20 ºC.

- **Sample Pre-Mix and samples**

In a new centrifuge tube, the Sample Pre-Mix was prepared as shown below in Table 20. Then 3.3 µl of the Sample Pre-Mix were added to each well of a 96-well plate together with 2.7 µl of the samples. The plate was vortexed for 20 sec and centrifuged at 1000 x g for 30 sec.

Table 20: Sample Pre-Mix

	Component	Volume per inlet (µl)	Volume per inlet with overage (µl)
Sample Pre-mix	2 × SsoFast EvaGreen Supermix with low ROX	2.5	3
	20 × DNA Binding Dye	0.25	0.3
	PreAmp and Exo I-treated sample	2.25	2.7
	Total volume (µl)	5	6

- **The Assay Mix**

The forward and reverse primers were mixed and then 0.6 µl were added to a 96-well plate. The Assay Mix was prepared as shown in Table 21 and then 5.4 µl of the Assay Mix were added to each well of a 96-well plate.

Table 21: Assay Mix

	Component	Volume per inlet (µl)	Volume per inlet with overage (µl)
Assay mix	2 × Assay Loading Reagent	2.5	3
	1 × DNA Suspension Buffer	2	2.4
	Combined forward and reverse primers (50 µM)	0.5	0.6
	Total volume (µl)	5	6

The plate was vortexed for 20 sec and centrifuged at 1000 x g for 30 sec.

- **The Dynamic Array Integrated Fluidic Circuit**

The 48.48 (Integrated Fluidic Circuit) IFC plate was used. Before the usage the 48.48 IFC must be primed with the control line fluid which was injected into the two accumulators and then the film on the bottom of the plate was removed. The IFC was placed in an IFC Controller MX, and the program: Prime (113×) was started. After, 5 µl of the assay and 5 µl of each sample were pipetted into the IFC plate, the plate was then loaded into the IFC Controller MX, and the program Load Mix (113×) was started. Then the plate was run with the Biomark Gene expression Data Collection software with the protocol GE 48 × 48 PCR + Melt v2.pcl. The data were analyzed using the ΔΔCt method and normalized to the house-keeping gene (*Hprt*).

2.2.2.8 Colon permeability assay with Evans Blue dye

Evans blue (EB) assay was performed to evaluate the permeability of the intestinal epithelium. The colon was removed and flushed with PBS to remove contents. The rectal end was closed with surgical thread and the colon was filled with 0.3 ml of 0.02% EB solution in PBS, then the oral end of the colon was closed. The colon sack was incubated on ice for 1 hr. After the incubation the colon washed with 0.1 M acetylcysteine and then dried at 37°C overnight. The day after the colon was weighted, cut into small pieces, and incubated in 1 ml of formamide at 56°C for 24 hrs. in order to extract the dye. The colon samples were then centrifuged at 5000 x g for 30 min and 100 µl of the supernatant were pipetted into Nunc Immuno™ MicroWell™ 96-well plate. The absorption was measured at a wavelength of 620 nm (Muzzi et al. 2021).

2.2.2.9 Colon permeability assay with FITC-Dextran

The mice were weighted and fasted overnight. The day after 600mg/kg of FITC-dextran were administrated by oral gavage. After 5h the mice were sacrificed, and the serum was collected by heart puncture. The serum was stored at -20 °C until the day of the analysis. The day of the analysis the standards were prepared for the standard curve and 100 µl were pipette into a Black 96-Well Immuno Plates. The samples were diluted 1:2 with distilled water to a final volume of 100 µl. The fluorescence was measured in a plate reader with 488 excitation and 520 emissions.

2.2.2.10 Enzyme-Linked Immunosorbent Assay

The level of IL-6 in the serum was measured by enzyme-linked immunosorbent assay (ELISA). At day 1, 100 µl of coating buffer were added to ELISA Nunc-Immuno™ MicroWell™ 96-well plates, the plate was sealed and incubated at 4 °C overnight. The day after, the plate was washed 4 times with PBST, then 200 µl assay diluent was added and the plate was incubated on a shaker at RT for 1 hr. After the incubation the plate was washed 4 times and the serum samples were diluted with assay diluent (1:2) and added to the wells in duplicates, the standards were pipetted in triplicates,

the final volume of each well was of 100 µl. The plate was sealed and incubated on a shaker at RT for 2 hrs. Then the plate was washed, subsequently 100 µl detection antibody diluted in assay diluent was added and the plate was incubated on the shaker for 1 hr. The plate was washed 4 times and 100 µl diluted of Avidin- Horse Radish Peroxidase (HRP) solution was added to each well and incubated for 30 min on a shaker. Next, the plate was washed 5 times, soaking for 1 min per wash and 100 µl of TMB substrate solution were added, the plate was incubated in the dark for around 20 min, then to stop the reaction, 100 µl Stop solution were added to each well, the color change was read at 450 nm and 570 nm.

2.2.2.11 Flow cytometric analysis of LPCs and IECs

Both LPCs and IECs were used for FACS analysis. LPCs were analyzed to quantify inflammatory cells in the different mice while IECs were analyzed to assess their purity. Regarding IECs, after cells isolation, 10.000 cells were transferred into a FACS tube, 4 ml of FACS buffer were added for washing and then the tubes were centrifuged at 350 x g for 7 min. After the washing step, IECs were stained with 20 µl of APC Rat IgG2a κ Isotype Ctrl APC and 20 µl anti-mouse CD326 (Ep-cam) separately. Tubes were incubated for 20 min at 4°C in the dark, then washed as described before and used for FACS analysis.

For the LPCs, 100.000 cells for each sample were transferred into FACS tubes, each sample was washed as described before, treated with the Fc blocker, and incubated for 20 min at 4°c in the dark and then washed. Next, the samples were stained with 20 µl of APC/cy7 anti-mouse Ly-6C, 20 µl of APC anti-mouse Ly-6G and 20 µl of PE-Cy7 anti-mouse CD11b antibodies and incubated in the dark for 20 min at 4°C. After the incubation time the samples were washed and used for FACS analysis.

2.2.2.12 Biolegend LEGENDplex™ Multiplex Assay

The Biolegend LEGENDplex™ Multiplex Assay is a bead-based immunoassays that allows to quantify multiple soluble analytes simultaneously in biological samples using the flow cytometer. Cytokines of the colon supernatant were measured with

this kit according to the manufacturers protocol. In brief, the V-bottom plate was loaded with the 25 µl standards or samples and diluted with 25 µl of assay buffer, then 25 µl of beads were added to a final volume of 75 µl. The plate was sealed and placed on a shaker at 800 rpm for 2 h. After the incubation time, the plate was centrifuged at 1020 rpm for 5 min. The supernatant was discarded by quickly inverting and flicking the plate in one continues and forceful movement. The plate was washed with 200 µl of 1x washing buffer, then the plate was centrifuged, and the supernatant discarded again as described before. 25 µl of the detection antibody were added and then the plate was sealed and placed on a shaker at 800 rpm for 1 h. After the incubation time 25 µl of SA-PE buffer were added and incubated for 30 min with shaking. Afterwards the plate was centrifuged, and the supernatant was discarded as described above. Then the plate was washed again with 200 µl of washing medium, centrifuged and the supernatant discarded. 150 µl of washing buffer were added to each well and the beads were resuspended, then the content of each well was transferred in 4 ml FACS tubes separately and the flow cytometer was used to acquire the data.

2.2.3 Histology

Histological analyses were performed in collaboration with Dr. Hanibal Bohnenberger at the Institute for Pathology of the University Medical Center Göttingen.

2.2.3.1 Histological examination using swiss-roll

For histological examination of the colon, the “swiss-roll” technique was performed. The colon was opened longitudinally, fixed on a moistened Whatman paper, and rolled up from the rectal to the proximal end. The tissue roll was insert into a tissue cassette and left for fixation in 4 % PFA for 24 h. The samples were dehydrated and embedded in paraffin at the Institute of Pathology of the University Medical Center Göttingen.

2.2.3.2 H&E Staining

The samples were cut at a thickness of 2 µm with the help of a microtome and then hematoxylin and eosin (H&E) staining was performed as shown in Table 22.

Table 22: H&E staining

Reagent	Time
Drying	10 min
Xylol	2:30 min; 2:30 min
Ethanol 100 %	1 min
Ethanol 95 %	1 min
Ethanol 70 %	1 min
ddH2O	1 min
Hematoxylin (Meyer's)	6 min
HCl Ethanol	0:05 min
ddH2O	8 min
Eosin	3 min
ddH2O	0:15 min
Ethanol 70 %	0:30 min
Ethanol 95%	1:30 min
Ethanol 100 %	2 min
Xylol	2 min

Hematoxylin shows the acid components of the cells such as the nucleus with a violet color while Eosin stains alkaline components of the cell like the cytoplasm with a red color.

2.2.3.3 Scoring of the histological samples

The glass slides with the stained colon were placed under the microscope and the score of the inflammation was performed. The scoring is dived into four stages of inflammation and for each sample, a number was assigned to each inflammation stage for a total of 100 as shown in Table 23.

Table 23: Score of the H&E-stained colon swiss-Roll

Inflammation	No inflammation	Slight inflammation	Medium inflammation	Severe inflammation
Description	No immune cells infiltration. Regular crypts and number of goblet cells	Little immune cells infiltration, crypts intact to slightly changed, regular number of goblet cells	Clear immune cells infiltration, crypts partially damaged reduced number of goblet cells	Massive immune cells infiltration, crypts structure completely destroyed. Loss of goblet cells

2.2.4 Statistical Analysis

One-way ANOVA followed by a Newman-Keuls multiple comparison test or Student's t-test were used. Statistical analysis was performed using GraphPad Prism software. Data are presented as mean and standard error (SEM) and considered significant if p-value was ≤ 0.05, the significance was depicted as: n.s., $p > 0.05$; *, $p < 0.05$; **, $p < 0.01$; ***, $p < 0.001$.

3. Results

3.1 Influence of impaired GR dimerization on intestinal inflammation and tumorigenesis

3.1.1 Impaired GR dimerization ameliorates DSS-induced colitis

GR^{dim} and GR^{wt} mice were treated with AOM and 3.5% DSS via the drinking water for 8 days and then received tap water until day 12. The control group received only tap water and the AOM injection. The DAI score, which represents the 3 major clinical hallmarks of the colitis (weight, stool consistency and fecal blood) increased in the DSS-treated mice. The highest peak was observed at day 8 but it was significantly higher in GR^{wt} mice compared to GR^{dim} mice at day 12, while the DAI of control mice of both genotypes remained low (Figure 5A). Therefore, samples for further analyses were taken on day 8 and 12.

The relative colon length was measured since DSS-colitis is known to be associated with a shortening of the colon. At day 12 the colon was significantly shorter in GR^{wt} mice compared to GR^{dim} mice (Figure 5B).

IL-6 levels in the serum were also analyzed. IL-6 is a pro-inflammatory cytokine and usually present at higher concentrations in the serum during inflammation. IL-6 levels were higher at day 8 in GR^{wt} mice compared to GR^{dim} mice while at day 12 they were back to normal in both groups. The control group did not show any significant differences neither in colon length nor IL-6 serum levels (Figure 5C).

These results together demonstrate that impaired GR dimerization exerts beneficial effects on DSS-induced colitis especially in the recovery phase.

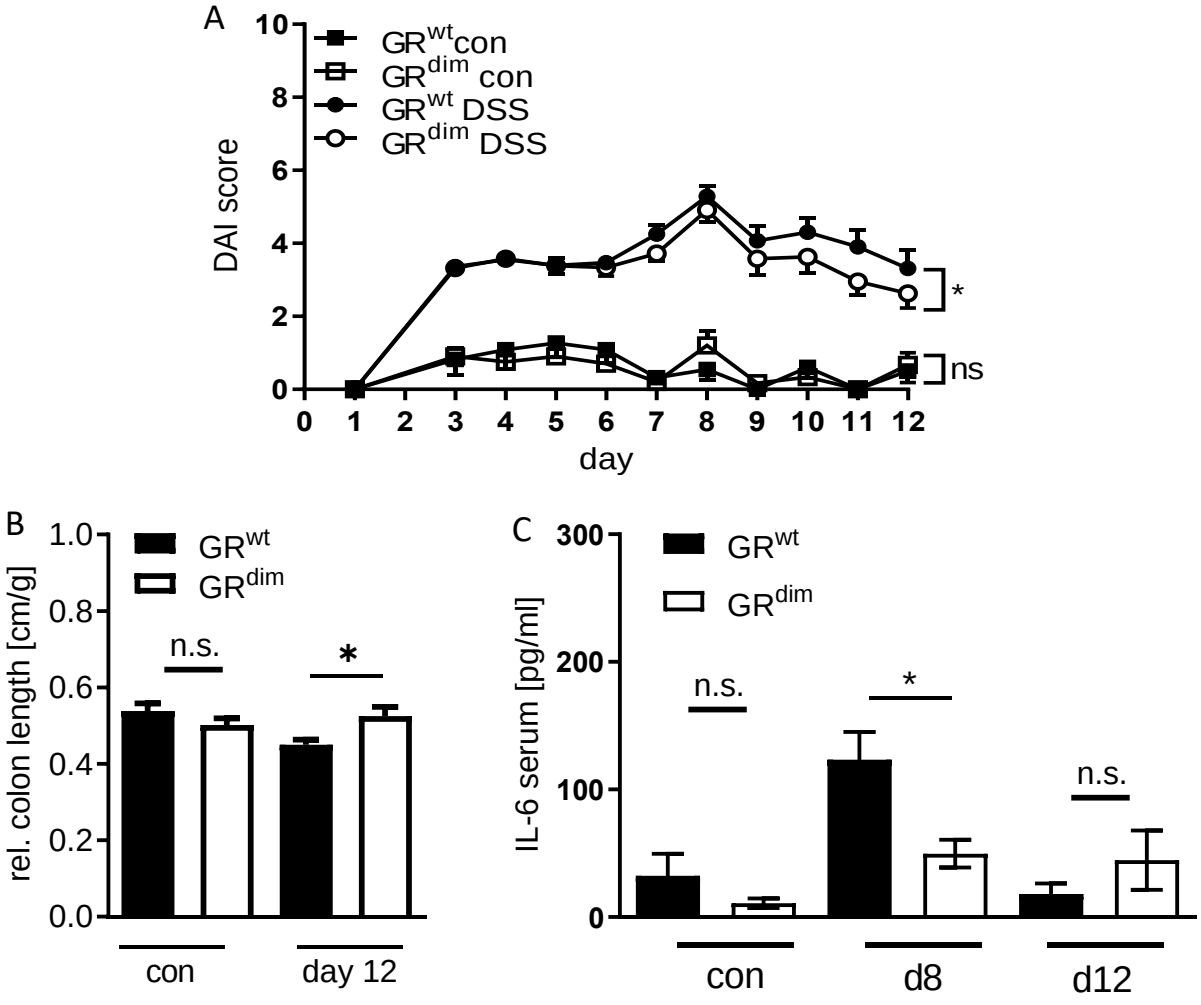

Figure 5: Impact of impaired GR dimerization on DSS-induced colitis.

Mice received 3.5% DSS via drinking water for 8 days and then tap water until day 12. Control mice received only tap water. A) The DAI score was calculated based on stool consistence, intestinal bleeding, and weight loss. GR^{wt} mice: n =11/53, GR^{dim} mice: n =10/52 (con/DSS). B) The colon length of mice sacrificed at day 12 of DSS treatment and control mice was measured and is represented in relation to the body weight. GR^{wt} mice: n =11/19, GR^{dim} mice: n =10/24 (con/day 12). C) IL-6 serum levels of mice sacrificed at day 8 or 12 of DSS treatment or control mice were analyzed by ELISA. GR^{wt} mice: n = 5/12/4, GR^{dim} mice: n = 5/12/3 (con/day 8/ day 12). Data in all panels are depicted as the mean ± SEM. Statistical analysis was performed by One-way ANOVA and followed by Newman-Keuls Multiple Comparison test. Levels of significance: *: $p < 0.05$; n.s. (non-significant): $p > 0.05$. The graph in panel A contains some data from former students.

3.1.2 Histological analysis of the colon reveals a reduced IEC damage and immune cell infiltrate in the colon of GR^{dim} mice

GR^{dim} and GR^{wt} mice were treated with AOM and received 3.5% DSS for 8 days and then tap water until day 12 as in the experiment before. Control mice received tap water and only the AOM injection. The colon was removed, opened longitudinally, and rolled to form colon swiss-rolls. The tissue was stained with H&E and scored histologically (Figure 6A and B). Immune cell infiltration and IEC damage were evaluated with the help of a microscope. At day 12 the colon of GR^{wt} mice revealed an exacerbated immune cells infiltration and IEC damage compared to the colon of the mutant mice while at day 8, so at the peak of the inflammation, no significant differences were observed. Control mice did not show any inflammatory features (Figure 6C).

Results

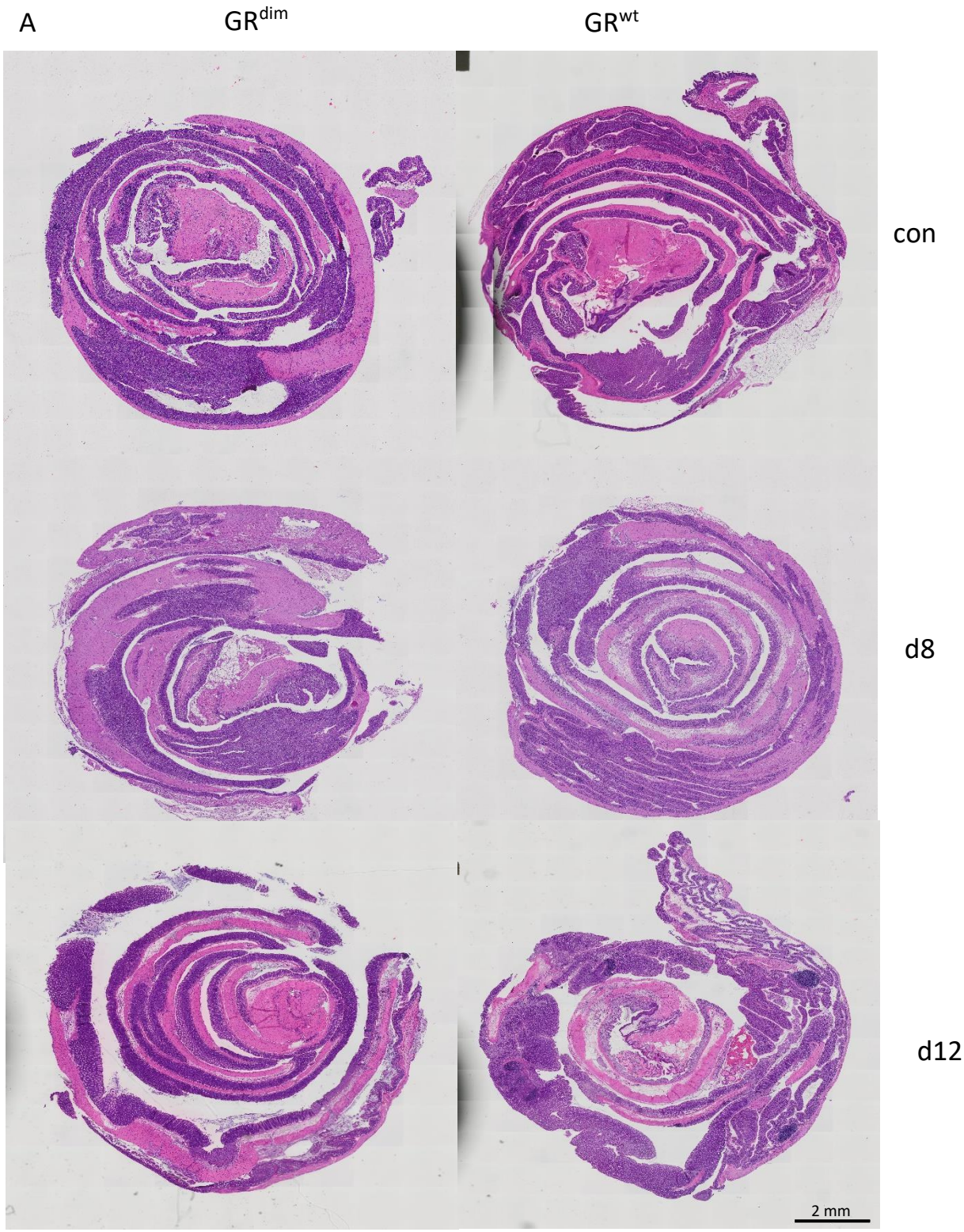

Results

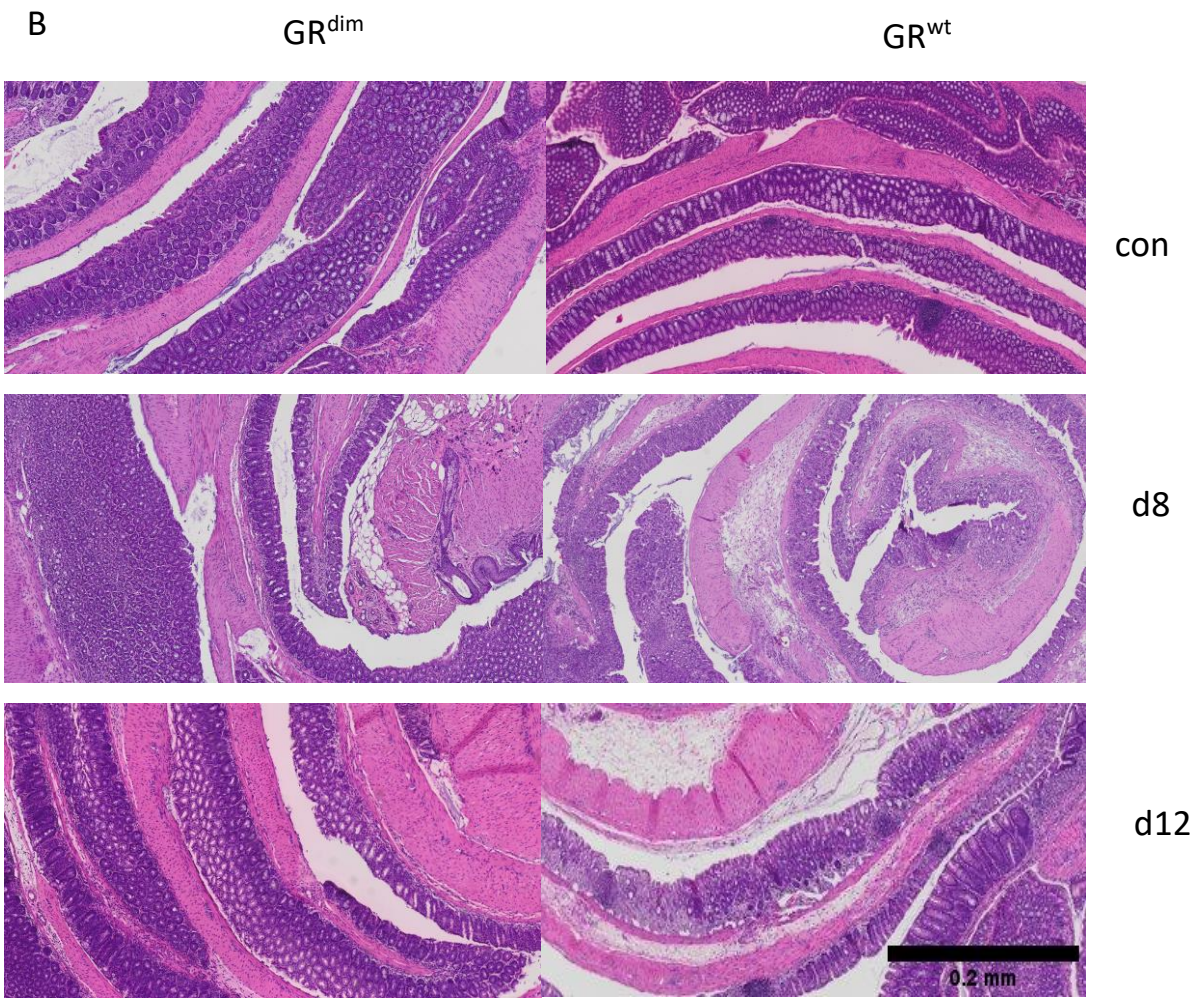

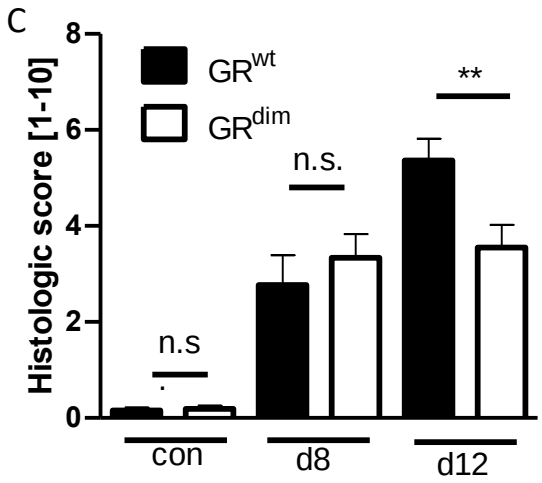

Figure 6: Histological assessment of tissue damage in the colon of GR^{dim} and GR^{wt} mice

Colon swiss-rolls prepared from AOM/DSS-treated and AOM treated control mice at day 8 and 12 were stained with H&E and evaluated for tissue damage A) Representative images of colonic tissue of DSS-treated or control mice; scale bar = 2 mm. One representative image is shown each. B) Higher magnification photographs of colon tissue; scale bar = 0.2 mm. C) Histological score according to the parameter's crypt distortion, loss of goblet cells and immune cell infiltration. GR^{wt} mice: n = 7/5/12, GR^{dim} mice: n = 8/5/15 (con/day 8/day 12). Data in panel C are depicted as the mean ± SEM. Statistical analysis was performed by One-way ANOVA and followed by Newman-Keuls Multiple Comparison test. Levels of significance: **: $p < 0.01$; n.s. (non-significant): $p > 0.05$. The graphs contain some data from former students.

3.1.3 High-throughput gene expression analysis of the colon of GR^{dim} mice during DSS-colitis

A Fluidigm® gene chip assay was performed to analyze mRNA levels in whole colon pieces to obtain a general impression of the gene expression profile in the colon. Altogether, 24 genes were analyzed in the colon of both healthy and DSS-treated mice.

The first group of genes are typical pro-inflammatory cytokines: *Il6*, *Tnfα* and *Il1b*. No differences were observed in the control group. At day 8, so at the peak of the inflammation, the genes were highly expressed in the GR^{wt} mice while in the mutant mice the expression remained normal. At day 12, cytokines were again normally expressed in both mutant and non-mutant mice.

The second group of genes analyzed are chemokines from the CXCL-family which are mostly expressed by IECs as well as those of the CCL-family which are known to be expressed by infiltrating immune cells such as macrophages. Chemokines of the CXCL-family at day 8 were highly expressed in GR^{wt} mice while in GR^{dim} mice only *Cxcl5* seemed to be upregulated but still less than in GR^{wt} mice. At day 12 the expression of *Cxcl1* and *Cxcl2* was low in both groups but the expression of *Cxcl5* remained high, especially in GR^{wt} mice. For the chemokines of the CCL-family no changes were observed, neither in wildtype nor mutant mice.

Genes associated with an M2 macrophage polarization were also analyzed. *Arg1* was downregulated in GR^{dim} mice at day 12 and a slight downregulation was also observed at day 8 while *Ym1* was downregulated in GR^{dim} mice at day 8.

Differences in TLRs were observed already in the control group. *Tlr2* and *Tlr4* were upregulated in the colon of mutant mice compared to GR^{wt} mice. At day 8 and day 12 no differences were observed between the two groups.

Expression of *Cox2* and *Alox15*, encoding enzymes involved in pro-inflammatory pathways, namely in prostaglandin production and cancer development, was similar

in both groups. Only for *Cox2* at day 12 a slight downregulation was observed in GR^{dim} mice.

The last group of genes analyzed are involved in colon permeability and TJs. An upregulation was already observed in control mutant mice where all TJ-associated genes were overexpressed. At day 8 and 12 the genes were slightly higher expressed in GR^{wt} mice (Figure 7).

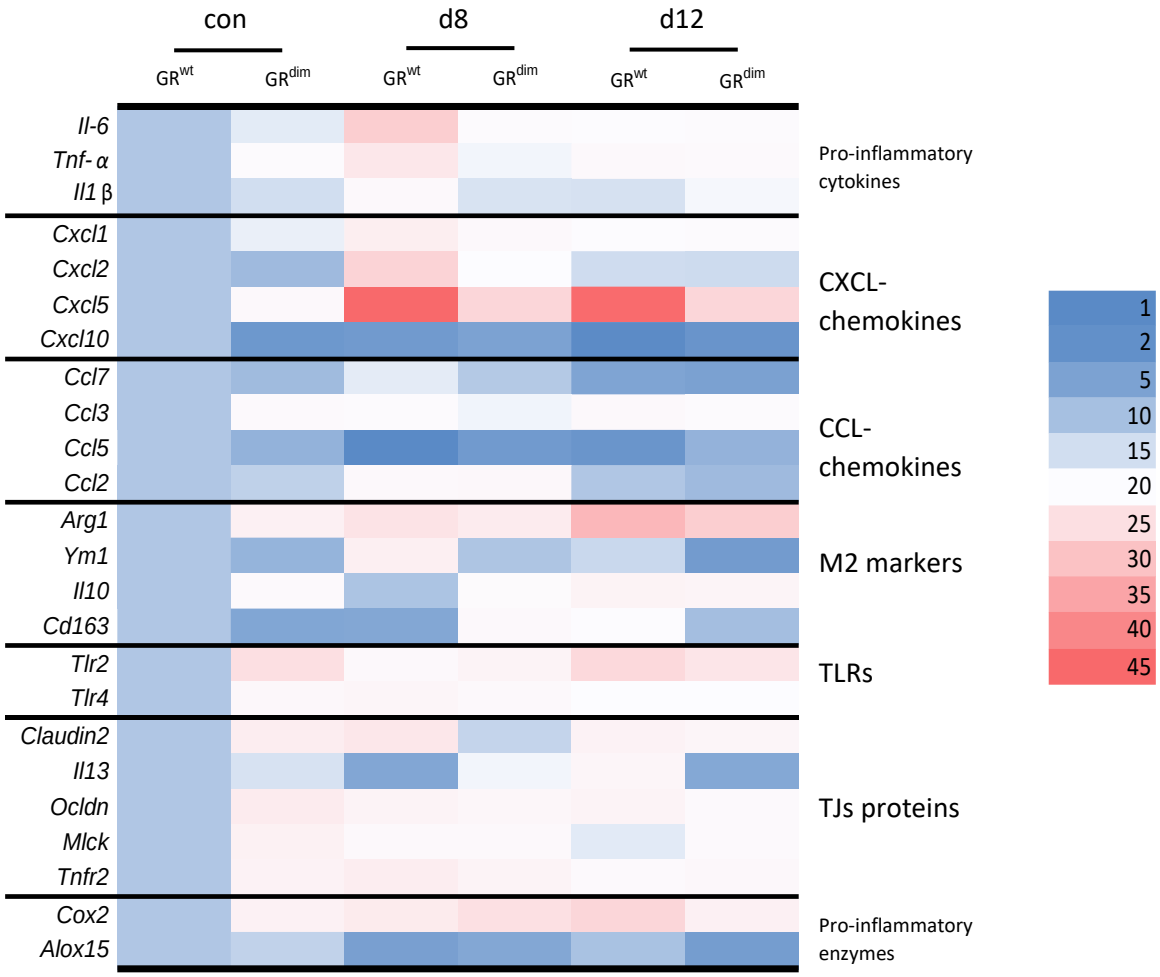

Figure 7: Fluidigm® gene chip analysis of colon tissue.

Mice were treated with 3.5% DSS and sacrificed at day 8 and 12. The control group received tap water and AOM injection. Total RNA and subsequently mRNA were isolated. Gene expression analysis was done using Fluidigm Chip. A color code is used to show the different levels of gene expression, the lowest expression is represented in blue and the highest expression in red. Gene expression of control GR^{wt} mice was set to 1. GR^{wt} mice: n = 4/5/6, GR^{dim} mice: n = 5/8/6 (con/day 8/day 12).

3.1.4 Analysis of the protein levels in colon supernatants using the BioLegend's LEGENDplex™ flow cytometric assay

Levels of pro-inflammatory cytokines in the colon supernatant were measured with the BioLegend's LEGENDplex™ assay to verify whether gene regulation impacts on protein levels, too. Mice were treated with AOM and received 3.5% DSS for 8 days and then tap water until day 12. Control mice received only the AOM injection and tap water. Colon pieces from the rectal part of the colon were weighted and placed in a 24-well plate with $RPMI^{++}$ medium for 24 hrs. at 37°C. In the end, the supernatants were used for protein analysis.

Two groups of genes were investigated, the first are chemokines: CXCL1, CXCL10 and CCL2. Their concentration was higher in GR^{wt} mice at day 8 while at day 12 the concentration was slightly higher in GR^{wt} mice but less than at day 8.

The second group are pro-inflammatory cytokines encompassing GM-CSF, IFN-β, IL-6 and TNF-α. The concentration of most of them were higher in the colon of GR^{wt} mice than in GR^{dim} mice at both day 8 and 12. No significant differences were observed in the control mice.

These results are in line with the hypothesis that impaired GR dimerization attenuates DSS-induced colitis since most pro-inflammatory genes were present at higher levels in colon supernatant of GR^{wt} mice compared to GR^{dim} mice (Figure 8).

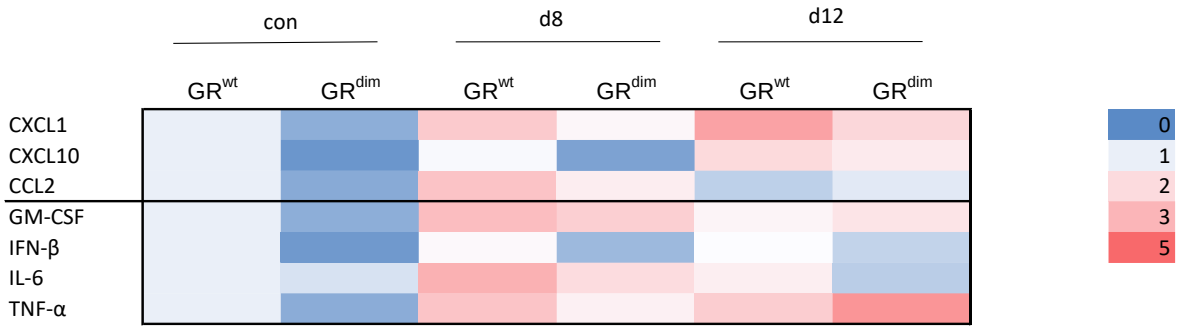

Figure 8: Analysis of the protein levels in the colon supernatant with the BioLegend's LEGENDplex™ flow cytometric assay.

Mice were treated with 3.5% DSS and sacrificed at day 8 and 12. Control mice received tap water. The colon was removed and cut in pieces. The colon pieces were placed in $RPMI^{++}$ medium and then protein levels were measured after 24 hrs. A color code is used to show the different concentrations, the lowest concentration is represented in blue and the highest concentration in red. Protein levels in control GR^{wt} mice was set to 1. GR^{wt} mice: n = 11/11/6, GR^{dim} mice: n = 8/11/8 (con/day 8/day 12).

3.1.5 Analysis of colon permeability in untreated control mice

Due to the different expression of genes associated with TJs and colon permeability in the control group, the permeability of the colon was tested in control GR^{wt} and GR^{dim} mice using two different assays. Firstly, the diffusion to the inorganic dye EB from the lumen into the colon tissue was determined. Mice were sacrificed, and the colon was filled with EB, incubated on ice for 1h and subsequently the excess amount of EB was washed out allowing to determine the amount of EB dye in the tissue by photometric quantification. Additionally, the permeability of the colonic epithelium for FITC-labelled dextran was investigated in control mice as well. The mice were fastened overnight and then treated with FITC-dextran via oral gavage. After 5 hrs., the serum was collected, and the fluorescence was measured in a spectrophotometer. Both experiments showed a slight difference between mutant and non-mutant mice, which did not reach significance (Figure 9A and B). GR^{wt} mice showed an increased colon permeability compared to GR^{dim} mice. The higher expression of TJ-associated genes in GR^{dim} mice thus seems to have a protective effect on epithelial integrity and thus reduces colon permeability already in control mice.

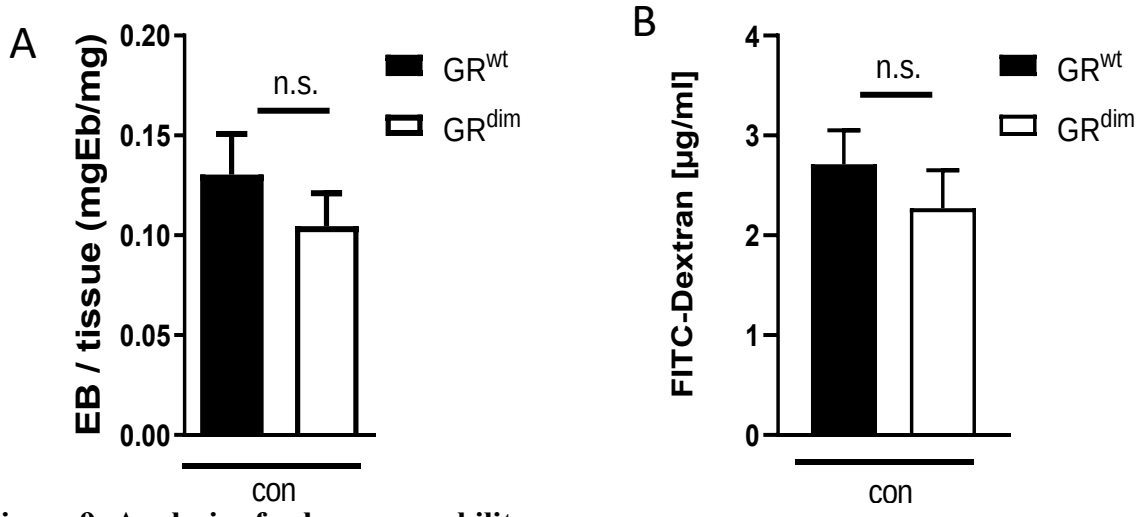

Figure 9: Analysis of colon permeability

A) The colon was removed from control mice and filled with EB dye solution for 1 hour. EB that had diffused into the tissue was quantified by spectrophotometry. GR^{wt} mice: n = 5, GR^{dim} mice: n = 5. B) Control mice were fastened overnight and treated with FITC-dextran via oral gavage. After 5 hrs. the serum was collected and used for quantification of FITC-Dextran by spectrophotometry. GR^{wt} mice: n = 5, GR^{dim} mice: n = 3. Data are depicted as the mean ± SEM. Statistical analysis was performed by student's t-test. Levels of significance: n.s. (non-significant): $p > 0.05$.

3.1.6 Analysis of bacterial content in the mesenteric lymph nodes

Due to the increased expression of TLRs in the colon of GR^{dim} control mice we investigated whether there were any differences in the bacterial content in mesenteric lymph nodes.

Control mice were scarified, and the mesenteric lymph nodes were isolated. Total RNA was analyzed via RT-qPCR. The 16s rRNA of bacteria was identified using a primer which amplifies conserved regions of this gene.

We observed an increased uptake of luminal bacteria into the mesenteric lymph nodes of GR^{dim} mice (Figure 10), probably linked to the higher expression of TLRs in the mutant control mice. We assume that the high expression of the TLRs in GR^{dim} mice leads to an increased bacteria clearance thus reducing inflammation.

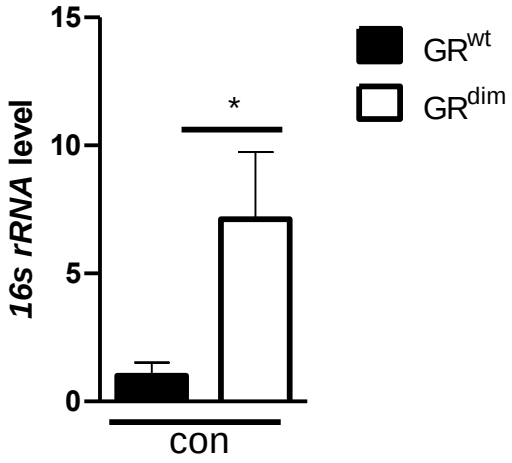

Figure 10: Analysis of bacterial content in mesenteric lymph nodes.

Mesenteric lymph nodes were removed, and total RNA was isolated. Gene expression of *16s rRNA* was performed via RT-qPCR and normalized to the housekeeping gene *Hprt*. GR^{wt} mice con = 5, GR^{dim} mice con = 4. All values are depicted as the mean ± SEM. Statistical analysis was performed by student's t-test. Levels of significance: *: $p < 0.05$. (non-significant): $p > 0.05$.

3.1.7 Analysis of lamina propria infiltrating cells via FACS

In order to better understand whether impaired GR dimerization affects the number of infiltrating cells in the LP, FACS analysis was performed. LPCs were isolated from AOM/DSS-treated mice at day 8 and 12 and from control mice. Neutrophils were identified as $CD11b^{+}Ly6G^{+}$ cells, total macrophages were identified as $CD11b^{+}$ $Ly6G^{-}$ cells and inflammatory macrophages within this population were identified as $Ly6C^{+}$ cells (Figure 11A).

Chemoattractants were more abundant on the protein level in colon supernatants and on the gene expression level in the colon tissue of GR^{wt} mice, and in line with these results we observed an increased percentage of neutrophils in the colon of GR^{wt} mice at day 8. Total macrophages were similar in mutant and non-mutant mice, but the percentage of pro-inflammatory macrophages was higher in GR^{wt} mice at day 8 (Figure 11 B, C, D).

These data support our finding that GR^{wt} mice suffer from an exacerbated DSS-induced intestinal inflammation compared to the GR^{dim} mice.

Results

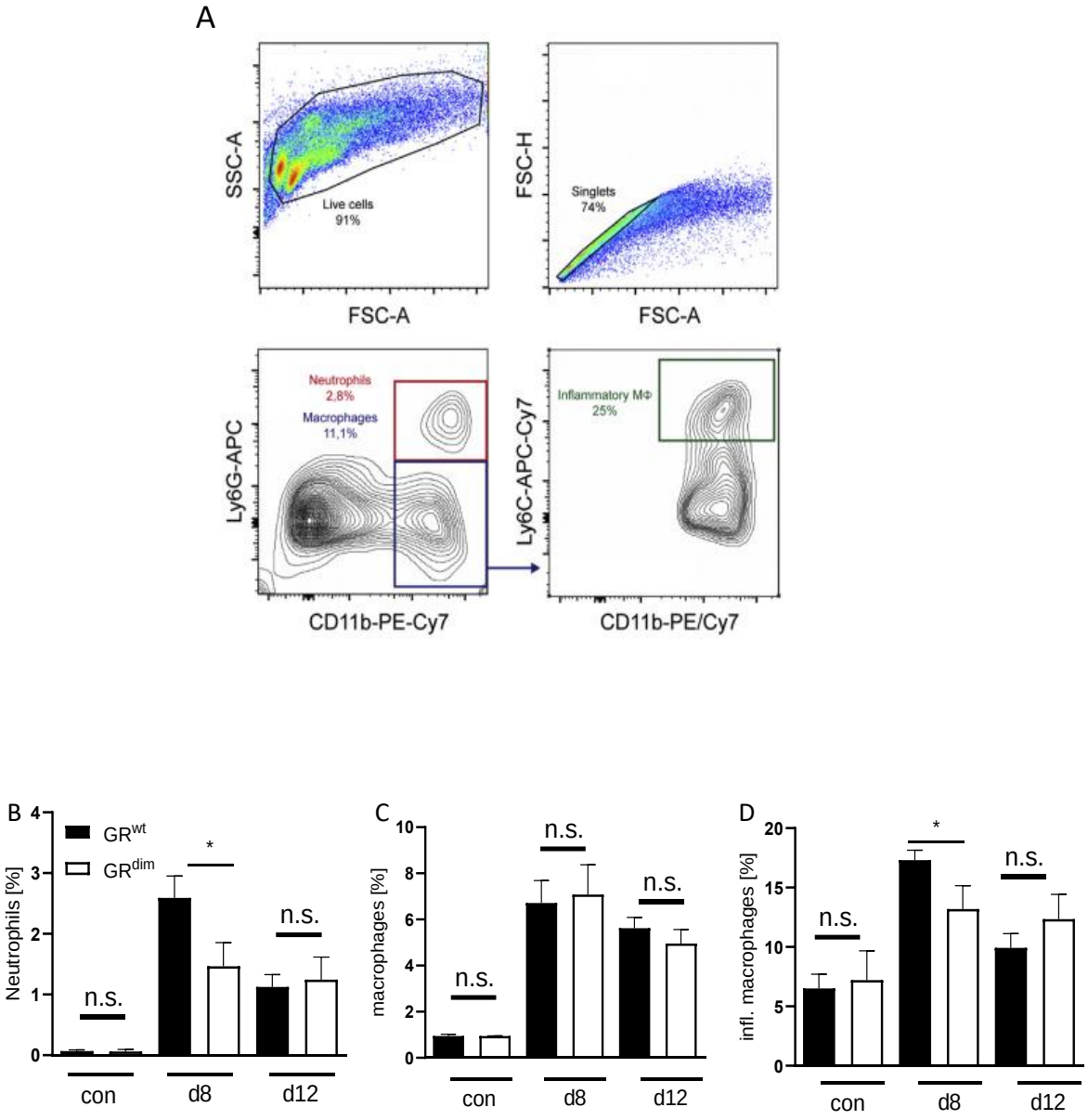

Figure 11: Flow cytometric analysis of LP-infiltrating cells

GR^{wt} and GR^{dim} mice were treated with AOM and 3.5% DSS to induce colitis for 8 days and then they received tap water until day 12. Control mice received tap water and only the AOM injection. LPCs, prepared by enzymatic digestion from the colon of DSS-treated mice at day 8 and 12 and AOM treated control mice, were analyzed by flow cytometry. A) Illustration of the gating strategy used in the experiment. Neutrophils: $CD11b^{+}Ly6G^{+}$ cells. Macrophages: $CD11b^{+}Ly6G^{-}$ cells. Inflammatory macrophages: $CD11b^{+}Ly6G^{-}Ly6C^{+}$ cells. B) The percentages of neutrophils, C) total macrophages a mongst all LPCs, and D) inflammatory macrophage amongst $CD11b^{+}Ly6G^{-}$ macrophages are depicted. GR^{wt} mice con: n = 4, GR^{wt} mice DSS: n=13–12, GR^{dim} mice control: n=3, GR^{dim} mice DSS: n =9-12. All values are depicted as the mean ± SEM. Statistical analysis was performed student t-test. Levels of significance: *: $p < 0.05$; n.s. (non-significant): $p > 0.05$.

3.1.8 Analysis of gene expression in LPCs

Since GR^{wt} mice have increased numbers of infiltrating neutrophils and inflammatory macrophages in the LP during AOM/DSS-induced colitis and since the clinical and histological hallmarks of colitis were more severe in GR^{wt} mice, we analyzed the expression of genes related to an inflammatory response in LPCs.

Il6 was higher expressed in GR^{wt} mice compared to GR^{dim} mice at both day 8 and day 12 and *Il1b* was higher expressed in GR^{wt} mice at day 12 (Figure 12A and B). This high expression in non-mutant mice can be linked to their exacerbated inflammation and it is in line with the Fluidigm Chip results. Moreover, the *Ptgs2* gene, which encodes Cox-2 was significantly higher in GR^{wt} mice at day 12, as observed in the analysis of whole colon tissue where the gene was slightly upregulated (Figure 12C).

Cxcl1, a chemoattractant, was slightly higher expressed in GR^{wt} mice at day 8 as observed before in the gene expression analysis of whole colon tissue (Figure 12D). No differences were observed for these genes in the control group.

Ym1 a marker of anti-inflammatory macrophages was slightly higher expressed in GR^{wt} mice while in GR^{dim} mice its expression remained low (Figure 12E). The increased presence of M2 macrophages in the LP of GR^{wt} mice is probably caused by the increased tissue damage and inflammation. We assume that due to the severe colitis M2 macrophages try to dampen the inflammatory response and heal the damaged colon tissue.

No differences were observed in the expression of *Il10* which is known for its anti-inflammatory activity (Figure 12F).

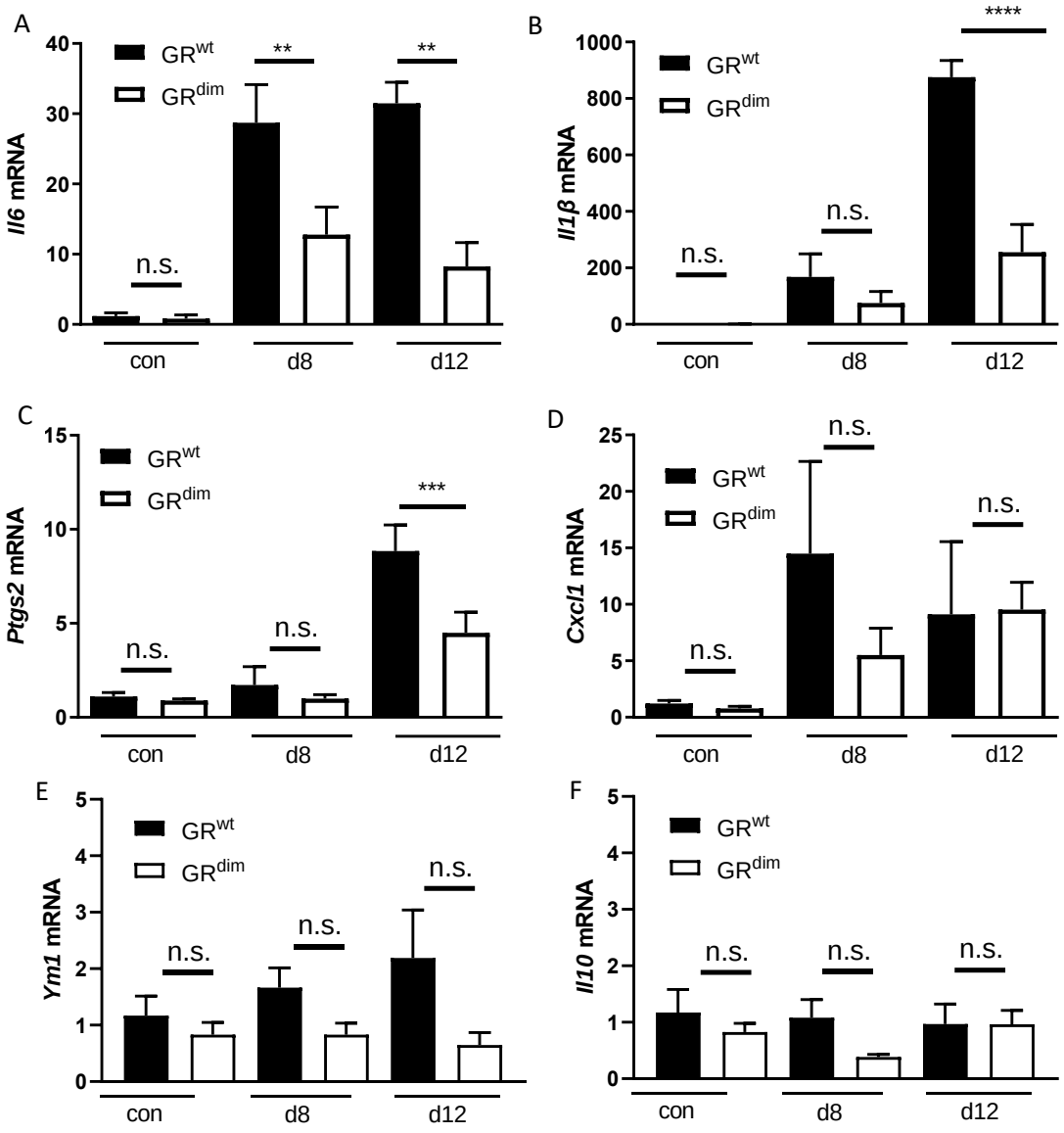

Figure 12: Gene expression analysis in LPCs.

LPCs were isolated from the colon of AOM/DSS-treated mice at day 8 and 12 and AOM treated control mice. Gene expression analysis was performed by RT-qPCR. Relative expression levels of *Cxcl1*, *Cxcl10*, *Il1b*, *Il6*, *Il10* and *Ym1* were determined by normalization to the housekeeping gene *Hprt.* GR^{wt} mice con: n = 3, GR^{wt} mice DSS: n = 4–3, GR^{dim} mice con: n = 3, GR^{dim} mice DSS: n = 7–4. All values are depicted as the mean ± SEM. Statistical analysis was performed by One-way ANOVA followed by Newman-Keuls Multiple Comparison test. Levels of significance: **: $p < 0.01$; ***: $p < 0.001$; ****: $p < 0.0001$; n.s. (non-significant): $p > 0.05$.

3.1.9 Analysis of colon tumorigenesis in the GR^{dim} mouse model

In order to quantify the tumor growth in GR^{dim} and GR^{wt} mice treated with AOM and 3.5% DSS, the number and the size of the tumors were analyzed. Colonoscopy was performed from week 6 on to monitor tumor growth. When the tumors were big enough (reaching a score of S3), the mice were sacrificed. The colon was opened, and the tumors were counted, and their size measured. The total number of tumors was significantly higher in GR^{wt} mice compared to GR^{dim} mice. Moreover, the tumor area was bigger in GR^{wt} mice compared to the mutant mice (Figure 13A and B). No tumors were observed in control mice.

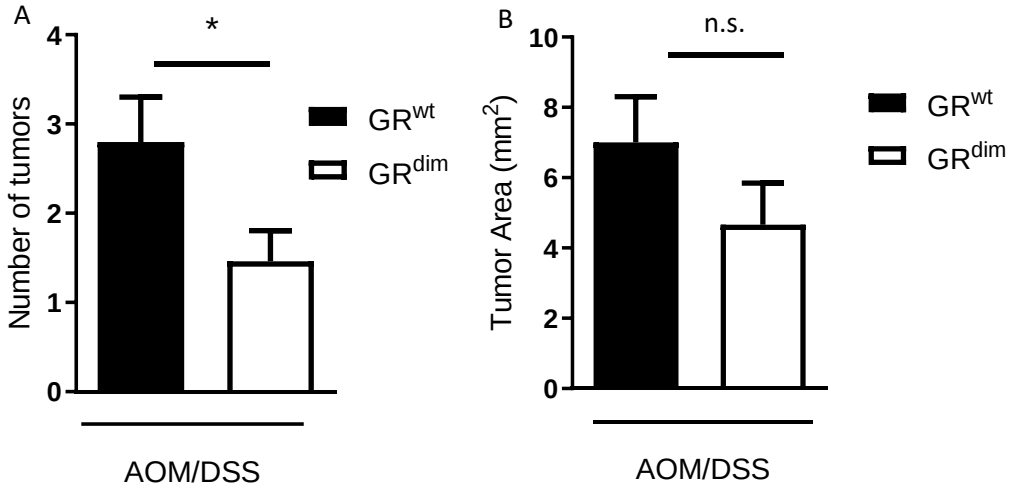

Figure 13: Quantitative tumor analysis.

Mice were treated with 3.5% DSS and AOM for 8 days and then the tumor growth was checked with colonoscopy every week starting from week 6. When S3 tumors were detected, the mice were sacrificed. The colon was opened longitudinally, and the tumors were counted (A) and their size quantified. The tumor area was calculated according to the formula $[(\text{length} + \text{width}) \times 0.5]^2$ (B). Control mice are not shown since no tumors were detected. GR^{wt} mice AOM/DSS = 22 GR^{dim} mice AOM/DSS = 23. Data include some from another student's experiments. All values are depicted as the mean ± SEM. Statistical analysis was performed Student t-test. Levels of significance: *: $p < 0.05$; n.s. (non-significant): $p > 0.05$. The graphs contain some data from former students.

3.1.10 Gene expression in tumor and mucosa tissue

A Fluidigm® gene chip assay was used for the evaluation of gene expression in both mucosa and tumor tissue. Mice were treated with AOM and then they received 3.5% DSS via the drinking water for 8 days. Control mice received tap water and an AOM injection. When a first S3 tumor was detected, the mice were sacrificed, tumors were harvested together with normal mucosa. The mRNA levels of several genes were analyzed in the tissue.

The first group of genes are chemokines and their receptors, most of them were highly expressed in both mucosa and tumor tissue of GR^{wt} mice except for *Cxcl10* which was higher in tumor tissue of GR^{dim} mice. The majority of chemokines and their receptors are associated with tumor development and infiltration. The second group of genes are associated with tumor development, angiogenesis, and metastasis; they were highly expressed in the tumor tissue of GR^{wt} mice while for the mucosa tissue no big differences were observed.

The enzymes *Arg1* and *Arg2* are involved in polyamine production and therefore linked to cell proliferation. Additionally, they impact NO production as they deprive NO synthase of its substrate arginine. *Arg1* is therefore also a marker for M2 macrophages and hence linked to tumor infiltrating macrophages. Both genes were highly expressed in the tumor tissue of GR^{wt} mice while in the mucosa the expression remained low.

The last group are metalloproteinases that are associated with tumor infiltration. They were both highly expressed in tumor tissue of GR^{wt} and GR^{dim} mice. *Mmp13* was higher expressed in tumor tissue of GR^{wt} mice. In mucosa tissue the genes were slightly higher expressed than in the GR^{wt} mice. Regarding control mice no differences were observed in the mucosa of GR^{wt} and GR^{dim} mice (Figure 14).

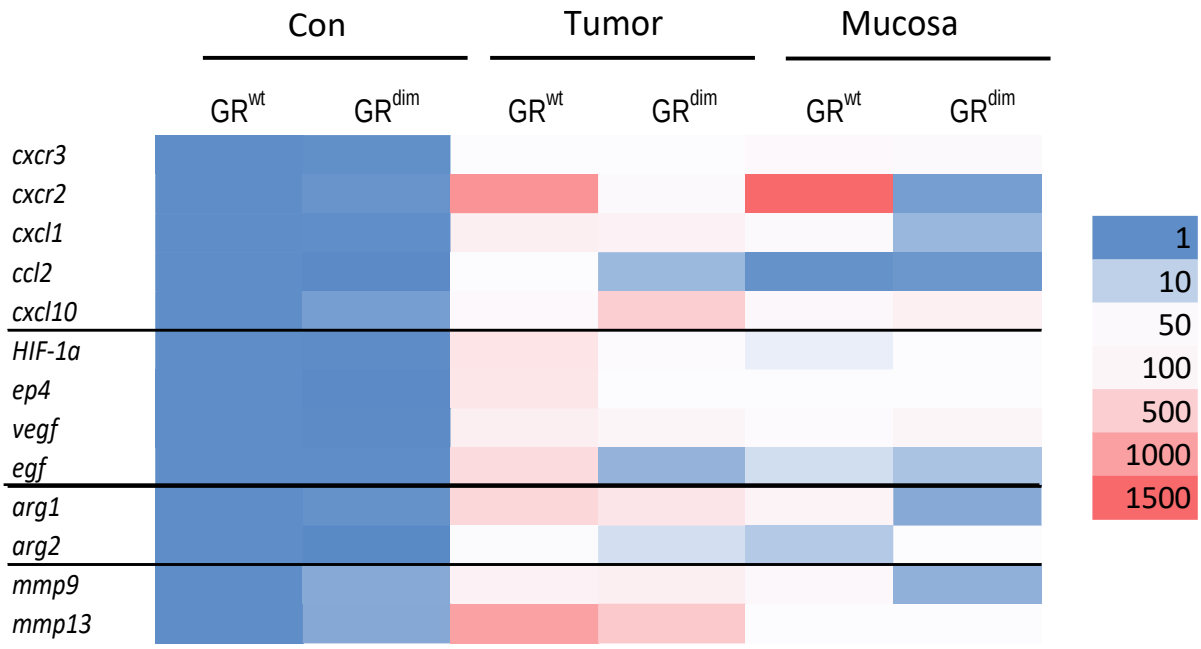

Figure 14: Fluidigm® gene chip analysis of mucosa and tumor tissue.

Mice were treated with AOM and 3.5% DSS. Control group received tap water and AOM injection. Mice were sacrificed when the tumors reached an S3 score. Total RNA and subsequently the mRNA were isolated. Gene expression analysis was done using Fluidigm Chip analysis. A color code is used to show the different gene expression, the lowest expression is represented in blue and the highest expression in red. Gene expression of control GR^{wt} mice was arbitrarily set to 1. GR^{wt} mice: n = 3/4/4, GR^{dim} mice: n = 3/5/4 (con/tumor /mucosa).

3.1.11 Establishment of GR^{dim} and GR^{wt} mice colonic organoids

Colonic organoids are one of the newest methods that allow the study of how cells interact and how diseases or drugs can affect them. The *in vitro* culture makes the organoids easy to manipulate and moreover it is a useful tool to spare animals. GR^{wt} and GR^{dim} mice were treated with 3.5% DSS for 8 days and with AOM, control mice received only tap water and the AOM injection. We then adapted a method to prepare and culture organoids from healthy mucosa tissue and from tumor tissue of BALB/c mice to be able to further investigate tumor development by making use of matched pair analysis (Klemke et al., 2021). Intestinal crypts were isolated from both colonic mucosa and tumors (Figure 15A). For the first time we isolated intestinal crypts from both GR^{wt} and GR^{dim} mice and used them for organoid culture (15B and C). These experiments open new perspective for GR^{dim} mice experiments since it is possible to study the colon environment of this mouse strain *in vitro*.

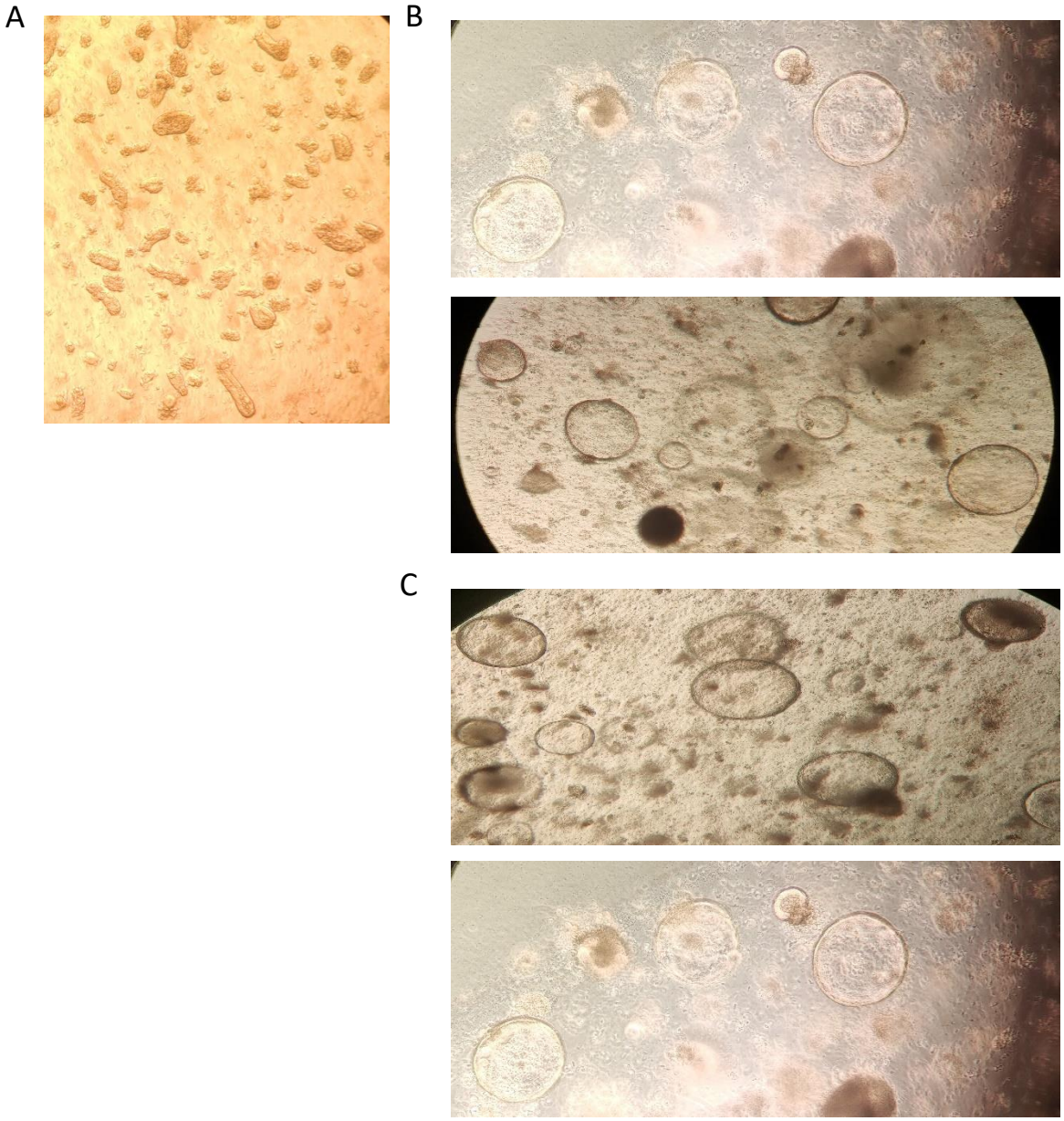

Figure 15: Organoid cultures from mucosa and tumor tissue.

Mice were treated with AOM and 3.5% DSS, control mice received tap water and only AOM. When the tumors reached the S3 stage, mice were sacrificed. A) Intestinal crypts were isolated from both tumors and mucosa tissue. B) Organoids culture from mucosa tissue. C) Organoids culture from tumor tissue.

3.2 The deletion of the GR in IECs aggravates DSS-induced colitis

3.2.1 DSS-induced colitis is aggravated in GR^{villin} mice

GR^{villin} and GR^{flox} were treated with tamoxifen by oral gavage to induce a knock-out of the GR in IECs in mutant mice. 1.2% DSS was then administrated via the drinking water for 8 days and then switched to tap water until day 10 while the control group received only tap water. DSS treatment resulted in a loss of body weight in the treated group, and the effect was increased in GR^{villin} mice compared to GR^{flox} mice. In contrast, the control group did not show any significant weight loss (Figure 16B). The DAI score of the mice, which represent the 3 major clinical hallmarks of colitis (weight, stool consistency and fecal blood), increased in DSS-treated mice until day 10 and it was significantly higher in GR^{villin} mice compared to GR^{flox} mice. The DAI score of the control mice remained unaltered (Figure 16A).

In addition, the colon of the mice was measured. No significant differences were observed at day 8 between DSS-treated mutant and non-mutant mice while at day 10 the colon was significantly shorter in GR^{villin} mice compared to GR^{flox} mice (Figure 16D).

IL-6 levels in the serum were measured via ELISA and higher at day 10 in GR^{villin} mice compared to GR^{flox} mice. The control group did not show any differences neither in colon length nor IL-6 serum levels (Figure 16C).

These results collectively demonstrate that the lack of the GR in IECs exacerbates DSS-induced colitis and that even after stopping the DSS-treatment at day 8 GR^{villin} mice cannot recover from colitis as well as GR^{wt} mice.

Results

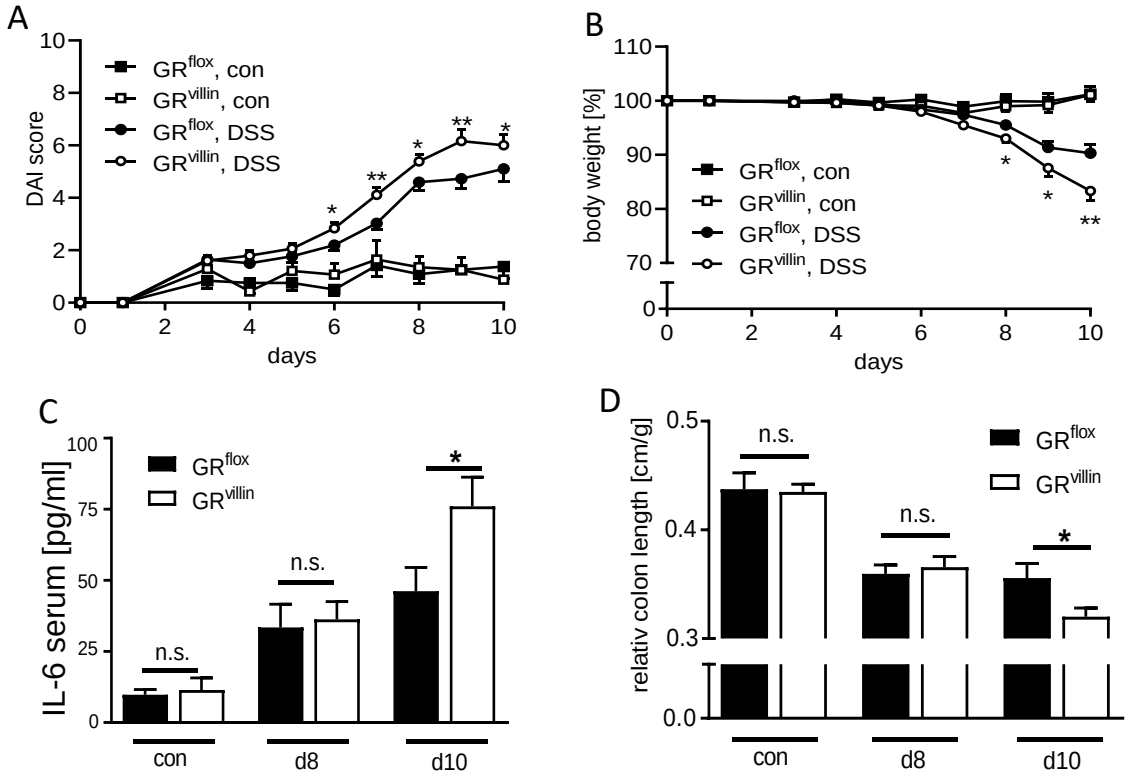

Figure 16: The impact of GR deletion in IECs on DSS-induced colitis.

A/B) Mice were treated with 1.2% DSS for 8 days and then with tap water until day 10. Control group received only tap water. The body weight is relative to the weight measured at day 0, and the DAI score were calculated based on stool consistence, intestinal bleeding, and weight loss. GR^{flox} mice: n =6/31, GR^{villin} mice: n =7/39 (con/DSS). C) The colon length of mice sacrificed at day 8 and 10 of DSS-treatment or control mice was measured. GR^{flox} mice: n =4/7/9, GR^{villin} mice: n =3/9/13 (con/ day 8/day 10). D) IL-6 serum levels of mice sacrificed at day 8 or 10 of DSS-treatment or control mice were analyzed by ELISA. GR^{flox} mice: n = 3/3/4, GR^{villin} mice: n = 2/7/6 (con/day 8/ day 10). All values are depicted as the mean ± SEM. Statistical analysis was performed by One-way ANOVA followed by Newman-Keuls Multiple Comparison test. Statistical analysis in panels A and B was performed individually for each day and is depicted for the comparison of DSS-treated GR^{flox} and GR^{villin} mice. Levels of significance: *: $p < 0.05$; n.s. (non-significant): $p > 0.05$. The graphs in panel A and B contain some data from former students. (Muzzi et al., 2021).

3.2.2 Increased intestinal permeability in DSS-treated GR^{villin} mice

DSS-treatment causes damage to IECs and thus compromises tissue permeability. To investigate the role of the GR in this process, an EB assay was performed to analyze epithelial permeability. The colon was removed, washed, filled with EB dye, and incubated on ice for 1 hour. The amount of EB dye that had diffused from the lumen of the colon into the tissue was quantified with the help of a standard curve and calculated relative to the weight of the colon. Treated mice, as expected, retained more EB in the colon compared to the control group. The relative amount of EB was significantly higher in the DSS-treated GR^{villin} mice compared to the GR^{flox} mice (Figure 17A and B). This result demonstrates that the GR in IECs plays a role in tissue permeability and that its deletion increases the permeability of the gut thus increasing the inflammatory response due to the increased diffusion of pathogens into the LP.

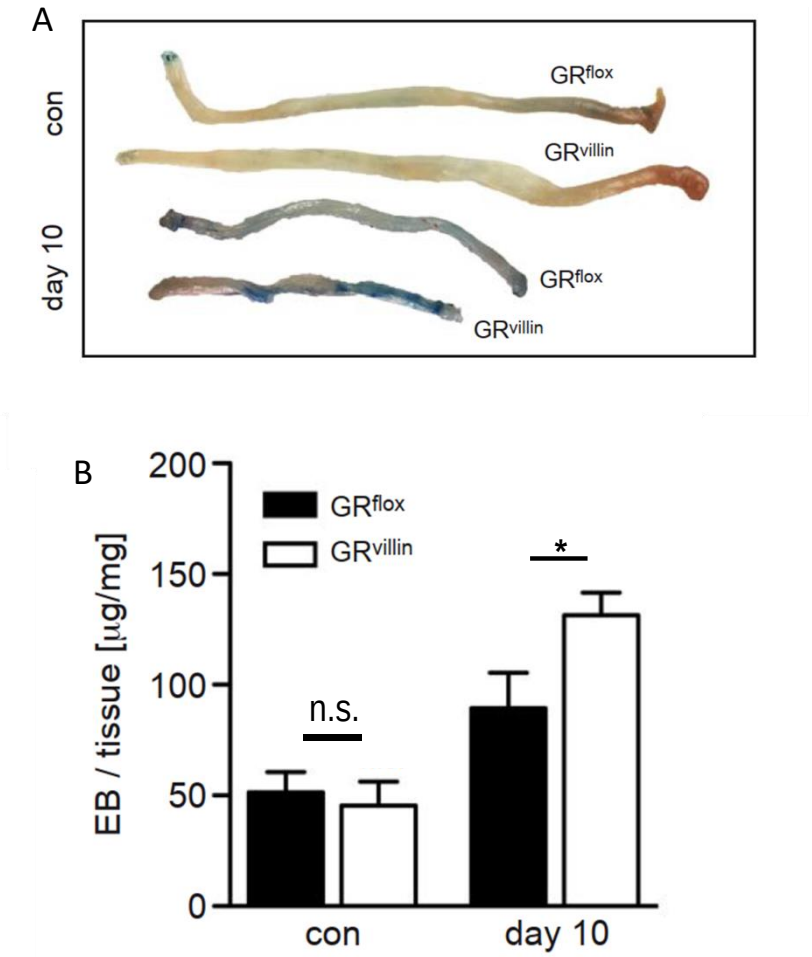

Figure 17: Analysis of the epithelial barrier integrity in DSS-induced colitis.

The colon was removed from 1.2% DSS-treated and control mice at day 10 and then filled with EB dye solution. EB that had diffused into the tissue was quantified by spectrophotometry. The amount of EB is depicted in relation to the weight of the colon. GR^{flox} mice: n = 4/7, GR^{villin} mice: n = 3/6 (con/day 10). A) Photographs of the colon after incubation with EB. B) The amount of EB in the tissue is depicted as the mean ± SEM. Statistical analysis was performed by One-way ANOVA followed by Newman-Keuls Multiple Comparison test and is depicted for the comparison of GR^{flox} and GR^{villin} mice at each time point. Levels of significance: *: $p < 0.05$; n.s. (non-significant): $p > 0.05$ (Muzzi et al., 2021).

3.2.3 Gene expression analysis of the whole colon

A Fluidigm® gene chip assay was performed with whole colon tissue to obtain a general impression of the gene expression profile in the entire organ. In total, 12 genes were analyzed in colon samples of both healthy and DSS-treated mice at day 8 and 12.

The first group of genes belongs to the CXCL family: *Cxcl1*, *Cxcl2* and *Cxcl5*. They are chemoattractants and mainly produced by IECs. Due to the aggravated colitis observed in GR^{villin} mice we expected a higher expression of these chemoattractants in mutant mice. Surprisingly, however, we observed a downregulation in GR^{villin} mice at day 10 compared to GR^{flox} mice.

The second group, chemokines of the CCL family and associated genes such as *Ccl2*, *Ccl3*, *Ccl5*, C*cl7* and *Cx3Cr1* were higher expressed in GR^{villin} mice compared to GR^{flox} mice. These molecules are chemoattractants that are mainly expressed by infiltrating cells as macrophages. CXCL- and CCL- family members are both involved in the recruitment of infiltrating cells and the regulation of the inflammatory response; moreover, they are also involved in cancer development.

The TLRs genes *Tlr2* and *Tlr4* were highly expressed in GR^{villin} mice compared to GR^{flox} mice. In contrast, the *Oct* gene, which encodes for ornithine transcarboxylase, and which is usually expressed in IECs, was expressed at lower levels in treated mice compared to healthy controls (Figure 18).

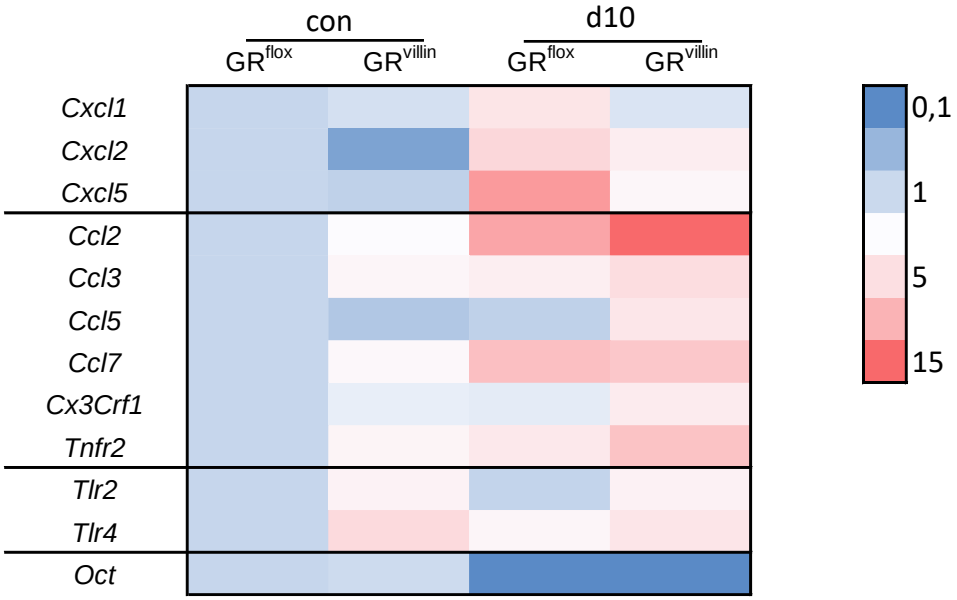

Figure 18: Fluidigm® gene chip analysis of whole colon tissue.

Mice were treated with 1.2% DSS and sacrificed at day 10. The control group received tap water. Total RNA and subsequently the mRNA were isolated and transcribed into cDNA. Gene expression analysis was done using a Fluidigm Microarray Chip. A color code is used to show the different gene expression, the lowest expression is represented in blue and the highest expression in red. Gene expression of control GR^{flox} mice was arbitrarily set to 1. GR^{flox} mice: n = 3/3, GR^{villin} mice: n = 3/5 (con/day 10). (Muzzi et al., 2021).

3.2.4 Gene expression analysis of purified IECs

Considering the fact that IECs in the mutant mice are devoid of the GR, a gene expression analysis of isolated IECs was performed by RT-qPCR. Expression of *Cxcl1*, *Cxcl5* and *Ccl5* were higher expressed in GR^{flox} mice but not in GR^{villin} mice compared to the respective control mice (Figure 19A, B, C). The high expression of these molecules in GR^{flox} mice indicates that the GR in IECs plays an important role for the induction of chemokine expression during an inflammatory response. Moreover, *Tlr4* which is involved in pathogen sensing, *Tnfr2* and *Mlck* which are important for the maintenance of barrier integrity were overexpressed in GR^{villin} mice compared to GR^{flox} and control mice (Figure 19D, E, F). Based on these data, we conclude that the GR in IECs is involved in the regulating of several different pathways for the control of the inflammation.

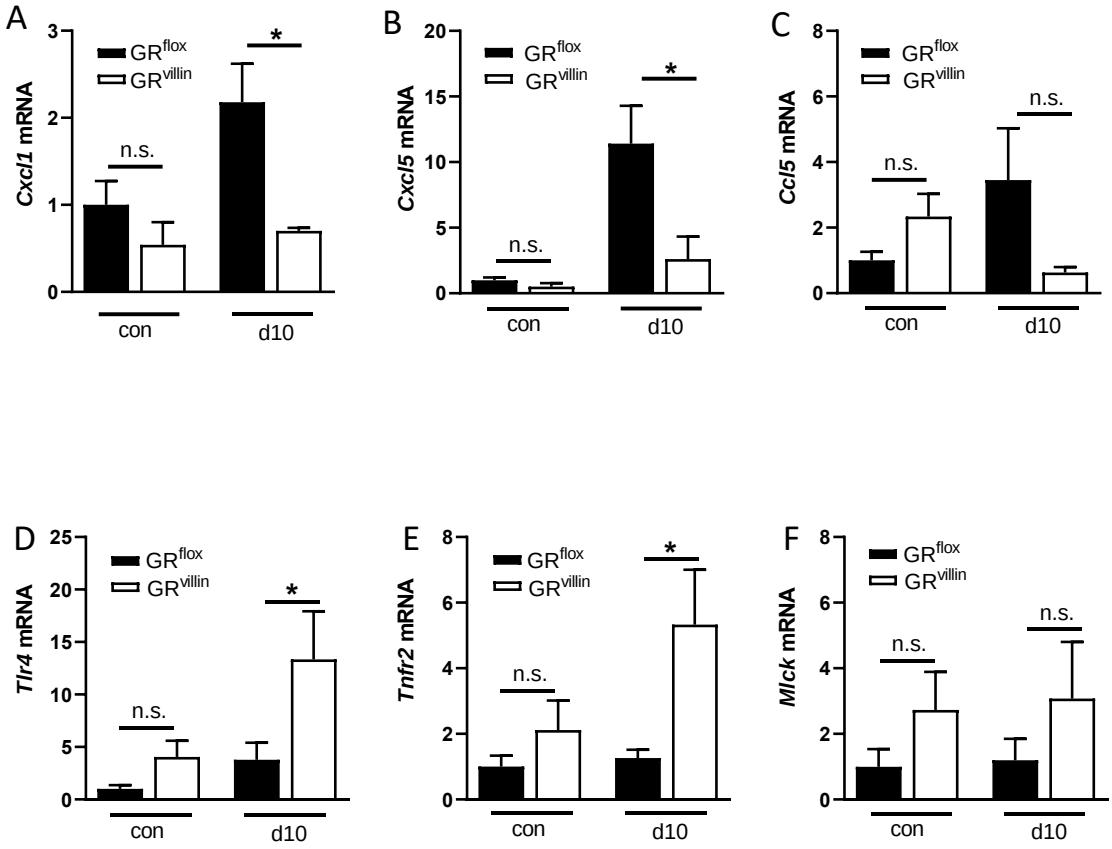

Figure 19: Gene expression analysis of purified IECs.

After tamoxifen treatment, GR^{flox} and GR^{villin} mice received 1.2% DSS to induce colitis for 8 days. Control (con) mice were treated with tamoxifen but received only tap water. IECs were isolated from the colon of control and DSS-treated mice at day 10 and gene expression analysis was performed using RT-qPCR. Relative mRNA levels were determined by normalization to the housekeeping gene *Hprt*. GR^{flox}, con: n = 5–6, GR^{flox}, DSS: n =6–11, GR^{villin}, con: n = 5–8, GR^{villin}, DSS: n=3–7. All values are depicted as the mean ± SEM. Statistical analysis was performed by One-way ANOVA followed by Newman-Keuls Multiple Comparison test and is depicted for the comparison of GR^{flox} and GR^{villin} mice at each time point. Levels of significance: *: $p < 0.05$; n.s. (non-significant): $p > 0.05$ (Muzzi et al., 2021).

3.2.5 FACS analysis of LPCs reveals reduced leukocyte infiltration in GR^{villin} mice

We previously observed that the chemokines CXCL1, CXCL5, and CCL5 were highly expressed in IECs of GR^{flox} but not of GR^{villin} mice. These chemoattractants play a fundamental role in attracting leukocytes such as neutrophils and monocytes. Consistently, we therefore decided to investigate if the lower expression in GR^{villin} mice also had an impact in the recruitment of immune cells into the LP during DSS-induced colitis. LPCs were isolated from control and DSS-treated mice at day 10 and analyzed by FACS. As previously outlined (Figure 11A), neutrophils were identified as $CD11b^{+}Ly6G^{+}$ cells, $CD11b^{+}Ly6G^{-}$ cells were identified as macrophages and inflammatory macrophages were distinguished thanks to their expression of Ly6C.

In agreement with the gene expression found in IECs, the presence of neutrophils, total macrophages, and inflammatory macrophages in the LP of GR^{villin} mice was reduced during DSS-induced colitis compared with GR^{flox} mice. This finding indicates that the recruitment of myeloid cells into the inflamed colon is diminished in the absence of the GR in IECs (Figure 20A, B, C).

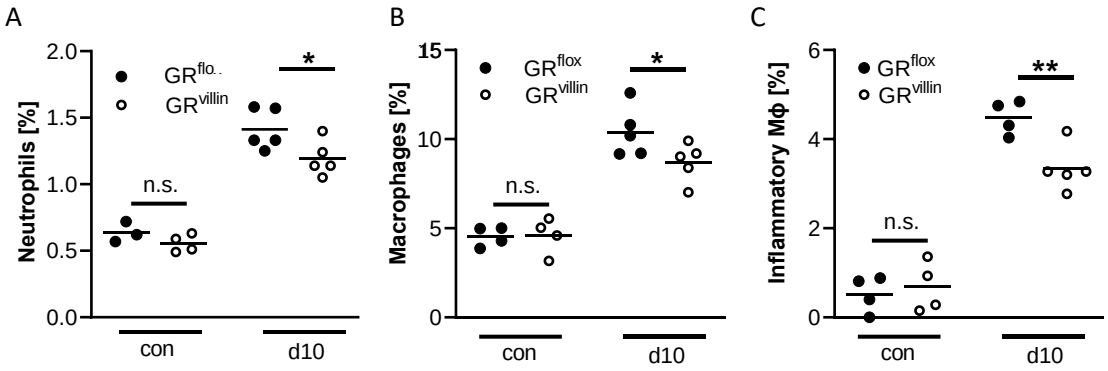

Figure 20: FACS analysis of infiltrating cells in the LP.

GR^{flox} and GR^{villin} mice were treated with tamoxifen to induce the deletion of GR in IECs and then received 1.2% DSS to induce colitis. Control mice received only tap water. LPCs were isolated from the colon of treated mice at day 10 and control mice and then used for FACS analysis. The graphs illustrate as a dot plot the percentages of neutrophils (A) and macrophages (B) as well as the percentage of inflammatory macrophage (Ly6C-) amongst all macrophages (C). Each dot corresponds to an individual mouse. GR^{flox}, con: n = 3–4, GR^{flox}, DSS: n=4–5, GR^{villin}, con: n= 4, GR^{villin}, DSS: n = 5. Statistical analysis was performed by One-way ANOVA followed by Newman-Keuls Multiple Comparison test. Levels of significance: *: $p < 0.05$; **: $p < 0.01$; n.s. (non-significant): $p > 0.05$ (Muzzi et al., 2021).

3.2.6 Infiltrating leukocytes in the colon of GR^{villin} mice are hyperactivated

GR^{villin} mice had a lower number of infiltrating neutrophils and macrophages in the LP during colitis but the clinical and histological hallmarks of the disease were exacerbated in GR^{villin} mice. Additionally, our gene expression analysis of whole colon tissue showed a higher expression of cytokines of the CCL family, which are mainly expressed by macrophages. In view of this fact, we investigated the expression of pro-inflammatory genes in LPCs

Cxcl1, *Cxcl5* and *Ccl5* expression in LPCs of GR^{villin} mice were higher than in GR^{flox} mice (Figure 21A, B, C). Moreover, expression of *Il1β*, *Il6* and *Ptgs2* was higher in LPCs of GR^{villin} mice during colitis (Figure 21D, E, F). These results reveal that LPCs in GR^{villin} mice are hyperactive. Because the GR is expressed at normal levels in these cells, we assume that the hyperactivation is a result of the aggravated colitis and increased barrier disruption in GR^{villin} mice. Since a lower number of immune cells is recruited to the site of inflammation in mutant mice, the clearance of pathogens is presumably inefficient and results in hyperactivation of the recruited immune cells.

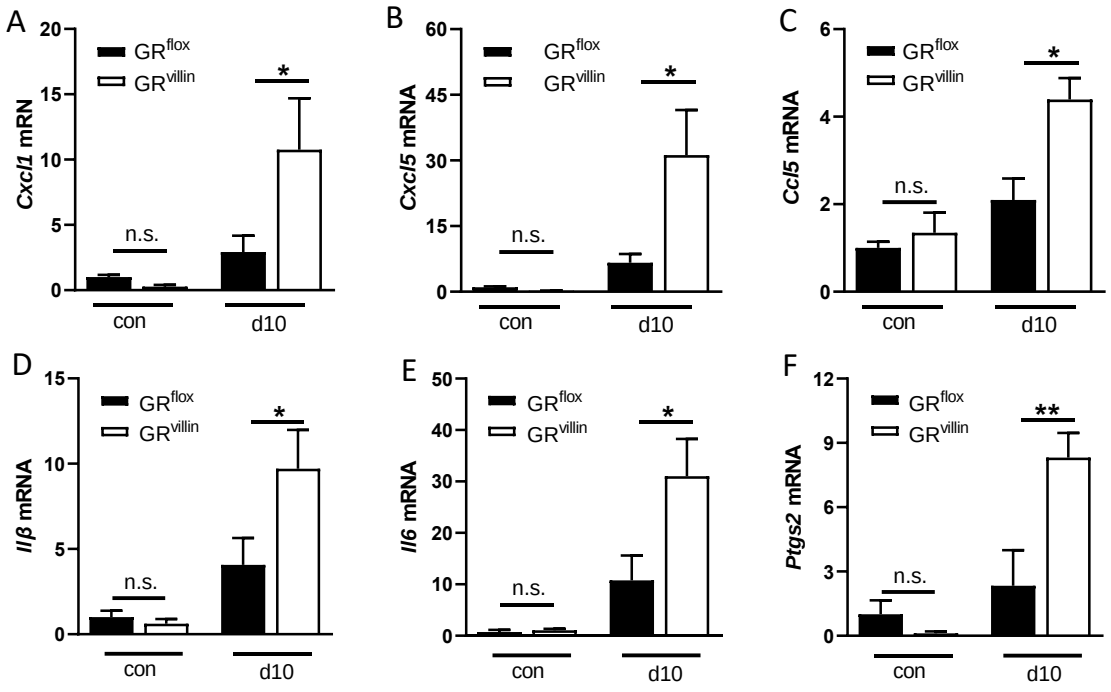

Figure 21: Gene expression analysis of LPCs.

LPCs were isolated from the colon of DSS-treated mice at day 10 or control mice. Gene expression analysis was performed by RT-qPCR. Relative expression of *Cxcl1*, *Cxcl2*, *Ccl5*, *Il1b*, *IL6*, and *Ptgs2* (Cox2) were determined by normalization to the housekeeping gene *Hprt*. GR^{flox}, con: n = 4, GR^{flox}, DSS: n = 4–8, GR^{villin}, con: n = 4, GR^{villin}, DSS: n = 4–9 (day8/ day12). Values are depicted as the mean ± SEM. Statistical analysis was performed by One-way ANOVA followed by Newman-Keuls Multiple Comparison test and is depicted for the comparison of GR^{flox} and GR^{villin} mice at each time point. Levels of significance: *: $p < 0.05$; **: $p < 0.01$; n.s. (non-significant): $p > 0.05$ (Muzzi et al., 2021).

4. Discussion

4.1 AOM/DSS-induced colitis and tumorigenesis in GR^{dim} mice

GR^{dim} mice are characterized by a point mutation, which impairs GR dimerization and DNA-binding. This mouse strain therefore allowed us to investigate the role of GR activities that are independent of dimers-formation and to test the receptor activity during crosstalk with other transcription factors in inflammation and tumorigenesis (Reichardt et al., 1998). GCs are known to mainly have anti-inflammatory activity, but their role is more extensive than this and we can define their action as pleiotropic. Studies have shown that GCs can act immunosuppressive and immunoenhancing depending on distinct factors. For instance, GCs induced by the circadian rhythm can enhance both B and T lymphocytes responses (Shimba et al., 2021). Moreover, due to the GRs broad expression in all body cells, the use of exogenous GCs is usually associated with side-effects (Poetker & Reh, 2010). Induction of AOM/DSS-colitis and subsequent tumorigenesis in GR^{dim} mice can provide a deeper insight into how the GR regulates intestinal inflammatory process and cancer development.

4.1.1 Impaired GR dimerization in GR^{dim} mice alleviates AOM/DSS- induced colitis and its clinical hallmarks in mice

It was previously demonstrated that GR dimers are essential in the protection against TNF-induced colitis (Ballegeer et al., 2018). In the context of DSS-induced colitis in GR^{dim} and GR^{wt} mice we observed that during treatment, the DAI increased with a peak at day 8 for both GR^{dim} and GR^{wt} mice. Interestingly, the mutant mice showed a faster recovery capability compared to GR^{wt} mice, and the clinical symptoms from day 8 to day 12 were less severe. At day 12 the DAI was significantly lower in the GR^{dim} mice compared to the GR^{wt} mice. We also analyzed colon length, which was observed to be shorter in IBD-affected patients and, and it was observed the same in DSS-treated mice (Nordgren et al., 1997). As expected from the disease course in both strains of mice, the relative colon length in GR^{dim} mice was greater at day 12 compared to GR^{wt} mice.

Moreover, IL-6 levels in the serum were reduced in GR^{dim} mice already at day 8. The GR can repress *Il6* gene expression independently from the presence of an nGRE in its promoter region: in fact, interaction with transcription factors such as NF-κB or AP-1 can successfully reduce IL-6 levels (de Bosscher et al., 2003). We conclude that the selective loss of GR dimerization, probably linked to the GCs pleiotropic effects, has a beneficial effect on colitis compared to mice with the full range of GR functions.

Histological features of IBD in humans are crypt architectural distortion, shortening and branching of the crypts, and the presence of infiltrating immune cells (DeRoche et al., 2014). DSS-induced colitis in mice shows a similar inflammatory pattern as crypts loss, IECs damage and inflammatory cells infiltration (Kitajima et al., 2000). To evaluate the DSS-induced damage of the colon in GR^{dim} and GR^{wt} mice, swiss-rolls of the whole colon were stained with H&E. After 4 days from terminating DSS treatment, colon damage and infiltrating cells were still abundant in GR^{wt} mice while in GR^{dim} mice inflammation and tissue damage were significantly reduced. These histological findings are in line with the DAI score in which we observed a reduced remission from colitis in GR^{wt} compared to GR^{dim} mice.

We assume that the impaired GR dimerization influences immune cell infiltration and tissue healing, which is aggravated in mice with normal GR gene regulation.

4.1.2 Gene expression analysis of the colon reveals different expression patterns in control and DSS-treated mice

In order to obtain a general impression of the gene expression pattern in colon tissue, Fluidigm Chip analysis of whole colon RNA was performed. *Il6, Tnfa* and *Il1b* are classic pro-inflammatory cytokines and their role in UC and cancer development has been elucidated in several studies. *Il6* has a key role in the uncontrolled intestinal inflammation. Its expression is also linked to an increased activation of the STAT3 pathway and the subsequent expression of anti-apoptotic genes such as Bcl-xL, which leads to apoptosis-resistant T cells, the perpetuation of the colonic inflammation and an increased risk to develop CACRC (Atreya & Neurath, 2005). *Il1b*, similarly to *Il6* perpetuates inflammation, and seems to be linked to an increased presence of Th17 cells in the colon during UC which is known to be deleterious during the disease (Coccia et al., 2012). *Tnfa* is a key player in UC, and. in fact, several drugs targeting this molecule were developed. *Tnfa* participates in macrophages activation, T cell responses, expression of adhesion molecules and recruitment of immune cells (Sands & Kaplan, 2007). Moreover, *Il6* and *Tnfa* regulate intestinal permeability in DSS-induced colitis, and neutralization of these two cytokines during colitis ameliorates the disease (Xiao et al., 2016). These three genes were observed to be expressed at lower levels in GR^{dim} mice at day 8 compared to GR^{wt} mice. The high expression of pro-inflammatory cytokines that perpetuates inflammation then also increased the expression of chemoattractive molecules such as *Cxcl1*, *Cxcl2* and *Cxcl5* in GR^{wt} mice at day 8, and *Cxcl5* expression remained high even at day 12. In GR^{dim} mice, expression of these molecules was low, only *Cxcl5* expression was slightly higher but still lower compared to GR^{wt} mice. *Ccl7*, *Ccl3*, *Ccl5* and *Ccl2* expressions were almost similar in both genotypes. These genes are involved in leukocytes recruitment, mainly of neutrophils and macrophages (Sawant et al., 2016; Wang et al., 2009). The lower expression of these molecules in GR^{dim} mice can be linked to the faster recovery from colitis and the lower number of infiltrating cells observed in the histological staining. It was demonstrated that a reduction of these molecules can be efficiently achieved even without the formation of GR dimers. Interaction with

transcription factors such as NF-κB or AP-1 in a dimer-independent way can lead to a reduced production of cytokines and chemokines (T. Liu et al., 2017)

We observed a differential gene expression also between untreated control mice of both genotypes. In untreated GR^{dim} mice, the TLR genes *Tlr2* and *Tlr4* were upregulated compared to untreated GR^{wt} mice. It is worth mentioning that GCs are known to induce expression of *Tlr2* as an anti-inflammatory mechanism (Hoppstädter et al., 2019). In our mouse model, we observed that impaired GR dimerization increases not only *Tlr2* but also *Tlr4* expression. This upregulation in mutant mice could have a protective effect since the uptake of antigens could be improved.

Regarding genes involved in macrophages polarization, *Ym1* was downregulated in GR^{dim} mice at day 8 and *Arg1* was slightly downregulated at day 12 in GR^{dim} mice. *Arg1*, which converts l-arginine into ornithine and urea, is not only a murine M2 macrophage marker but it is also associated with an impaired resolution from colitis by altering the microbiome. Moreover, it is also associated with cancer development (Baier et al., 2020; Raes et al., 2005; You et al., 2018). GCs are known for their role in directing macrophage polarization towards the M2 phenotype thereby promoting tissue healing and the anti-inflammatory activity (Desgeorges et al., 2019). The increased presence of alternatively activated M2 macrophages in GR^{wt} mice could be associated with the increased tissue damage observed in the histological results.

We also observed a differential expression of genes associated with TJs in control mice. Intestinal permeability is compromised during UC in humans (Michielan & D'Incà, 2015), a dysregulation which is also present in DSS-induced colitis in mice. Genes such as *Claudin2*, *Occludin*, *Mlck* and *Tnfr2* are usually dysregulated during colonic inflammation and their upregulation is associated with a leaky colon (Luettig et al., 2015; Su et al., 2013; Yamamoto-Furusho et al., 2012). It was demonstrated that the increased expression of *Claudin2* in the colon before induction of colitis has a protection effect. A high expression of this gene is associated with an increased anergy of the immune cell in the LP thus reducing the abnormal immune response during colitis. In line with this observation, GR^{dim} control mice, which have an

increased expression of *Claudin2*, showed a less severe colitis after DSS treatment (Ahmad et al., 2014). In order to better understand if the permeability of the gut in GR^{dim} mice was less compromised compared to GR^{wt} mice, we also performed two preliminary experiments with different methods to study colon permeability. EB and FITC-Dextran experiments were performed in untreated mice to determine whether the differential TJ gene expression had any real impact on the permeability or not. Both experiments unveiled an increased permeability in control GR^{wt} mice whereas the permeability of the colonic epithelium in GR^{dim} mice was slightly lower. However, further experiments must be done to confirm this finding. In any way, we assume that an impaired GR dimerization exerts a protective effect on colon permeability and regulates the expression of genes that contribute to it.

The high expression of TLRs in the whole colon of GR^{dim} control mice described before was investigated, too. Since we hypothesized that this alteration was associated with a better clearance of bacterial antigens, we isolated the mesenteric lymph nodes, and investigated the bacterial content. In line with our hypothesis, expression of the bacterial 16S rRNA gene was elevated in the mesenteric lymph nodes of control GR^{dim} mice compared to control GR^{wt} mice. This indicates an increased bacterial uptake thanks to TLR overexpression and a reactive immune system that confers a protective environment in the colon of GR^{dim} mice during DSS-colitis.

Finally, cytokine concentrations in the rectal part of the colon were also analyzed in organ culture supernatants. In this case no differences were observed in untreated control mice. In DSS-treated mice the concentration of CXCL1 was lower in colon supernatants of GR^{dim} mice at both day 8 and 12, and the same pattern was found for CXCL10 and CCL2, highlighting again the increased presence of chemoattractants in the colon of GR^{wt} mice. The concentration of pro-inflammatory cytokines was lower in colon supernatants of GR^{dim} mice as well, except for GM-CSF which was almost equally abundant in both GR^{dim} and GR^{wt} mice at day 8 and 12. These results are well in line with the gene expression data and reinforce the idea that impaired GR

dimerization reduces inflammation during DSS-colitis, while normal GR gene regulation rather impairs the recovery from colitis and aggravates it.

4.1.3 Decreased cellular infiltration and reduced expression of pro-inflammatory genes in the LP of GR^{dim} mice

Due to the differential gene expression in the whole colon, we decided to verify it in LP cells and test whether there were differences in infiltrating cells during DSS-induced colitis, too.

The infiltrating cells in the LP play a crucial role in DSS-induced colitis; an increased number of cells could be associated with an exacerbated disease (Maltby et al., 2010). For instance, the inhibition of adhesion molecules, which mediates the recruitment of inflammatory cells ameliorates colitis (Kato et al., 2000). By contrast, we observed that a higher number of infiltrating cells is not necessarily correlated with more severe colitis but that the expression of pro-inflammatory cytokines by LPCs also plays a crucial role in colitis (Muzzi et al., 2021). For this purpose, we first investigated the inflammatory infiltrates in the LP via FACS analysis.

Flow cytometry revealed an increased percentage of neutrophils at day 8 in GR^{wt} mice while in GR^{dim} mice the percentage remained low. No differences were observed in the percentage of total macrophages, but the relative proportion of inflammatory macrophages amongst all macrophages was significantly lower in GR^{dim} mice at day 8 compared to GR^{wt} mice. Hence, we observed an increased immune cell infiltration in GR^{wt} mice which corroborates the histological findings as well as the high expression of chemoattractants observed on the level of gene expression and in colon supernatants.

Then, we evaluated the expression of genes in LPCs, since pro-inflammatory genes as well as chemoattractants were downregulated in GR^{dim} mice at day 8. Hence, we analyzed their expression specifically in LPCs to understand the role of impaired GR dimerization in these cells.

Discussion

Il6 was highly expressed in GR^{wt} mice in LPCs which confirms the Fluidigm results, while *Il1b* was higher in GR^{wt} mice at day 12. *Il1b* was highly expressed in the whole colon of GR^{wt} mice at day 8 while in LPCs the highest expression was observed at day 12. Accordingly, we assume that at day 8, *Il1b* was regulated by different cell types within the colon. Expression of the *Ptgs2* gene (Cox2) was downregulated in GR^{dim} mice at day 12 with a significant difference compared to the GR^{wt} mice. All these three genes play an important role not only in the propagation of inflammation but also in tumor development. Cox2 promotes tumor growth and suppresses anti-tumor immunity (B. Liu et al., 2015), and the same role can be fulfilled by *Il6* and *Il1b* (Atreya & Neurath, 2005; Gelfo et al., 2020). The mechanism of GCs in the regulation of these genes is known to be both DNA-dependent and -independent as nGREs are present in the promoter of the *IL1B* and *IL6* genes. Downregulation of these genes takes place also thanks to the interaction with transcription factors such as STAT family members and NF-κB, or due to the induction of inhibitors of the JAK-STAT signaling pathways (Cain & Cidlowski, 2017). Therefore, we observed that protein-protein interaction alone has a beneficial effect in dampening the pro-inflammatory response by lowering the production of inflammatory mediators. *Cxcl1* expression in LP showed only slight differences between the genotypes a day 8 while at day 12 the expression was the same. This is similar to what we observed in the Fluidigm Chip analysis where the different gene expression was not markedly changed especially at day 12.

When we investigated anti-inflammatory genes, no differences were observed in *Il10* expression. *Ym1* is a marker for alternatively activated M2 macrophages (Raes et al., 2005) and slightly downregulated in GR^{dim} mice at both day 8 and day 12, although not significantly. The higher expression of this gene in GR^{wt} mice could be linked to the increased tissue damage, which leads to an increased presence of M2 macrophages required for tissue healing. Moreover, the presence of M2 macrophages is also linked to the development of CACRC. The anti-inflammatory activity of these cells impairs the immune response against cancer cells, so M2 macrophages could be

associated with a higher risk to develop tumors in GR^{wt} mice (Wang et al., 2015). GCs are known to regulate macrophages polarization, promoting anti-inflammatory M2 macrophages to limit the immune response, so the increased presence of these cells in GR^{wt} mice is probably linked to the full spectrum of GR action. Hence, the overall non-specific immunosuppression of GCs can also have undesirable effects for cancer progression.

4.1.4 GR^{dim} mice develop less tumors and show reduced expression of genes involved in cancer development

UC is known to be associated with the development of CACRC, and the extent and the duration of colitis are key factors in this process (Kulaylat & Dayton, 2010). Since we observed a more severe colitis in GR^{wt} mice compared to the mutant mice in terms of infiltrating cells, recovery time, histological findings, gene expression and clinical hallmarks, we investigated the consequences on cancer development.

Mice were treated with AOM and then received DSS via the drinking water for 8 days. Tumors formation then required around 6-9 weeks. During this time, the mice were monitored via colonoscopy. Once stage S3-4 tumors were identified, the mice were sacrificed, the tumors counted, and their size measured. The number of tumors was significantly lower in GR^{dim} mice compared to GR^{wt} mice, whereas no significant difference was observed in tumor size although the area of GR^{dim} mice tumors was slightly smaller. So, in line with the colitis results, GR^{dim} mice showed a reduced tumors burden compared to GR^{wt} mice.

We additionally investigated gene expression in both tumors and mucosa tissue in GR^{dim} and GR^{wt} mice. Noteworthy, no differences were observed in control mice. Firstly, chemokines and their receptors were analyzed: *Cxcr3* was equally expressed in mucosa and tumor tissue of both GR^{dim} and GR^{wt} mice. *Cxcr2* was downregulated in GR^{dim} mucosa and tumor tissue compared to the high expression observed in GR^{wt} mice. *Cxcr2* has a role in cancer progression and angiogenesis (Jaffer & Ma, 2016) and the presence of this receptor in colorectal cancer is associated with poor prognosis in humans (Zhao et al., 2017). No differences were observed in *Cxcl1* expression in

tumor tissue of GR^{dim} and GR^{wt} mice, but the gene was downregulated in the mucosa of GR^{dim} mice. Overexpression of this gene is associated with an increased growth of murine fibroblast in colorectal cancer and its expression in mucosa tissue could be linked to the higher number of tumors in GR^{wt} mice (le Rolle et al., 2015). *Ccl2* was slightly downregulated in tumor tissue of GR^{dim} mice and the same was observed in mucosa tissue. In contrast, *Cxcl10* was upregulated in both mucosa and tumor tissue of GR^{dim} mice. *Ccl2* is associated with cancer development in several cancer entities and shapes a tumor permissive microenvironment (Chun et al., 2015). *Cxcl10* expression in tumor tissue is usually associated with T cell recruitment, which is beneficial for anti-cancer immunity (Mowat et al., 2021). Regarding this first group of genes, our results reveal a high expression of genes that are associated with tumor progression in GR^{wt} mice whereas *Cxcl10* which is rather associated with anti-cancer immunity, is upregulated in GR^{dim} mice.

Next, we investigated the expression of some genes which are associated with tumor progression, angiogenesis, and metastasis. *Hif1a* plays a crucial role in tumor hypoxia and contributes to tumor aggressiveness (Ioannou et al., 2015). The prostaglandin E receptor *Ep4* increases the survival and tumor vasculature in colon cancer cells via the Cox2 pathway (Karpisheh et al., 2020), *Vegf* is known for its role in tumor angiogenesis and *Egf* seems to be associated with an M2 polarization in the cancer microenvironment and the regulation of cancer stem cell proliferation (Ahluwalia et al., 2014; Feng et al., 2012; Lian et al., 2019). All these genes were higher expressed in tumor tissue of GR^{wt} mice compared to GR^{dim} mice while no significant differences were observed in mucosa tissue.

Arg1 and *Arg2* expression in cancer is generally high and linked to the regulation of tumor growth and metastasis. Moreover, *Arg1* is a marker of poor prognosis in humans (Ma et al., 2019; Niu et al., 2022). Both genes were downregulated in tumor tissue of GR^{dim} mice, especially *Arg2*.

The last group of genes that we analyzed are the matrix metalloproteinases *Mmp9* and *Mmp13*. These genes regulate tumor infiltration and are associated with

metastasis and poor prognosis (Yamada et al., 2010; Yang et al., 2014). In tumor tissue, *Mmp9* expression was the same in GR^{wt} and GR^{dim} mice while *Mmp13* was downregulated in GR^{dim} mice. In the mucosa, slight differences were observed but didn't reach significance.

Collectively, gene expression analysis of tumor and mucosa tissue of GR^{dim} and GR^{wt} mice unveils, as expected, an increased susceptibility to tumor formation in GR^{wt} mice. The development of CACRC is strongly associated with the immune response during colitis and tissue damage, and the subsequent immune response against it can reduce or increase the risk of cancer. Impaired GR dimerization also attenuates colitis and its clinical hallmarks, and moreover, LPCs infiltration and the expression of pro-inflammatory genes by infiltrating cells are reduced in GR^{dim} mice. Therefore, the altered gene regulation in GR^{dim} mice seems to confer a protective effect for both colitis and tumorigenesis.

4.1.5 Organoids from the colon of GR^{dim} and GR^{wt} mice, a new prospective for animal studies

Colonic murine organoids are three-dimensional crypts growing *in vitro* that allow the study of a specific mouse model and a specific disease thanks to their realistic microanatomy. Organoids enable the investigation of the pathophysiology of several disease such as DSS-induced colitis and CACRC. Moreover, they are a useful tool to spare animals (Fan et al., 2016). Organoids from both colon and small intestine have been widely used in the last years for the analysis of several mechanism involved in colon cancer and inflammation.

We adapted a protocol to grow murine organoids from colonic mucosa and tumors tissue of GR^{dim} and GR^{wt} mice on the BALB/c background, with the aim to mimic the environment during the disease and to analyze them in an easy way since tumors formation in mice requires a long time. The use of organoids allows the culture of tumors harvested from both GR^{dim} and GR^{wt} mice and the possibility to use them for experiments such as the investigation of proliferation in both genotypes, while *in vivo*

research is limited to the analysis of tumor numbers and by the time needed for tumor formation.

4.1.6 Conclusions from the GR^{dim} mice project

Endogenous GCs regulate several aspects of the immune system through different pathways. Gene regulation employs two major mechanisms, which are either GR dimerization-dependent or -independent. The role of CGs in the immune system is mainly believed to be anti-inflammatory but it is better to be defined as pleiotropic since GCs can act also act as immune enhancers and cooperate with pro-inflammatory molecules such as TNF-α (Lannan et al., 2012). However, all the mechanisms exerted by GCs are believed to prepare the immune system to better react to the stress of inflammation. We decided to better elucidate the mechanism by which endogenous GCs regulate DSS-induced colitis and the subsequent CACRC formation and to test if gene regulation exerted by GR dimerization has a beneficial effect on the disease or not. We observed that the impaired GR dimerization in GR^{dim} mice is beneficial in colitis and cancer development, whereas in contrast GR^{wt} mice were more likely to developed cancer and colitis. We assume that the gene expression in GR^{dim} mice favors a colonic environment in which the immune response during colitis is better controlled thus also reducing subsequent cancer development.

Studies suggested that the type of stress and the level of GCs at the basal state have a key role in shaping the GCs immune response and that these factors can contribute to a pro- or anti-inflammatory response (Cruz-Topete & Cidlowski, 2015). Even if the level of GCs in both mutant and non-mutant mice should be the same under basal and inflamed conditions, it is possible that the impaired GR dimerization in GR^{dim} mice reduces the pro-inflammatory gene regulation exerted by GCs during colitis as well as in control mice since different gene expression was also observed in the control group. This also opens the question whether a treatment, which only targets the DNA-binding-independent mechanism, e.g., by using SEGRAMs, could be more effective for UC and in preventing cancer. Moreover, in this study we only analyzed the role of GR dimerization in DSS-induced colitis but effects in other chronic diseases could

be potentially investigated as well to better understand the gene regulation exerted by GCs on the immune system.

4.2 GR deletion in IECs in DSS-induced colitis

IECs are one of the main barriers against pathogen invasion and segregate the immune system from the microbiota. This prevents an abnormal immune response against it, which can eventually result in chronic inflammatory disorders such as IBD. Moreover, IECs express a variety of receptors and interact with both immune cells and bacteria to regulate them. During UC, IECs have a key role in the control of immune cells and in the regulation of inflammation. The role of GR in IECs during UC was unclear until recently. Studies have shown that GCs in IECs can regulate T cell responses (Cima et al., 2004) and that the deletion of the GR in IECs upregulates cytokines in the gut under basal conditions (Aranda et al., 2019). However, the role of the GR during DSS-induced colitis had not been investigated so far. Since GC treatment is widely used during UC and since GCs can act on all cell types, it is important to better understand the role of endogenous GCs during inflammation in a specific tissue or cell type. So, we decide to elucidate the role of the GR in IECs during inflammation in a mouse model, which carries an inducible deletion of the GR in IECs. These $GR^{VillinCreERT2}$ mice are dedicated here as GR^{villin} mice.

4.2.1 Lack of the GR in IECs aggravates DSS-induced colitis and increases colon permeability

The lack of the GR in IECs during DSS treatment unveiled that its regular presence is essential for controlling intestinal inflammation. The DAI of GR^{villin} mice was significantly higher compared to GR^{flox} mice, and the recovery phase was impaired in mutant mice. Furthermore, the bodyweight of GR^{villin} mice was significantly lower compared to wildtype littermates. The reduction of the colon length and the increased IL-6 level in the serum of GR^{villin} mice highlight the importance of the GR in the control of intestinal inflammation. Colon permeability, which was tested with an EB experiment, confirmed the importance of the GR in regulating epithelial integrity in the colon and TJ gene expression. Deletion of the GR in IECs increased the

permeability of the colon during colitis thus enhancing the passage of bacteria into the LP. All these findings together unveil the role of the GR and endogenous GCs in DSS-colitis and their protective role exerted in IECs since the GR's absence in IECs aggravates inflammation and enhances the permeability of the colon (Muzzi et al., 2021).

4.2.2 Gene expression in colon tissue revealed a differential gene regulation in GR^{villin} and GR^{flox} mice

Fluidigm chip analysis provided an overview of gene expression in whole colon tissue. An increased expression of the chemoattractants *Cxcl1*, *Cxcl2* and *Cxcl5* was observed in GR^{flox} mice even though colitis in these mice was less severe. These molecules are required for immune cells recruitment into the inflamed area. GCs were previously associated with the expression of chemoattracts in several tissues such as *Ccl20* in the airway epithelium (Zijlstra et al., 2014), or with increased chemotaxis of monocytes in multiple sclerosis patients (Fischer et al., 2019).

The expression of cytokines and their receptor was upregulated in the colon of GR^{villin} mice, which can be attributed to the more severe colitis. The same was observed for *Tlr* genes. Moreover, *Tlr* genes were also upregulated in control GR^{villin} mice, which received tamoxifen treatment but not DSS, so the lack of the GR in IECs seems to influence *Tlr* expression even without inflammatory stimuli.

Albeit a differential gene regulation in the colon was observed between GR^{villin} and GR^{flox} mice in DSS-induced colitis, but deeper insights are required to understand how the lack of the GR in IECs affects individual cell types in the colon (Muzzi et al., 2021).

4.2.3 IEC gene expression unveils a low expression of chemoattractants in the colon of GR^{villin} mice

The gene expression analysis of isolated IECs of GR^{villin} and GR^{flox} mice at day 10, two days after termination of the DSS treatment, revealed a high expression of chemoattractants in the colon of GR^{flox} mice. These genes were downregulated in GR^{villin} mice, which is in line with the results from the Fluidigm® chip analysis of the whole colon tissue. As mentioned above, the role of GCs in inducing chemotaxis has already been described in other tissues. In our study we demonstrated that the GR in IECs is essential for a full induction of chemokine expression. This finding was in line with our analysis of infiltrating cells in the LP of the colon.

GCs were previously reported to regulate *Tlr4* gene expression (Curtale et al., 2017), and consequently we also observed an upregulation of *Tlr4* in IECs of GR^{villin} mice at day 10. At normal levels, the GR in GR^{flox} mice can probably control expression of *Tlr4* in order to sense pathogens, while in GR^{villin} mice the lack of the GR in IECs results in an enhanced expression of *Tlr4* thus increasing the activation of pro-inflammatory pathways such as NF-κB.

The *Mlck* and *Tnfr2* genes are associated with TJs and colon permeability and were upregulated in GR^{villin} mice at day 10. Their high expression is usually associated with increased colon permeability (Su et al., 2013), for this reason these results are in line with our EB experiment (Muzzi et al., 2021).

4.2.4 FACS analysis of LPCs reveals a reduced leukocyte infiltration in GR^{villin} Mice

To corroborate the low expression of chemoattractants in GR^{villin} mice, infiltrating cells in the LP were investigated by flow cytometry. We observed that the number of infiltrating cells in the LP was significantly lower in GR^{villin} mice compared to GR^{flox} mice. This concerned neutrophils, total macrophages, and inflammatory macrophages. It had already been demonstrated that GCs affect neutrophil motility and function (Ronchetti et al., 2018; Zak-Nejmark et al., 1996), and the same was observed for macrophages (Desgeorges et al., 2019). However, in this case the lower percentage of infiltrating cells in the LP is probably caused by regulation of chemoattractant expression in IECs via the GR rather than direct effects of GCs on inflammatory cells. We assume that the increased presence of these cell in the LP of GR^{flox} mice has a protective effect, which helps in the clearance of pathogens while in GR^{villin} mice their lower number results in an impaired eradication of invading pathogens leading to an aggravated DSS-induced colitis and a slower recovery.

Despite being less abundant, the infiltrating cells in the LP of GR^{villin} mice are hyperactivated due to their inability to resolve the inflammation. *Cxcl1*, *Cxcl5* and *Ccl5* are upregulated in the LP of GR^{villin} mice, thus indicating that immune cells are trying to recruit more infiltrating cells to resolve the inflammation. *Il6*, *Il1b* and *Ptgs2* are also upregulated in GR^{villin} mice contributing to the abnormal immune response usually observed in UC. Moreover, the high expression of these genes is also associated with the increased cancer development that we observed in GR^{villin} mice (Muzzi et al., 2021).

4.2.5 Conclusions from the GR^{villin} project

In this study we unveiled a specific role of the GR during DSS-induced colitis in a specific cell type, namely the IECs, which play a key role in the regulation of UC. We provide evidence that the GR in IECs is essential for controlling DSS-induced colitis, since the clinical hallmarks and pathological features were higher in GR^{villin} mice, and since it could be shown that the GR has a significant role in the regulation of the epithelial barrier permeability.

The gene regulation by the GR also unveiled their vital role for chemotaxis of immune cells. Expression of the GR in IECs is essential for the full induction of chemokines and for the recruitment of inflammatory cells into the LP, which leads to an increased clearance of pathogens. The lack of the receptor is associated with a decreased number of infiltrating cells in the LP, although these cells are hyperactivated probably due to the inability in controlling the inflammation. Moreover, the high expression of pro-inflammatory cytokines in GR^{villin} mice may also play a role in tumor formation (Muzzi et al., 2021).

Collectively, we provide evidence that the presence of the GR in IECs is essential in the control of colonic inflammation, and that a targeted therapy could be a beneficial option to reduce the adverse effects, which are associated with GC treatment. Further studies must be conducted to better understand if the use of specific therapies such as NPs which target the GR in IECs is a promising option for UC treatment.

5. References

Ahluwalia, A., Jones, M. K., Matysiak-Budnik, T., & Tarnawski, A. S. (2014). VEGF and colon cancer growth beyond angiogenesis: does VEGF directly mediate colon cancer growth via a non-angiogenic mechanism?. *Current pharmaceutical design*, *20*(7), 1041–1044. https://doi.org/10.2174/13816128199991312181759O5

Ahmad, R., Chaturvedi, R., Olivares-Villagómez, D., Habib, T., Asim, M., Shivesh, P., Polk, D. B., Wilson, K. T., Washington, M. K., Van Kaer, L., Dhawan, P., & Singh, A. B. (2014). Targeted colonic claudin-2 expression renders resistance to epithelial injury, induces immune suppression, and protects from colitis. *Mucosal immunology*, *7*(6), 1340–1353. https://doi.org/10.1038/mi.2014.21

Ahmed, A., Schmidt, C., & Brunner, T. (2019). Extra-Adrenal Glucocorticoid Synthesis in the Intestinal Mucosa: Between Immune Homeostasis and Immune Escape. *Frontiers in immunology*, *10*, 1438.
https://doi.org/10.3389/fimmu.2019.01438

Anderson, W. C., 3rd, & Szefler, S. J. (2019). Cost-effectiveness and comparative effectiveness of biologic therapy for asthma: To biologic or not to biologic?. *Annals of allergy, asthma & immunology : official publication of the American College of Allergy, Asthma, & Immunology*, *122*(4), 367–372.
https://doi.org/10.1016/j.anai.2019.01.018

Antoni, L., Nuding, S., Wehkamp, J., & Stange, E. F. (2014). Intestinal barrier in inflammatory bowel disease. *World journal of gastroenterology*, *20*(5), 1165–1179. https://doi.org/10.3748/wjg.v20.i5.1165

Aranda, C. J., Arredondo-Amador, M., Ocón, B., Lavín, J. L., Aransay, A. M., Martínez-Augustin, O., & Sánchez de Medina, F. (2019). Intestinal epithelial deletion of the glucocorticoid receptor NR3C1 alters expression of inflammatory mediators and barrier function. *FASEB journal : official publication of the Federation of American Societies for Experimental Biology*, *33*(12), 14067–14082. https://doi.org/10.1096/fj.201900404RR

Aratari, A., Papi, C., Clemente, V., Moretti, A., Luchetti, R., Koch, M., Capurso, L., & Caprilli, R. (2008). Colectomy rate in acute severe ulcerative colitis in the infliximab era. *Digestive and liver disease : official journal of the Italian Society of Gastroenterology and the Italian Association for the Study of the Liver*, *40*(10), 821–826. https://doi.org/10.1016/j.dld.2008.03.014

References

Arnone, D., Vallier, M., Hergalant, S., Chabot, C., Ndiaye, N. C., Moulin, D., Aignatoaei, A. M., Alberto, J. M., Louis, H., Boulard, O., Mayeur, C., Dreumont, N., Peuker, K., Strigli, A., Zeissig, S., Hansmannel, F., Chamaillard, M., Kökten, T., & Peyrin-Biroulet, L. (2021). Long-Term Overconsumption of Fat and Sugar Causes a Partially Reversible Pre-inflammatory Bowel Disease State. *Frontiers in nutrition*, *8*, 758518. https://doi.org/10.3389/fnut.2021.758518

Artis D. (2008). Epithelial-cell recognition of commensal bacteria and maintenance of immune homeostasis in the gut. *Nature reviews. Immunology*, *8*(6), 411–420. https://doi.org/10.1038/nri2316

Atarashi, K., Tanoue, T., Oshima, K., Suda, W., Nagano, Y., Nishikawa, H., Fukuda, S., Saito, T., Narushima, S., Hase, K., Kim, S., Fritz, J. V., Wilmes, P., Ueha, S., Matsushima, K., Ohno, H., Olle, B., Sakaguchi, S., Taniguchi, T., Morita, H., … Honda, K. (2013). Treg induction by a rationally selected mixture of Clostridia strains from the human microbiota. *Nature*, *500*(7461), 232–236. https://doi.org/10.1038/nature12331

Atreya, R., & Neurath, M. F. (2005). Involvement of IL-6 in the pathogenesis of inflammatory bowel disease and colon cancer. *Clinical reviews in allergy & immunology*, *28*(3), 187–196. https://doi.org/10.1385/CRIAI:28:3:187

Atsuta, J., Plitt, J., Bochner, B. S., & Schleimer, R. P. (1999). Inhibition of VCAM-1 expression in human bronchial epithelial cells by glucocorticoids. *American journal of respiratory cell and molecular biology*, *20*(4), 643–650. https://doi.org/10.1165/ajrcmb.20.4.3265

Auphan, N., DiDonato, J. A., Rosette, C., Helmberg, A., & Karin, M. (1995). Immunosuppression by glucocorticoids: inhibition of NF-kappa B activity through induction of I kappa B synthesis. *Science (New York, N.Y.)*, *270*(5234), 286–290. https://doi.org/10.1126/science.270.5234.286

Baier, J., Gänsbauer, M., Giessler, C., Arnold, H., Muske, M., Schleicher, U., Lukassen, S., Ekici, A., Rauh, M., Daniel, C., Hartmann, A., Schmid, B., Tripal, P., Dettmer, K., Oefner, P. J., Atreya, R., Wirtz, S., Bogdan, C., & Mattner, J. (2020). Arginase impedes the resolution of colitis by altering the microbiome and metabolome. *The Journal of clinical investigation*, *130*(11), 5703–5720. https://doi.org/10.1172/JCI126923

Bain, C. C., & Schridde, A. (2018). Origin, Differentiation, and Function of Intestinal Macrophages.*Frontiers in immunology*, *9*, 2733. https://doi.org/10.3389/fimmu.2018.02733

References

Ballegeer, M., Van Looveren, K., Timmermans, S., Eggermont, M., Vandevyver, S., Thery, F., Dendoncker, K., Souffriau, J., Vandewalle, J., Van Wyngene, L., De Rycke, R., Takahashi, N., Vandenabeele, P., Tuckermann, J., Reichardt, H. M., Impens, F., Beyaert, R., De Bosscher, K., Vandenbroucke, R. E., & Libert, C. (2018). Glucocorticoid receptor dimers control intestinal STAT1 and TNF-induced inflammation in mice. *The Journal of clinical investigation*, *128*(8), 3265–3279. https://doi.org/10.1172/JCI96636

Becker, C., Fantini, M. C., & Neurath, M. F. (2006). High resolution colonoscopy in live mice. *Nature protocols*, *1*(6), 2900–2904.
https://doi.org/10.1038/nprot.2006.446

Bording-Jorgensen M, Armstrong H, Wickenberg M, LaPointe P, Wine (2002) E. Macrophages and Epithelial Cells Mutually Interact through NLRP3 to Clear Infection and Enhance the Gastrointestinal Barrier. *Immuno*.; 2(1):13-25. https://doi.org/10.3390/immuno2010002

Bros, M., Jährling, F., Renzing, A., Wiechmann, N., Dang, N. A., Sutter, A., Ross, R., Knop, J., Sudowe, S., & Reske-Kunz, A. B. (2007). A newly established murine immature dendritic cell line can be differentiated into a mature state, but exerts tolerogenic function upon maturation in the presence of glucocorticoid. *Blood*, *109*(9), 3820–3829. https://doi.org/10.1182/blood-2006-07-035576

Bros, M., Jährling, F., Renzing, A., Wiechmann, N., Dang, N. A., Sutter, A., Ross, R., Knop, J., Sudowe, S., & Reske-Kunz, A. B. (2007). A newly established murine immature dendritic cell line can be differentiated into a mature state, but exerts tolerogenic function upon maturation in the presence of glucocorticoid. *Blood*, *109*(9), 3820–3829. https://doi.org/10.1182/blood-2006-07-035576

Bruscoli, S., Febo, M., Riccardi, C., & Migliorati, G. (2021). Glucocorticoid Therapy in Inflammatory Bowel Disease: Mechanisms and Clinical Practice. *Frontiers in immunology*, *12*, 691480. https://doi.org/10.3389/fimmu.2021.691480

Cain, D. W., & Cidlowski, J. A. (2017). Immune regulation by glucocorticoids. *Nature reviews. Immunology*, *17*(4), 233–247.
https://doi.org/10.1038/nri.2017.1

Casalegno Garduño, R., & Däbritz, J. (2021). New Insights on $CD8^+$ T Cells in Inflammatory Bowel Disease and Therapeutic Approaches. *Frontiers in immunology*, *12*, 738762. https://doi.org/10.3389/fimmu.2021.738762

References

Chassaing, B., Aitken, J. D., Malleshappa, M., & Vijay-Kumar, M. (2014). Dextran sulfate sodium (DSS)-induced colitis in mice. *Current protocols in immunology*, *104*, 15.25.1–15.25.14. https://doi.org/10.1002/0471142735.im1525s104

Chen, S. Q., Song, Y. Q., Wang, C., Tao, S., Yu, F. Y., Lou, H. Y., Hu, F. Q., & Yuan, H. (2020). Chitosan-modified lipid nanodrug delivery system for the targeted and responsive treatment of ulcerative colitis. *Carbohydrate polymers*, *230*, 115613. https://doi.org/10.1016/j.carbpol.2019.115613

Chibbar, R., & Moss, A. C. (2020). Mesalamine in the Initial Therapy of Ulcerative Colitis. *Gastroenterology clinics of North America*, *49*(4), 689–704. https://doi.org/10.1016/j.gtc.2020.07.002

Chieppa, M., Rescigno, M., Huang, A. Y., & Germain, R. N. (2006). Dynamic imaging of dendritic cell extension into the small bowel lumen in response to epithelial cell TLR engagement. *The Journal of experimental medicine*, *203*(13), 2841–2852. https://doi.org/10.1084/jem.20061884

Chun, E., Lavoie, S., Michaud, M., Gallini, C. A., Kim, J., Soucy, G., Odze, R., Glickman, J. N., & Garrett, W. S. (2015). CCL2 Promotes Colorectal Carcinogenesis by Enhancing Polymorphonuclear Myeloid-Derived Suppressor Cell Population and Function. *Cell reports*, *12*(2), 244–257. https://doi.org/10.1016/j.celrep.2015.06.024

Cima, I., Corazza, N., Dick, B., Fuhrer, A., Herren, S., Jakob, S., Ayuni, E., Mueller, C., & Brunner, T. (2004). Intestinal epithelial cells synthesize glucocorticoids and regulate T cell activation. *The Journal of experimental medicine*, *200*(12), 1635–1646. https://doi.org/10.1084/jem.20031958

Coccia, M., Harrison, O. J., Schiering, C., Asquith, M. J., Becher, B., Powrie, F., & Maloy, K. J. (2012). IL-1β mediates chronic intestinal inflammation by promoting the accumulation of IL-17A secreting innate lymphoid cells and CD4(+) Th17 cells. *The Journal of experimental medicine*, *209*(9), 1595–1609. https://doi.org/10.1084/jem.20111453

Coskun M. (2014). Intestinal epithelium in inflammatory bowel disease. *Frontiers in medicine*, *1*, 24. https://doi.org/10.3389/fmed.2014.00024

Cronstein, B. N., Kimmel, S. C., Levin, R. I., Martiniuk, F., & Weissmann, G. (1992). A mechanism for the antiinflammatory effects of corticosteroids: the glucocorticoid receptor regulates leukocyte adhesion to endothelial cells and expression of endothelial-leukocyte adhesion molecule 1 and intercellular adhesion molecule 1. *Proceedings of the National Academy of Sciences of the United States of America*, *89*(21), 9991–9995. https://doi.org/10.1073/pnas.89.21.9991

References

Cruz-Topete, D., & Cidlowski, J. A. (2015). One hormone, two actions: anti- and pro-inflammatory effects of glucocorticoids. *Neuroimmunomodulation*, *22*(1-2), 20–32. https://doi.org/10.1159/000362724

Curtale, G., Renzi, T. A., Drufuca, L., Rubino, M., & Locati, M. (2017). Glucocorticoids downregulate TLR4 signaling activity via its direct targeting by miR-511-5p. *European journal of immunology*, *47*(12), 2080–2089. https://doi.org/10.1002/eji.201747044

da Silva, B. C., Lyra, A. C., Rocha, R., & Santana, G. O. (2014). Epidemiology, demographic characteristics and prognostic predictors of ulcerative colitis. *World journal of gastroenterology*, *20*(28), 9458–9467. https://doi.org/10.3748/wjg.v20.i28.9458

D'Amico, F., Parigi, T. L., Fiorino, G., Peyrin-Biroulet, L., & Danese, S. (2019). Tofacitinib in the treatment of ulcerative colitis: efficacy and safety from clinical trials to real-world experience. *Therapeutic advances in gastroenterology*, *12*, 1756284819848631. https://doi.org/10.1177/1756284819848631

Damsker, J. M., Conklin, L. S., Sadri, S., Dillingham, B. C., Panchapakesan, K., Heier, C. R., McCall, J. M., & Sandler, A. D. (2016). VBP15, a novel dissociative steroid compound, reduces NFκB-induced expression of inflammatory cytokines in vitro and symptoms of murine trinitrobenzene sulfonic acid-induced colitis. *Inflammation research : official journal of the European Histamine Research Society ... [et al.]*, *65*(9), 737–743. https://doi.org/10.1007/s00011-016-0956-8

De Bosscher, K., Vanden Berghe, W., & Haegeman, G. (2003). The interplay between the glucocorticoid receptor and nuclear factor-kappaB or activator protein-1: molecular mechanisms for gene repression. *Endocrine reviews*, *24*(4), 488–522. https://doi.org/10.1210/er.2002-0006

DeRoche, T. C., Xiao, S. Y., & Liu, X. (2014). Histological evaluation in ulcerative colitis. *Gastroenterology report*, *2*(3), 178–192. https://doi.org/10.1093/gastro/gou031

Desgeorges, T., Caratti, G., Mounier, R., Tuckermann, J., & Chazaud, B. (2019). Glucocorticoids Shape Macrophage Phenotype for Tissue Repair. *Frontiers in immunology*, *10*, 1591. https://doi.org/10.3389/fimmu.2019.01591

References

Dhir, M., Montgomery, E. A., Glöckner, S. C., Schuebel, K. E., Hooker, C. M., Herman, J. G., Baylin, S. B., Gearhart, S. L., & Ahuja, N. (2008). Epigenetic regulation of WNT signaling pathway genes in inflammatory bowel disease (IBD) associated neoplasia. *Journal of gastrointestinal surgery : official journal of the Society for Surgery of the Alimentary Tract*, *12*(10), 1745–1753. https://doi.org/10.1007/s11605-008-0633-5

Dianzani, C., Foglietta, F., Ferrara, B., Rosa, A. C., Muntoni, E., Gasco, P., Della Pepa, C., Canaparo, R., & Serpe, L. (2017). Solid lipid nanoparticles delivering anti-inflammatory drugs to treat inflammatory bowel disease: Effects in an *in vivo* model. *World journal of gastroenterology*, *23*(23), 4200–4210. https://doi.org/10.3748/wjg.v23.i23.4200

Dieleman, L. A., Ridwan, B. U., Tennyson, G. S., Beagley, K. W., Bucy, R. P., & Elson, C. O. (1994). Dextran sulfate sodium-induced colitis occurs in severe combined immunodeficient mice. *Gastroenterology*, *107*(6), 1643–1652. https://doi.org/10.1016/0016-5085(94)90803-6

Du, L., & Ha, C. (2020). Epidemiology and Pathogenesis of Ulcerative Colitis. *Gastroenterology clinics of North America*, *49*(4), 643–654. https://doi.org/10.1016/j.gtc.2020.07.005

Egger, B., Bajaj-Elliott, M., MacDonald, T. T., Inglin, R., Eysselein, V. E., & Büchler, M. W. (2000). Characterisation of acute murine dextran sodium sulphate colitis: cytokine profile and dose dependency. *Digestion*, *62*(4), 240–248. https://doi.org/10.1159/000007822

Ehrchen, J. M., Roth, J., & Barczyk-Kahlert, K. (2019). More Than Suppression: Glucocorticoid Action on Monocytes and Macrophages. *Frontiers in immunology*, *10*, 2028. https://doi.org/10.3389/fimmu.2019.02028

Eichele, D. D., & Kharbanda, K. K. (2017). Dextran sodium sulfate colitis murine model: An indispensable tool for advancing our understanding of inflammatory bowel diseases pathogenesis. *World journal of gastroenterology*, *23*(33), 6016–6029. https://doi.org/10.3748/wjg.v23.i33.6016

Ekbom, A., Helmick, C., Zack, M., & Adami, H. O. (1990). Ulcerative colitis and colorectal cancer. A population-based study. *The New England journal of medicine*, *323*(18), 1228–1233. https://doi.org/10.1056/NEJM199011013231802.

El Aidy, S., Hooiveld, G., Tremaroli, V., Bäckhed, F., & Kleerebezem, M. (2013). The gut microbiota and mucosal homeostasis: colonized at birth or at adulthood, does it matter?. *Gut microbes*, *4*(2), 118–124. https://doi.org/10.4161/gmic.23362

References

Fan, Y. Y., Davidson, L. A., & Chapkin, R. S. (2019). Murine Colonic Organoid Culture System and Downstream Assay Applications. *Methods in molecular biology (Clifton, N.J.)*, *1576*, 171–181. https://doi.org/10.1007/7651_2016_8

Feng, Y., Dai, X., Li, X., Wang, H., Liu, J., Zhang, J., Du, Y., & Xia, L. (2012). EGF signalling pathway regulates colon cancer stem cell proliferation and apoptosis. *Cell proliferation*, *45*(5), 413–419. https://doi.org/10.1111/j.1365-2184.2012.00837.x

Feuerstein, J. D., & Cheifetz, A. S. (2014). Ulcerative colitis: epidemiology, diagnosis, and management. *Mayo Clinic proceedings*, *89*(11), 1553–1563. https://doi.org/10.1016/j.mayocp.2014.07.002

Feuerstein, J. D., Moss, A. C., & Farraye, F. A. (2019). Ulcerative Colitis. *Mayo Clinic proceedings*, *94*(7), 1357–1373 https://doi.org/10.1016/j.mayocp.2019.01.018

Fischer, H. J., Finck, T., Pellkofer, H. L., Reichardt, H. M., & Lühder, F. (2019). Glucocorticoid Therapy of Multiple Sclerosis Patients Induces Anti-inflammatory Polarization and Increased Chemotaxis of Monocytes. *Frontiers in immunology*, *10*, 1200. https://doi.org/10.3389/fimmu.2019.01200

Fogt, F., Vortmeyer, A. O., Goldman, H., Giordano, T. J., Merino, M. J., & Zhuang, Z. (1998). Comparison of genetic alterations in colonic adenoma and ulcerative colitis-associated dysplasia and carcinoma. *Human pathology*, *29*(2), 131–136. https://doi.org/10.1016/s0046-8177(98)90222-2

Franchimont, D., Galon, J., Gadina, M., Visconti, R., Zhou, Y., Aringer, M., Frucht, D. M., Chrousos, G. P., & O'Shea, J. J. (2000). Inhibition of Th1 immune response by glucocorticoids: dexamethasone selectively inhibits IL-12-induced Stat4 phosphorylation in T lymphocytes. *Journal of immunology (Baltimore, Md. : 1950)*, *164*(4), 1768–1774. https://doi.org/10.4049/jimmunol.164.4.1768

Frank, D. N., St Amand, A. L., Feldman, R. A., Boedeker, E. C., Harpaz, N., & Pace, N. R. (2007). Molecular-phylogenetic characterization of microbial community imbalances in human inflammatory bowel diseases. *Proceedings of the National Academy of Sciences of the United States of America*, *104*(34), 13780–13785. https://doi.org/10.1073/pnas.0706625104

Frei, P., Biedermann, L., Nielsen, O. H., & Rogler, G. (2013). Use of thiopurines in inflammatory bowel disease. *World journal of gastroenterology*, *19*(7), 1040–1048. https://doi.org/10.3748/wjg.v19.i7.1040

Funderburg, N. T., Stubblefield Park, S. R., Sung, H. C., Hardy, G., Clagett, B., Ignatz-Hoover, J., Harding, C. V., Fu, P., Katz, J. A., Lederman, M. M., & Levine,

References

A. D. (2013). Circulating CD4(+) and CD8(+) T cells are activated in inflammatory bowel disease and are associated with plasma markers of inflammation. *Immunology*, *140*(1), 87–97. https://doi.org/10.1111/imm.12114

Furukawa, A., Wisel, S. A., & Tang, Q. (2016). Impact of Immune-Modulatory Drugs on Regulatory T Cell. *Transplantation*, *100*(11), 2288–2300. https://doi.org/10.1097/TP.0000000000001379

Gajendran M, Loganathan P, Jimenez G, Catinella AP, Ng N, Umapathy C, Ziade N, Gajendran, M., Loganathan, P., Jimenez, G., Catinella, A. P., Ng, N., Umapathy, C., Ziade, N., & Hashash, J. G. (2019). A comprehensive review and update on ulcerative colitis. *Disease-a-month : DM*, *65*(12), 100851. https://doi.org/10.1016/j.disamonth.2019.02.004

Gelfo, V., Romaniello, D., Mazzeschi, M., Sgarzi, M., Grilli, G., Morselli, A., Manzan, B., Rihawi, K., & Lauriola, M. (2020). Roles of IL-1 in Cancer: From Tumor Progression to Resistance to Targeted Therapies. *International journal of molecular sciences*, *21*(17), 6009. https://doi.org/10.3390/ijms21176009

Gensler L. S. (2013). Glucocorticoids: complications to anticipate and prevent. *The Neurohospitalist*, *3*(2), 92–97. https://doi.org/10.1177/1941874412458678

González, M. V., Jiménez, B., Berciano, M. T., González-Sancho, J. M., Caelles, C., Lafarga, M., & Muñoz, A. (2000). Glucocorticoids antagonize AP-1 by inhibiting the Activation/phosphorylation of JNK without affecting its subcellular distribution. *The Journal of cell biology*, *150*(5), 1199–1208. https://doi.org/10.1083/jcb.150.5.1199

Goto Y. (2019). Epithelial Cells as a Transmitter of Signals From Commensal Bacteria and Host Immune Cells. *Frontiers in immunology*, *10*, 2057. https://doi.org/10.3389/fimmu.2019.02057

Grivennikov, S., Karin, E., Terzic, J., Mucida, D., Yu, G. Y., Vallabhapurapu, S., Scheller, J., Rose-John, S., Cheroutre, H., Eckmann, L., & Karin, M. (2009). IL-6 and Stat3 are required for survival of intestinal epithelial cells and development of colitis-associated cancer. *Cancer cell*, *15*(2), 103–113. https://doi.org/10.1016/j.ccr.2009.01.001

Gutzeit, C., Magri, G., & Cerutti, A. (2014). Intestinal IgA production and its role in host-microbe interaction. *Immunological reviews*, *260*(1), 76–85. https://doi.org/10.1111/imr.12189

Halpin, S. J., Hamlin, P. J., Greer, D. P., Warren, L., & Ford, A. C. (2013). Efficacy of infliximab in acute severe ulcerative colitis: a single-centre experience. *World journal of gastroenterology*, *19*(7), 1091–1097.

References

https://doi.org/10.3748/wjg.v19.i7.1091

Heller, F., Florian, P., Bojarski, C., Richter, J., Christ, M., Hillenbrand, B., Mankertz, J., Gitter, A. H., Bürgel, N., Fromm, M., Zeitz, M., Fuss, I., Strober, W., & Schulzke, J. D. (2005). Interleukin-13 is the key effector Th2 cytokine in ulcerative colitis that affects epithelial tight junctions, apoptosis, and cell restitution. *Gastroenterology*, *129*(2), 550–564.
https://doi.org/10.1016/j.gastro.2005.05.002

Henderson, P., van Limbergen, J. E., Schwarze, J., & Wilson, D. C. (2011). Function of the intestinal epithelium and its dysregulation in inflammatory bowel disease. *Inflammatory bowel diseases*, *17*(1), 382–395.
https://doi.org/10.1002/ibd.21379

Herath, M., Hosie, S., Bornstein, J. C., Franks, A. E., & Hill-Yardin, E. L. (2020). The Role of the Gastrointestinal Mucus System in Intestinal Homeostasis: Implications for Neurological Disorders. *Frontiers in cellular and infection microbiology*, *10*, 248. https://doi.org/10.3389/fcimb.2020.00248

Herrlich P. (2001). Cross-talk between glucocorticoid receptor and AP-1. *Oncogene*, *20*(19), 2465–2475. https://doi.org/10.1038/sj.onc.1204388

Heuberger, C., Pott, J., & Maloy, K. J. (2021). Why do intestinal epithelial cells express MHC class II?. *Immunology*, *162*(4), 357–367.
https://doi.org/10.1111/imm.13270

Hoppstädter, J., Dembek, A., Linnenberger, R., Dahlem, C., Barghash, A., Fecher-Trost, C., Fuhrmann, G., Koch, M., Kraegeloh, A., Huwer, H., & Kiemer, A. K. (2019). Toll-Like Receptor 2 Release by Macrophages: An Anti-inflammatory Program Induced by Glucocorticoids and Lipopolysaccharide. *Frontiers in immunology*, *10*, 1634. https://doi.org/10.3389/fimmu.2019.01634.

Hossain, Z., & Hirata, T. (2008). Molecular mechanism of intestinal permeability: interaction at tight junctions. *Molecular bioSystems*, *4*(12), 1181–1185. https://doi.org/10.1039/b800402a

Hua, G., Zein, N., Daubeuf, F., & Chambon, P. (2019). Glucocorticoid receptor modulators CpdX and CpdX-D3 exhibit the same in vivo antiinflammatory activities as synthetic glucocorticoids. *Proceedings of the National Academy of Sciences of the United States of America, 116*(28), 14191–14199.
https://doi.org/10.1073/pnas.1908258116

References

Humphries, A., Jawad, N., Ignjatovic, A., East, J., & Leedham, S. (2012). Carcinogenesis in Ulcerative Colitis. In (Ed.), Ulcerative Colitis from Genetics to Complications. IntechOpen. https://doi.org/10.5772/25306Hussenbux A, & de Silva A. (2021). Steroids in inflammatory bowel disease: a clinical review. Journal of Prescribing Practice, 3. https://doi.org/10.1080/14656566.2016

Ioannou, M., Paraskeva, E., Baxevanidou, K., Simos, G., Papamichali, R., Papacharalambous, C., Samara, M., & Koukoulis, G. (2015). HIF-1α in colorectal carcinoma: review of the literature. *Journal of B.U.ON. : official journal of the Balkan Union of Oncology*, *20*(3), 680–689.

Isidro, R. A., & Appleyard, C. B. (2016). Colonic macrophage polarization in homeostasis, inflammation, and cancer. *American journal of physiology. Gastrointestinal and liver physiology*, *311*(1), G59–G73. https://doi.org/10.1152/ajpgi.00123.2016

Issa, J. P., Ahuja, N., Toyota, M., Bronner, M. P., & Brentnall, T. A. (2001). Accelerated age-related CpG island methylation in ulcerative colitis. *Cancer research*, *61*(9), 3573–3577.

Jaffer, T., & Ma, D. (2016). The emerging role of chemokine receptor CXCR2 in cancer progression. *Transl Cancer Res*, *5*(Suppl 4), S616-S28. https://doi.org/10.21037/tcr.2016.10.06

Jain, A., Wordinger, R. J., Yorio, T., & Clark, A. F. (2014). Role of the alternatively spliced glucocorticoid receptor isoform GRβ in steroid responsiveness and glaucoma. *Journal of ocular pharmacology and therapeutics : the official journal of the Association for Ocular Pharmacology and Therapeutics*, *30*(2-3), 121–127. https://doi.org/10.1089/jop.2013.0239

Kahai, P., Mandiga, P., Wehrle, C. J., & Lobo, S. (2021). Anatomy, Abdomen and Pelvis, Large Intestine. In *StatPearls*. StatPearls Publishing.

Karpisheh, V., Joshi, N., Zekiy, A. O., Beyzai, B., Hojjat-Farsangi, M., Namdar, A., Edalati, M., & Jadidi-Niaragh, F. (2020). EP4 receptor as a novel promising therapeutic target in colon cancer. *Pathology, research and practice*, *216*(12), 153247. https://doi.org/10.1016/j.prp.2020.153247

Kato, S., Hokari, R., Matsuzaki, K., Iwai, A., Kawaguchi, A., Nagao, S., Miyahara, T., Itoh, K., Ishii, H., & Miura, S. (2000). Amelioration of murine experimental colitis by inhibition of mucosal addressin cell adhesion molecule-1. *The Journal of pharmacology and experimental therapeutics*, *295*(1), 183–189.

References

Kaur, A., & Goggolidou, P. (2020). Ulcerative colitis: understanding its cellular pathology could provide insights into novel therapies. *Journal of inflammation (London, England)*, *17*, 15. https://doi.org/10.1186/s12950-020-00246-4

Kayal, M., & Shah, S. (2019). Ulcerative Colitis: Current and Emerging Treatment Strategies. *Journal of clinical medicine*, *9*(1), 94.
https://doi.org/10.3390/jcm9010094

Kedia, S., Ahuja, V., & Tandon, R. (2014). Management of acute severe ulcerative colitis. *World journal of gastrointestinal pathophysiology*, *5*(4), 579–588. https://doi.org/10.4291/wjgp.v5.i4.579

Kelsall, B. L., & Rescigno, M. (2004). Mucosal dendritic cells in immunity and inflammation. *Nature immunology*, *5*(11), 1091–1095.
https://doi.org/10.1038/ni1104-1091

Kerr, T. A., Ciorba, M. A., Matsumoto, H., Davis, V. R., Luo, J., Kennedy, S., Xie, Y., Shaker, A., Dieckgraefe, B. K., & Davidson, N. O. (2012). Dextran sodium sulfate inhibition of real-time polymerase chain reaction amplification: a poly-A purification solution. *Inflammatory bowel diseases*, *18*(2), 344–348. https://doi.org/10.1002/ibd.21763

Kim, D., Nguyen, Q. T., Lee, J., Lee, S. H., Janocha, A., Kim, S., Le, H. T., Dvorina, N., Weiss, K., Cameron, M. J., Asosingh, K., Erzurum, S. C., Baldwin, W. M., 3rd, Lee, J. S., & Min, B. (2020). Anti-inflammatory Roles of Glucocorticoids Are Mediated by Foxp3^{+} Regulatory T Cells via a miR-342-Dependent Mechanism. *Immunity*, *53*(3), 581–596.e5. https://doi.org/10.1016/j.immuni.2020.07.002

Kim, H. Y., Cheon, J. H., Lee, S. H., Min, J. Y., Back, S. Y., Song, J. G., Kim, D. H., Lim, S. J., & Han, H. K. (2020). Ternary nanocomposite carriers based on organic clay-lipid vesicles as an effective colon-targeted drug delivery system: preparation and in vitro/in vivo characterization. *Journal of nanobiotechnology*, *18*(1), 17. https://doi.org/10.1186/s12951-020-0579-7

Kirschke, E., Goswami, D., Southworth, D., Griffin, P. R., & Agard, D. A. (2014). Glucocorticoid receptor function regulated by coordinated action of the Hsp90 and Hsp70 chaperone cycles. *Cell*, *157*(7), 1685–1697.
https://doi.org/10.1016/j.cell.2014.04.038

Kitajima, S., Takuma, S., & Morimoto, M. (2000). Histological analysis of murine colitis induced by dextran sulfate sodium of different molecular weights. *Experimental animals*, *49*(1), 9–15. https://doi.org/10.1538/expanim.49.9

References

Klemke, L., De Oliveira, T., Witt, D., Winkler, N., Bohnenberger, H., Bucala, R., Conradi, L. C., & Schulz-Heddergott, R. (2021). Hsp90-stabilized MIF supports tumor progression via macrophage recruitment and angiogenesis in colorectal cancer. *Cell death & disease*, *12*(2), 155. https://doi.org/10.1038/s41419-021-03426-z

Krieglstein, C. F., Cerwinka, W. H., Sprague, A. G., Laroux, F. S., Grisham, M. B., Koteliansky, V. E., Senninger, N., Granger, D. N., & de Fougerolles, A. R. (2002). Collagen-binding integrin alpha1beta1 regulates intestinal inflammation in experimental colitis. *The Journal of clinical investigation*, *110*(12), 1773–1782. https://doi.org/10.1172/JCI15256

Krieglstein, C. F., Cerwinka, W. H., Sprague, A. G., Laroux, F. S., Grisham, M. B., Koteliansky, V. E., Senninger, N., Granger, D. N., & de Fougerolles, A. R. (2002). Collagen-binding integrin alpha1beta1 regulates intestinal inflammation in experimental colitis. *The Journal of clinical investigation*, *110*(12), 1773–1782. https://doi.org/10.1172/JCI15256

Kulaylat, M. N., & Dayton, M. T. (2010). Ulcerative colitis and cancer. *Journal of surgical oncology*, *101*(8), 706–712. https://doi.org/10.1002/jso.21505

Lakatos, P. L., & Lakatos, L. (2008). Risk for colorectal cancer in ulcerative colitis: changes, causes and management strategies. *World journal of gastroenterology*, *14*(25), 3937–3947. https://doi.org/10.3748/wjg.14.3937.

Landy, J., Ronde, E., English, N., Clark, S. K., Hart, A. L., Knight, S. C., Ciclitira, P. J., & Al-Hassi, H. O. (2016). Tight junctions in inflammatory bowel diseases and inflammatory bowel disease associated colorectal cancer. *World journal of gastroenterology*, *22*(11), 3117–3126. https://doi.org/10.3748/wjg.v22.i11.3117

Lannan, E. A., Galliher-Beckley, A. J., Scoltock, A. B., & Cidlowski, J. A. (2012). Proinflammatory actions of glucocorticoids: glucocorticoids and TNFα coregulate gene expression in vitro and in vivo. *Endocrinology*, *153*(8), 3701–3712. https://doi.org/10.1210/en.2012-1020

Laroui, H., Ingersoll, S. A., Liu, H. C., Baker, M. T., Ayyadurai, S., Charania, M. A., Laroui, F., Yan, Y., Sitaraman, S. V., & Merlin, D. (2012). Dextran sodium sulfate (DSS) induces colitis in mice by forming nano-lipocomplexes with medium-chain-length fatty acids in the colon. *PloS one*, *7*(3), e32084. https://doi.org/10.1371/journal.pone.0032084

le Rolle, A. F., Chiu, T. K., Fara, M., Shia, J., Zeng, Z., Weiser, M. R., Paty, P. B., & Chiu, V. K. (2015). The prognostic significance of CXCL1 hypersecretion by human

colorectal cancer epithelia and myofibroblasts. *Journal of translational medicine*, *13*, 199. https://doi.org/10.1186/s12967-015-0555-4

Li, Q., Zhang, Q., Wang, M., Zhao, S., Ma, J., Luo, N., Li, N., Li, Y., Xu, G., & Li, J. (2008). Interferon-gamma and tumor necrosis factor-alpha disrupt epithelial barrier function by altering lipid composition in membrane microdomains of tight junction. *Clinical immunology (Orlando, Fla.)*, *126*(1), 67–80. https://doi.org/10.1016/j.clim.2007.08.017

Lian, G., Chen, S., Ouyang, M., Li, F., Chen, L., & Yang, J. (2019). Colon Cancer Cell Secretes EGF to Promote M2 Polarization of TAM Through EGFR/PI3K/AKT/mTOR Pathway. *Technology in cancer research & treatment*, *18*, 1533033819849068. https://doi.org/10.1177/1533033819849068.

Liberman, A. C., Refojo, D., Druker, J., Toscano, M., Rein, T., Holsboer, F., & Arzt, E. (2007). The activated glucocorticoid receptor inhibits the transcription factor T-bet by direct protein-protein interaction. *FASEB journal : official publication of the Federation of American Societies for Experimental Biology*, *21*(4), 1177–1188. https://doi.org/10.1096/fj.06-7452com

Lin, L., & Zhang, J. (2017). Role of intestinal microbiota and metabolites on gut homeostasis and human diseases. *BMC immunology*, *18*(1), 2. https://doi.org/10.1186/s12865-016-0187-3

Liu, B., Qu, L., & Yan, S. (2015). Cyclooxygenase-2 promotes tumor growth and suppresses tumor immunity. *Cancer cell international*, *15*, 106. https://doi.org/10.1186/s12935-015-0260-7

Liu, T., Zhang, L., Joo, D., & Sun, S. C. (2017). NF-κB signaling in inflammation. *Signal transduction and targeted therapy*, *2*, 17023–. https://doi.org/10.1038/sigtrans.2017.23

Löwenberg, M., Verhaar, A. P., van den Brink, G. R., & Hommes, D. W. (2007). Glucocorticoid signaling: a nongenomic mechanism for T-cell immunosuppression. *Trends in molecular medicine*, *13*(4), 158–163. https://doi.org/10.1016/j.molmed.2007.02.001

Lu, B., Niu, L. L., Xu, X. G., Yao, S. L., & Tan, X. Y. (2018). Ulcerative colitis in an adult patient mimicking Henoch-Schönlein purpura: A case report. *Medicine*, *97*(35), e12036. https://doi.org/10.1097/MD.0000000000012036

Lühder, F., & Reichardt, H. M. (2017). Novel Drug Delivery Systems Tailored for Improved Administration of Glucocorticoids. *International journal of molecular sciences*, *18*(9), 1836. https://doi.org/10.3390/ijms18091836

References

Ma, Z., Lian, J., Yang, M., Wuyang, J., Zhao, C., Chen, W., Liu, C., Zhao, Q., Lou, C., Han, J., & Zhang, Y. (2019). Overexpression of Arginase-1 is an indicator of poor prognosis in patients with colorectal cancer. *Pathology, research and practice*, *215*(6), 152383. https://doi.org/10.1016/j.prp.2019.03.012

Macpherson, A. J., & Harris, N. L. (2004). Interactions between commensal intestinal bacteria and the immune system. *Nature reviews. Immunology*, *4*(6), 478–485. https://doi.org/10.1038/nri1373

Mähler, M., Bristol, I. J., Leiter, E. H., Workman, A. E., Birkenmeier, E. H., Elson, C. O., & Sundberg, J. P. (1998). Differential susceptibility of inbred mouse strains to dextran sulfate sodium-induced colitis. *The American journal of physiology*, *274*(3), G544–G551. https://doi.org/10.1152/ajpgi.1998.274.3.G544

Maloy, K. J., & Powrie, F. (2011). Intestinal homeostasis and its breakdown in inflammatory bowel disease. *Nature*, *474*(7351), 298–306. https://doi.org/10.1038/nature10208

Maltby, S., Wohlfarth, C., Gold, M., Zbytnuik, L., Hughes, M. R., & McNagny, K. M. (2010). CD34 is required for infiltration of eosinophils into the colon and pathology associated with DSS-induced ulcerative colitis. *The American journal of pathology*, *177*(3), 1244–1254. https://doi.org/10.2353/ajpath.2010.100191

Matsuoka, K., Saito, E., Fujii, T., Takenaka, K., Kimura, M., Nagahori, M., Ohtsuka, K., & Watanabe, M. (2015). Tacrolimus for the Treatment of Ulcerative Colitis. *Intestinal research*, *13*(3), 219–226. https://doi.org/10.5217/ir.2015.13.3.219

Meers, G. K., Bohnenberger, H., Reichardt, H. M., Lühder, F., & Reichardt, S. D. (2018). Impaired resolution of DSS-induced colitis in mice lacking the glucocorticoid receptor in myeloid cells. *PloS one*, *13*(1), e0190846. https://doi.org/10.1371/journal.pone.0190846

Meier, J., & Sturm, A. (2011). Current treatment of ulcerative colitis. *World journal of gastroenterology*, *17*(27), 3204–3212. https://doi.org/10.3748/wjg.v17.i27.3204

Meijsing S. H. (2015). Mechanisms of Glucocorticoid-Regulated Gene Transcription. *Advances in experimental medicine and biology*, *872*, 59–81. https://doi.org/10.1007/978-1-4939-2895-8_3

Mezzina, N., Campbell Davies, S. E., & Ardizzone, S. (2018). Nonbiological therapeutic management of ulcerative colitis. *Expert opinion on pharmacotherapy*, *19*(16), 1747–1757. https://doi.org/10.1080/14656566.2018.1525361

References

Michielan, A., & D'Incà, R. (2015). Intestinal Permeability in Inflammatory Bowel Disease: Pathogenesis, Clinical Evaluation, and Therapy of Leaky Gut. *Mediators of inflammation*, *2015*, 628157. https://doi.org/10.1155/2015/628157

Miyata, M., Lee, J. Y., Susuki-Miyata, S., Wang, W. Y., Xu, H., Kai, H., Kobayashi, K. S., Flavell, R. A., & Li, J. D. (2015). Glucocorticoids suppress inflammation via the upregulation of negative regulator IRAK-M. *Nature communications*, *6*, 6062. https://doi.org/10.1038/ncomms7062

Mowat, C., Mosley, S. R., Namdar, A., Schiller, D., & Baker, K. (2021). Anti-tumor immunity in mismatch repair-deficient colorectal cancers requires type I IFN-driven CCL5 and CXCL10. *The Journal of experimental medicine*, *218*(9), e20210108. https://doi.org/10.1084/jem.20210108

Müller, S., Lory, J., Corazza, N., Griffiths, G. M., Z'graggen, K., Mazzucchelli, L., Kappeler, A., & Mueller, C. (1998). Activated CD4+ and CD8+ cytotoxic cells are present in increased numbers in the intestinal mucosa from patients with active inflammatory bowel disease. *The American journal of pathology*, *152*(1), 261–268.

Muzzi, C., Watanabe, N., Twomey, E., Meers, G. K., Reichardt, H. M., Bohnenberger, H., & Reichardt, S. D. (2021). The Glucocorticoid Receptor in Intestinal Epithelial Cells Alleviates Colitis and Associated Colorectal Cancer in Mice. *Cellular and molecular gastroenterology and hepatology*, *11*(5), 1505–1518. https://doi.org/10.1016/j.jcmgh.2020.12.006

Nava, P., Koch, S., Laukoetter, M. G., Lee, W. Y., Kolegraff, K., Capaldo, C. T., Beeman, N., Addis, C., Gerner-Smidt, K., Neumaier, I., Skerra, A., Li, L., Parkos, C. A., & Nusrat, A. (2010). Interferon-gamma regulates intestinal epithelial homeostasis through converging beta-catenin signaling pathways. *Immunity*, *32*(3), 392–402. https://doi.org/10.1016/j.immuni.2010.03.001

Neurath M. (2010). Thiopurines in IBD: What Is Their Mechanism of Action?. *Gastroenterology & hepatology*, *6*(7), 435–436.

Neurath M. F. (2019). IL-23 in inflammatory bowel diseases and colon cancer. *Cytokine & growth factor reviews*, *45*, 1–8.
https://doi.org/10.1016/j.cytogfr.2018.12.002

Nishida, A., Inoue, R., Inatomi, O., Bamba, S., Naito, Y., & Andoh, A. (2018). Gut microbiota in the pathogenesis of inflammatory bowel disease. *Clinical journal of gastroenterology*, *11*(1), 1–10. https://doi.org/10.1007/s12328-017-0813-5

References

Nissen, R. M., & Yamamoto, K. R. (2000). The glucocorticoid receptor inhibits NFkappaB by interfering with serine-2 phosphorylation of the RNA polymerase II carboxy-terminal domain. *Genes & development*, *14*(18), 2314–2329. https://doi.org/10.1101/gad.827900

Niu, F., Yu, Y., Li, Z., Ren, Y., Li, Z., Ye, Q., Liu, P., Ji, C., Qian, L., & Xiong, Y. (2022). Arginase: An emerging and promising therapeutic target for cancer treatment. *Biomedicine & pharmacotherapy = Biomedecine & pharmacotherapie*, *149*, 112840. https://doi.org/10.1016/j.biopha.2022.112840

Noddings, C. M., Wang, R. Y., Johnson, J. L., & Agard, D. A. (2022). Structure of Hsp90-p23-GR reveals the Hsp90 client-remodelling mechanism. *Nature*, *601*(7893), 465–469. https://doi.org/10.1038/s41586-021-04236-1

Nordgren, S., McPheeters, G., Svaninger, G., Oresland, T., & Hultén, L. (1997). Small bowel length in inflammatory bowel disease. *International journal of colorectal disease*, *12*(4), 230–234. https://doi.org/10.1007/s003840050095

Oakley, R. H., & Cidlowski, J. A. (2013). The biology of the glucocorticoid receptor: new signaling mechanisms in health and disease. *The Journal of allergy and clinical immunology*, *132*(5), 1033–1044. https://doi.org/10.1016/j.jaci.2013.09.007

Oakley, R. H., Sar, M., & Cidlowski, J. A. (1996). The human glucocorticoid receptor beta isoform. Expression, biochemical properties, and putative function. *The Journal of biological chemistry*, *271*(16), 9550–9559.
https://doi.org/10.1074/jbc.271.16.9550

Ocón, B., Aranda, C. J., Gámez-Belmonte, R., Suárez, M. D., Zarzuelo, A., Martínez-Augustin, O., & Sánchez de Medina, F. (2016). The glucocorticoid budesonide has protective and deleterious effects in experimental colitis in mice. *Biochemical pharmacology*, *116*, 73–88. https://doi.org/10.1016/j.bcp.2016.07.010

Okayasu, I., Hatakeyama, S., Yamada, M., Ohkusa, T., Inagaki, Y., & Nakaya, R. (1990). A novel method in the induction of reliable experimental acute and chronic ulcerative colitis in mice. *Gastroenterology*, *98*(3), 694–702. https://doi.org/10.1016/0016-5085(90)90290-h

Okumura, R., & Takeda, K. (2016). Maintenance of gut homeostasis by the mucosal immune system. *Proceedings of the Japan Academy. Series B, Physical and biological sciences*, *92*(9), 423–435. https://doi.org/10.2183/pjab.92.423

References

Okumura, R., & Takeda, K. (2017). Roles of intestinal epithelial cells in the maintenance of gut homeostasis. *Experimental & molecular medicine*, *49*(5), e338. https://doi.org/10.1038/emm.2017.20

Omenetti, S., & Pizarro, T. T. (2015). The Treg/Th17 Axis: A Dynamic Balance Regulated by the Gut Microbiome. *Frontiers in immunology*, *6*, 639. https://doi.org/10.3389/fimmu.2015.00639

Oshima, H., & Oshima, M. (2012). The inflammatory network in the gastrointestinal tumor microenvironment: lessons from mouse models. *Journal of gastroenterology*, *47*(2), 97–106. https://doi.org/10.1007/s00535-011-0523-6

Panea, C., Farkas, A. M., Goto, Y., Abdollahi-Roodsaz, S., Lee, C., Koscsó, B., Gowda, K., Hohl, T. M., Bogunovic, M., & Ivanov, I. I. (2015). Intestinal Monocyte-Derived Macrophages Control Commensal-Specific Th17 Responses. *Cell reports*, *12*(8), 1314–1324. https://doi.org/10.1016/j.celrep.2015.07.040

Proetzel G, Wiles M. V. Mouse Models for Drug Discovery, Methods and Protocols. (2010). Part of the book series: Methods in Molecular Biology (MIMB, volume 602).

Panettieri, R. A., Schaafsma, D., Amrani, Y., Koziol-White, C., Ostrom, R., & Tliba, O. (2019). Non-genomic Effects of Glucocorticoids: An Updated View. *Trends in pharmacological sciences*, *40*(1), 38–49. https://doi.org/10.1016/j.tips.2018.11.002

Parang, B., Barrett, C. W., & Williams, C. S. (2016). AOM/DSS Model of Colitis-Associated Cancer. *Methods in molecular biology (Clifton, N.J.)*, *1422*, 297–307. https://doi.org/10.1007/978-1-4939-3603-8_26

Park, S. C., & Jeen, Y. T. (2015). Current and emerging biologics for ulcerative colitis. *Gut and liver*, *9*(1), 18–27. https://doi.org/10.5009/gnl14226

Patrick, G. (2013). History of Cortisone and Related Compounds. In *eLS* John Wiley & Sons Ltd.. https://doi.org/10.1002/9780470015902.a0003627.pub2

Pelaseyed, T., Bergström, J. H., Gustafsson, J. K., Ermund, A., Birchenough, G. M., Schütte, A., van der Post, S., Svensson, F., Rodríguez-Piñeiro, A. M., Nyström, E. E., Wising, C., Johansson, M. E., & Hansson, G. C. (2014). The mucus and mucins of the goblet cells and enterocytes provide the first defense line of the gastrointestinal tract and interact with the immune system. *Immunological reviews*, *260*(1), 8–20. https://doi.org/10.1111/imr.12182

References

Petersen, C., & Round, J. L. (2014). Defining dysbiosis and its influence on host immunity and disease. *Cellular microbiology*, *16*(7), 1024–1033. https://doi.org/10.1111/cmi.12308

Petta, I., Dejager, L., Ballegeer, M., Lievens, S., Tavernier, J., De Bosscher, K., & Libert, C. (2016). The Interactome of the Glucocorticoid Receptor and Its Influence on the Actions of Glucocorticoids in Combatting Inflammatory and Infectious Diseases. *Microbiology and molecular biology reviews : MMBR*, *80*(2), 495–522. https://doi.org/10.1128/MMBR.00064-15

Piemonti, L., Monti, P., Allavena, P., Leone, B. E., Caputo, A., & Di Carlo, V. (1999). Glucocorticoids increase the endocytic activity of human dendritic cells. *International immunology*, *11*(9), 1519–1526. https://doi.org/10.1093/intimm/11.9.1519

Piemonti, L., Monti, P., Allavena, P., Sironi, M., Soldini, L., Leone, B. E., Socci, C., & Di Carlo, V. (1999). Glucocorticoids affect human dendritic cell differentiation and maturation. *Journal of immunology (Baltimore, Md. : 1950)*, *162*(11), 6473–6481.

Poetker, D. M., & Reh, D. D. (2010). A comprehensive review of the adverse effects of systemic corticosteroids. *Otolaryngologic clinics of North America*, *43*(4), 753–768. https://doi.org/10.1016/j.otc.2010.04.003

Poritz, L. S., Garver, K. I., Green, C., Fitzpatrick, L., Ruggiero, F., & Koltun, W. A. (2007). Loss of the tight junction protein ZO-1 in dextran sulfate sodium induced colitis. *The Journal of surgical research*, *140*(1), 12–19. https://doi.org/10.1016/j.jss.2006.07.050

Probert C. (2013). Steroids and 5-aminosalicylic acids in moderate ulcerative colitis: addressing the dilemma. *Therapeutic advances in gastroenterology*, *6*(1), 33–38. https://doi.org/10.1177/1756283X12461395

Raes, G., Van den Bergh, R., De Baetselier, P., Ghassabeh, G. H., Scotton, C., Locati, M., Mantovani, A., & Sozzani, S. (2005). Arginase-1 and Ym1 are markers for murine, but not human, alternatively activated myeloid cells. *Journal of immunology (Baltimore, Md. : 1950)*, *174*(11), 6561–6562. https://doi.org/10.4049/jimmunol.174.11.6561

Ramamoorthy, S., & Cidlowski, J. A. (2016). Corticosteroids: Mechanisms of Action in Health and Disease. *Rheumatic diseases clinics of North America*, *42*(1), 15–vii. https://doi.org/10.1016/j.rdc.2015.08.002

References

Reichardt, H. M., Kaestner, K. H., Tuckermann, J., Kretz, O., Wessely, O., Bock, R., Gass, P., Schmid, W., Herrlich, P., Angel, P., & Schütz, G. (1998). DNA binding of the glucocorticoid receptor is not essential for survival. *Cell*, *93*(4), 531–541. https://doi.org/10.1016/s0092-8674(00)81183-6

Reichardt, H. M., Tuckermann, J. P., Göttlicher, M., Vujic, M., Weih, F., Angel, P., Herrlich, P., & Schütz, G. (2001). Repression of inflammatory responses in the absence of DNA binding by the glucocorticoid receptor. *The EMBO journal*, *20*(24), 7168–7173. https://doi.org/10.1093/emboj/20.24.7168

Reichardt, S. D., Amouret, A., Muzzi, C., Vettorazzi, S., Tuckermann, J. P., Lühder, F., & Reichardt, H. M. (2021). The Role of Glucocorticoids in Inflammatory Diseases. *Cells*, *10*(11), 2921. https://doi.org/10.3390/cells10112921

Reichardt, S. D., Föller, M., Rexhepaj, R., Pathare, G., Minnich, K., Tuckermann, J. P., Lang, F., & Reichardt, H. M. (2012). Glucocorticoids enhance intestinal glucose uptake via the dimerized glucocorticoid receptor in enterocytes. *Endocrinology*, *153*(4), 1783–1794. https://doi.org/10.1210/en.2011-1747

Rescigno, M., & Di Sabatino, A. (2009). Dendritic cells in intestinal homeostasis and disease. *The Journal of clinical investigation*, *119*(9), 2441–2450. https://doi.org/10.1172/JCI39134

Reuter, K. C., Grunwitz, C. R., Kaminski, B. M., Steinhilber, D., Radeke, H. H., & Stein, J. (2012). Selective glucocorticoid receptor agonists for the treatment of inflammatory bowel disease: studies in mice with acute trinitrobenzene sulfonic acid colitis. *The Journal of pharmacology and experimental therapeutics*, *341*(1), 68–80. https://doi.org/10.1124/jpet.111.183947

Rocamora-Reverte, L., Tuzlak, S., von Raffay, L., Tisch, M., Fiegl, H., Drach, M., Reichardt, H. M., Villunger, A., Tischner, D., & Wiegers, G. J. (2019). Glucocorticoid Receptor-Deficient Foxp3^{+} Regulatory T Cells Fail to Control Experimental Inflammatory Bowel Disease. *Frontiers in immunology*, *10*, 472. https://doi.org/10.3389/fimmu.2019.00472

Roda, G., Sartini, A., Zambon, E., Calafiore, A., Marocchi, M., Caponi, A., Belluzzi, A., & Roda, E. (2010). Intestinal epithelial cells in inflammatory bowel diseases. *World journal of gastroenterology*, *16*(34), 4264–4271. https://doi.org/10.3748/wjg.v16.i34.4264

References

Ronchetti, S., Migliorati, G., & Riccardi, C. (2015). GILZ as a Mediator of the Anti-Inflammatory Effects of Glucocorticoids. *Frontiers in endocrinology*, *6*, 170. https://doi.org/10.3389/fendo.2015.00170

Ronchetti, S., Ricci, E., Migliorati, G., Gentili, M., & Riccardi, C. (2018). How Glucocorticoids Affect the Neutrophil Life. *International journal of molecular sciences*, *19*(12), 4090. https://doi.org/10.3390/ijms19124090

Rozkova, D., Horvath, R., Bartunkova, J., & Spisek, R. (2006). Glucocorticoids severely impair differentiation and antigen presenting function of dendritic cells despite upregulation of Toll-like receptors. *Clinical immunology (Orlando, Fla.)*, *120*(3), 260–271. https://doi.org/10.1016/j.clim.2006.04.567

Rutella, S., & Locatelli, F. (2011). Intestinal dendritic cells in the pathogenesis of inflammatory bowel disease. *World journal of gastroenterology*, *17*(33), 3761–3775. https://doi.org/10.3748/wjg.v17.i33.3761

Sandborn, W. J., Vermeire, S., Tyrrell, H., Hassanali, A., Lacey, S., Tole, S., Tatro, A. R., & Etrolizumab Global Steering Committee (2020). Etrolizumab for the Treatment of Ulcerative Colitis and Crohn's Disease: An Overview of the Phase 3 Clinical Program. *Advances in therapy*, *37*(7), 3417–3431. https://doi.org/10.1007/s12325-020-01366-2

Sands, B. E., & Kaplan, G. G. (2007). The role of TNFalpha in ulcerative colitis. *Journal of clinical pharmacology*, *47*(8), 930–941. https://doi.org/10.1177/0091270007301623

Satsangi, J., Silverberg, M. S., Vermeire, S., & Colombel, J. F. (2006). The Montreal classification of inflammatory bowel disease: controversies, consensus, and implications. *Gut*, *55*(6), 749–753. https://doi.org/10.1136/gut.2005.082909

Sawant, K. V., Poluri, K. M., Dutta, A. K., Sepuru, K. M., Troshkina, A., Garofalo, R. P., & Rajarathnam, K. (2016). Chemokine CXCL1 mediated neutrophil recruitment: Role of glycosaminoglycan interactions. *Scientific reports*, *6*, 33123. https://doi.org/10.1038/srep33123

Scheinman, R. I., Gualberto, A., Jewell, C. M., Cidlowski, J. A., & Baldwin, A. S., Jr (1995). Characterization of mechanisms involved in transrepression of NF-kappa B by activated glucocorticoid receptors. *Molecular and cellular biology*, *15*(2), 943–953. https://doi.org/10.1128/MCB.15.2.943

Scott, C. L., Aumeunier, A. M., & Mowat, A. M. (2011). Intestinal CD103+ dendritic cells: master regulators of tolerance?. *Trends in immunology*, *32*(9), 412–419. https://doi.org/10.1016/j.it.2011.06.003

References

Scribano M. L. (2018). Vedolizumab for inflammatory bowel disease: From randomized controlled trials to real-life evidence. *World journal of gastroenterology*, *24*(23), 2457–2467. https://doi.org/10.3748/wjg.v24.i23.2457

Seril, D. N., Liao, J., Yang, G. Y., & Yang, C. S. (2003). Oxidative stress and ulcerative colitis-associated carcinogenesis: studies in humans and animal models. *Carcinogenesis*, *24*(3), 353–362. https://doi.org/10.1093/carcin/24.3.353

Shen, Z. H., Zhu, C. X., Quan, Y. S., Yang, Z. Y., Wu, S., Luo, W. W., Tan, B., & Wang, X. Y. (2018). Relationship between intestinal microbiota and ulcerative colitis: Mechanisms and clinical application of probiotics and fecal microbiota transplantation. *World journal of gastroenterology*, *24*(1), 5–14. https://doi.org/10.3748/wjg.v24.i1.5

Sheng, J. A., Bales, N. J., Myers, S. A., Bautista, A. I., Roueinfar, M., Hale, T. M., & Handa, R. J. (2021). The Hypothalamic-Pituitary-Adrenal Axis: Development, Programming Actions of Hormones, and Maternal-Fetal Interactions. *Frontiers in behavioral neuroscience*, *14*, 601939. https://doi.org/10.3389/fnbeh.2020.601939

Shimba, A., Ejima, A., & Ikuta, K. (2021). Pleiotropic Effects of Glucocorticoids on the Immune System in Circadian Rhythm and Stress. *Frontiers in immunology*, *12*, 706951. https://doi.org/10.3389/fimmu.2021.706951

Simoni, R. D., Hill, R. L., & Vaughan, M. The Isolation of Thyroxine and Cortisone: the Work of Edward C. Kendall. Journal of Biological Chemistry, 2002. 277(21), 21–22. https://doi.org/10.1016/s0021-9258(20)85219-3

Snider, A. J., Bialkowska, A. B., Ghaleb, A. M., Yang, V. W., Obeid, L. M., & Hannun, Y. A. (2016). Murine Model for Colitis-Associated Cancer of the Colon. *Methods in molecular biology (Clifton, N.J.)*, *1438*, 245–254. https://doi.org/10.1007/978-1-4939-3661-8_14

Spencer, J., & Sollid, L. M. (2016). The human intestinal B-cell response. *Mucosal immunology*, *9*(5), 1113–1124. https://doi.org/10.1038/mi.2016.59

Stallmach, A., Hagel, S., & Bruns, T. (2010). Adverse effects of biologics used for treating IBD. *Best practice & research. Clinical gastroenterology*, *24*(2), 167–182. https://doi.org/10.1016/j.bpg.2010.01.002

Strehl, C., Ehlers, L., Gaber, T., & Buttgereit, F. (2019). Glucocorticoids-All-Rounders Tackling the Versatile Players of the Immune System. *Frontiers in immunology*, *10*, 1744. https://doi.org/10.3389/fimmu.2019.01744

References

Strugnell, R. A., & Wijburg, O. L. (2010). The role of secretory antibodies in infection immunity. *Nature reviews. Microbiology*, *8*(9), 656–667. https://doi.org/10.1038/nrmicro2384

Su, L., Nalle, S. C., Shen, L., Turner, E. S., Singh, G., Breskin, L. A., Khramtsova, E. A., Khramtsova, G., Tsai, P. Y., Fu, Y. X., Abraham, C., & Turner, J. R. (2013). TNFR2 activates MLCK-dependent tight junction dysregulation to cause apoptosis-mediated barrier loss and experimental colitis. *Gastroenterology*, *145*(2), 407–415. https://doi.org/10.1053/j.gastro.2013.04.011

Sun, T., Nguyen, A., & Gommerman, J. L. (2020). Dendritic Cell Subsets in Intestinal Immunity and Inflammation. *Journal of immunology (Baltimore, Md. : 1950)*, *204*(5), 1075–1083. https://doi.org/10.4049/jimmunol.1900710

Sundahl, N., Bridelance, J., Libert, C., De Bosscher, K., & Beck, I. M. (2015). Selective glucocorticoid receptor modulation: New directions with non-steroidal scaffolds. *Pharmacology & therapeutics*, *152*, 28–41. https://doi.org/10.1016/j.pharmthera.2015.05.001

Suzuki, R., Kohno, H., Sugie, S., Nakagama, H., & Tanaka, T. (2006). Strain differences in the susceptibility to azoxymethane and dextran sodium sulfate-induced colon carcinogenesis in mice. *Carcinogenesis*, *27*(1), 162–169. https://doi.org/10.1093/carcin/bgi205

Szebeni, B., Veres, G., Dezsõfi, A., Rusai, K., Vannay, A., Mraz, M., Majorova, E., & Arató, A. (2008). Increased expression of Toll-like receptor (TLR) 2 and TLR4 in the colonic mucosa of children with inflammatory bowel disease. *Clinical and experimental immunology*, *151*(1), 34–41. https://doi.org/10.1111/j.1365-2249.2007.03531.x

Tanaka, T., Kohno, H., Suzuki, R., Yamada, Y., Sugie, S., & Mori, H. (2003). A novel inflammation-related mouse colon carcinogenesis model induced by azoxymethane and dextran sodium sulfate. *Cancer science*, *94*(11), 965–973. https://doi.org/10.1111/j.1349-7006.2003.tb01386.x

Tatro, E. T., Everall, I. P., Kaul, M., & Achim, C. L. (2009). Modulation of glucocorticoid receptor nuclear translocation in neurons by immunophilins FKBP51 and FKBP52: implications for major depressive disorder. *Brain research*, *1286*, 1–12. https://doi.org/10.1016/j.brainres.2009.06.036

Thompson, A. I., & Lees, C. W. (2011). Genetics of ulcerative colitis. *Inflammatory bowel diseases*, *17*(3), 831–848. https://doi.org/10.1002/ibd.21375

References

Toyoda, H., Wang, S. J., Yang, H. Y., Redford, A., Magalong, D., Tyan, D., McElree, C. K., Pressman, S. R., Shanahan, F., & Targan, S. R. (1993). Distinct associations of HLA class II genes with inflammatory bowel disease. *Gastroenterology*, *104*(3), 741–748. https://doi.org/10.1016/0016-5085(93)91009-7

Tronche, F., Kellendonk, C., Kretz, O., Gass, P., Anlag, K., Orban, P. C., Bock, R., Klein, R., & Schütz, G. (1999). Disruption of the glucocorticoid receptor gene in the nervous system results in reduced anxiety. *Nature genetics*, *23*(1), 99–103. https://doi.org/10.1038/12703

Ungaro, R., Mehandru, S., Allen, P. B., Peyrin-Biroulet, L., & Colombel, J. F. (2017). Ulcerative colitis. *Lancet (London, England)*, *389*(10080), 1756–1770. https://doi.org/10.1016/S0140-6736(16)32126-2

van der Flier, L. G., & Clevers, H. (2009). Stem cells, self-renewal, and differentiation in the intestinal epithelium. *Annual review of physiology*, *71*, 241–260. https://doi.org/10.1146/annurev.physiol.010908.163145

Van der Sluis, M., De Koning, B. A., De Bruijn, A. C., Velcich, A., Meijerink, J. P., Van Goudoever, J. B., Büller, H. A., Dekker, J., Van Seuningen, I., Renes, I. B., & Einerhand, A. W. (2006). Muc2-deficient mice spontaneously develop colitis, indicating that MUC2 is critical for colonic protection. *Gastroenterology*, *131*(1), 117–129. https://doi.org/10.1053/j.gastro.2006.04.020

van Wijk, F., & Cheroutre, H. (2010). Mucosal T cells in gut homeostasis and inflammation. *Expert review of clinical immunology*, *6*(4), 559–566. https://doi.org/10.1586/eci.10.34

Vanderpool, C., Yan, F., & Polk, D. B. (2008). Mechanisms of probiotic action: Implications for therapeutic applications in inflammatory bowel diseases. *Inflammatory bowel diseases*, *14*(11), 1585–1596. https://doi.org/10.1002/ibd.20525

Varela, E., Manichanh, C., Gallart, M., Torrejón, A., Borruel, N., Casellas, F., Guarner, F., & Antolin, M. (2013). Colonisation by Faecalibacterium prausnitzii and maintenance of clinical remission in patients with ulcerative colitis. *Alimentary pharmacology & therapeutics*, *38*(2), 151–161. https://doi.org/10.1111/apt.12365

Villemin, C., Tranquet, O., Solé-Jamault, V., Smit, J. J., Pieters, R., Denery-Papini, S., & Bouchaud, G. (2020). Deamidation and Enzymatic Hydrolysis of Gliadins Alter Their Processing by Dendritic Cells in Vitro. *Journal of agricultural and food chemistry*, *68*(5), 1447–1456. https://doi.org/10.1021/acs.jafc.9b06075

References

Vogelstein, B., Fearon, E. R., Hamilton, S. R., Kern, S. E., Preisinger, A. C., Leppert, M., Nakamura, Y., White, R., Smits, A. M., & Bos, J. L. (1988). Genetic alterations during colorectal-tumor development. *The New England journal of medicine*, *319*(9), 525–532. https://doi.org/10.1056/NEJM198809013190901

Waldner, M. J., & Neurath, M. F. (2009). Colitis-associated cancer: the role of T cells in tumor development. *Seminars in immunopathology*, *31*(2), 249–256. https://doi.org/10.1007/s00281-009-0161-8

Wang, D., Dubois, R. N., & Richmond, A. (2009). The role of chemokines in intestinal inflammation and cancer. *Current opinion in pharmacology*, *9*(6), 688–696. https://doi.org/10.1016/j.coph.2009.08.003

Wang, W., Li, X., Zheng, D., Zhang, D., Peng, X., Zhang, X., Ai, F., Wang, X., Ma, J., Xiong, W., Li, G., Zhou, Y., & Shen, S. (2015). Dynamic changes and functions of macrophages and M1/M2 subpopulations during ulcerative colitis-associated carcinogenesis in an AOM/DSS mouse model. *Molecular medicine reports*, *11*(4), 2397–2406. https://doi.org/10.3892/mmr.2014.3018

Weikum, E. R., de Vera, I., Nwachukwu, J. C., Hudson, W. H., Nettles, K. W., Kojetin, D. J., & Ortlund, E. A. (2017). Tethering not required: the glucocorticoid receptor binds directly to activator protein-1 recognition motifs to repress inflammatory genes. *Nucleic acids research*, *45*(14), 8596–8608. https://doi.org/10.1093/nar/gkx509

Weikum, E. R., Knuesel, M. T., Ortlund, E. A., & Yamamoto, K. R. (2017). Glucocorticoid receptor control of transcription: precision and plasticity via allostery. *Nature reviews. Molecular cell biology*, *18*(3), 159–174. https://doi.org/10.1038/nrm.2016.152

Xavier, A. M., Anunciato, A. K., Rosenstock, T. R., & Glezer, I. (2016). Gene Expression Control by Glucocorticoid Receptors during Innate Immune Responses. *Frontiers in endocrinology*, *7*, 31. https://doi.org/10.3389/fendo.2016.00031

Xiao, Y. T., Yan, W. H., Cao, Y., Yan, J. K., & Cai, W. (2016). Neutralization of IL-6 and TNF-α ameliorates intestinal permeability in DSS-induced colitis. *Cytokine*, *83*, 189–192. https://doi.org/10.1016/j.cyto.2016.04.012

Xu, C. T., Meng, S. Y., & Pan, B. R. (2004). Drug therapy for ulcerative colitis. *World journal of gastroenterology*, *10*(16), 2311–2317. https://doi.org/10.3748/wjg.v10.i16.2311

References

Yamada, T., Oshima, T., Yoshihara, K., Tamura, S., Kanazawa, A., Inagaki, D., Yamamoto, N., Sato, T., Fujii, S., Numata, K., Kunisaki, C., Shiozawa, M., Morinaga, S., Akaike, M., Rino, Y., Tanaka, K., Masuda, M., & Imada, T. (2010). Overexpression of MMP-13 gene in colorectal cancer with liver metastasis. *Anticancer research*, *30*(7), 2693–2699.

Yamamoto-Furusho, J. K., Mendivil, E. J., & Fonseca-Camarillo, G. (2012). Differential expression of occludin in patients with ulcerative colitis and healthy controls. *Inflammatory bowel diseases*, *18*(10), E1999. https://doi.org/10.1002/ibd.22835

Yan, F., & Polk, D. B. (2010). Disruption of NF-kappaB signalling by ancient microbial molecules: novel therapies of the future?. *Gut*, *59*(4), 421–426. https://doi.org/10.1136/gut.2009.179614

Yang, B., Tang, F., Zhang, B., Zhao, Y., Feng, J., & Rao, Z. (2014). Matrix metalloproteinase-9 overexpression is closely related to poor prognosis in patients with colon cancer. *World journal of surgical oncology*, *12*, 24. https://doi.org/10.1186/1477-7819-12-24

You, J., Chen, W., Chen, J., Zheng, Q., Dong, J., & Zhu, Y. (2019). Corrigendum to "The Oncogenic Role of ARG1 in Progression and Metastasis of Hepatocellular Carcinoma". *BioMed research international*, *2019*, 6212386. https://doi.org/10.1155/2019/6212386

Zak-Nejmark, T., Jankowska, R., Małolepszy, J., Jutel, M., Kraus-Filarska, M., & Nadobna, G. (1996). Spontaneous motility and chemotaxis of neutrophils is influenced by glycocorticosteroid therapy. *Archivum immunologiae et therapiae experimentalis*, *44*(1), 77–80.

Zhang, Z., Dong, L., Jia, A., Chen, X., Yang, Q., Wang, Y., Wang, Y., Liu, R., Cao, Y., He, Y., Bi, Y., & Liu, G. (2020). Glucocorticoids Promote the Onset of Acute Experimental Colitis and Cancer by Upregulating mTOR Signaling in Intestinal Epithelial Cells. *Cancers*, *12*(4), 945. https://doi.org/10.3390/cancers12040945

Zhang, Z., Zhang, Z. Y., & Schluesener, H. J. (2009). Compound A, a plant origin ligand of glucocorticoid receptors, increases regulatory T cells and M2 macrophages to attenuate experimental autoimmune neuritis with reduced side effects. *Journal of immunology (Baltimore, Md. : 1950)*, *183*(5), 3081–3091. https://doi.org/10.4049/jimmunol.0901088

Zhao, J., Ou, B., Feng, H., Wang, P., Yin, S., Zhu, C., Wang, S., Chen, C., Zheng, M., Zong, Y., Sun, J., & Lu, A. (2017). Overexpression of CXCR2 predicts poor

prognosis in patients with colorectal cancer. *Oncotarget*, *8*(17), 28442–28454. https://doi.org/10.18632/oncotarget.16086

Zhu, W., Yu, J., Nie, Y., Shi, X., Liu, Y., Li, F., & Zhang, X. L. (2014). Disequilibrium of M1 and M2 macrophages correlates with the development of experimental inflammatory bowel diseases. *Immunological investigations*, *43*(7), 638–652. https://doi.org/10.3109/08820139.2014.909456

Zijlstra, G. J., Fattahi, F., Rozeveld, D., Jonker, M. R., Kliphuis, N. M., van den Berge, M., Hylkema, M. N., ten Hacken, N. H., van Oosterhout, A. J., & Heijink, I. H. (2014). Glucocorticoids induce the production of the chemoattractant CCL20 in airway epithelium. *The European respiratory journal*, *44*(2), 361–370. https://doi.org/10.1183/09031936.00209513

6. Appendix

6.1 Acknowledgements

I would like to thank many people who have been part of this journey.

First, I would sincerely thank my supervisor: Dr. Sybille Reichardt, thanks for your help, guidance, and patience during these years, for always helping me out during every step, and for always being open to questions and finding a solution to every problem I had. A big thanks to Prof. Dr. Holger Reichardt for his help and advice in improving my scientific research. Thanks to both of you for giving me the opportunity to be part of your team and for the scientific knowledge you offered me.

I would like to thank my thesis committee members: Prof. Dr. Matthias Dobbelstein and Prof. Dr. Lutz Walter for their suggestions and advice during our meetings and their interest in my project, and for giving me the opportunity to do experiments in your lab. Thanks also to Nico for helping me during the experiments.

Thanks to my lovely colleagues, Amina, Agathe, Fabian, Hu, Tina, Katja, and Leonie. Sharing this scientific journey with you was a great pleasure. Thanks also to the whole Department of Cellular and Molecular Immunology for your help.

I would like to thank my parents for always supporting me and always being present when I needed them. Thanks to my beautiful large family, my boyfriend, and his family for always being supportive and helpful during these years despite the distance. Thanks to my old and new friends for your help and support, I am glad to have you in my life.